Dtsch. Entomol. Z. 71 (1) 2024, 111–176 | DOI 10.3897/dez.71.112433

PENSOFT

für Natur MUSEUM FÜR NATURKUNDE BERLIN

Et latet et lucet: Discoveries from the Phyletisches Museum amber and copal collection in Jena, Germany

Brendon E. Boudinot[1,2,3], Bernhard L. Bock[1], Michael Weingardt[1], Daniel Tröger[1], Jan Batelka[4], Di Li[1,5], Adrian Richter[1,6], Hans Pohl[1], Olivia T. D. Moosdorf[1,2], Kenny Jandausch[1,7], Jörg U. Hammel[8], Rolf G. Beutel[1]

1 *Friedrich-Schiller-Universität Jena, Institut für Zoologie und Evolutionsforschung, Erbertstraße 1, 07743 Jena, Germany*
2 *National Museum of Natural History, Smithsonian Institution, 10th & Constitution Ave. NW, Washington, DC, USA*
3 *Senckenberg Naturmuseum Frankfurt, Senckenberganlage 25, 60325 Frankfurt, Germany*
4 *Department of Zoology, Faculty of Science, Charles University, Viničná 7, 128 43 Praha 2, Czech Republic*
5 *Department of Entomology, China Agricultural University, 100193 Beijing, China*
6 *Okinawa Institute of Science and Technology Graduate University, 1919-1 Tancha, Onna son, 904-0495, Japan*
7 *Institute for Anatomie I, Jena University Hospital, Teichgraben 7, 07743 Jena, Germany*
8 *Institute of Materials Physics, Helmholtz-Zentrum Hereon, Max-Planck-Straße 1, 21502 Geesthacht, Germany*

https://zoobank.org/050A157B-D712-4094-B4FA-E605151001EA

Corresponding authors: Brendon E. Boudinot (boudinotb@gmail.com, brendon.boudinot@senckenberg.de); Bernhard L. Bock (bernhard-leopold.bock@uni-jena.de); Michael Weingardt (michael.weingardt@uni-jena.de)

Academic editor: Sonja Wedmann ♦ **Received** 8 September 2023 ♦ **Accepted** 8 January 2024 ♦ **Published** 19 April 2024

Abstract

As the only direct records of the history of evolution, it is critical to determine the geological source of biota-bearing fossils. Through the application of synchrotron-radiation micro-computed tomography (SR-µ-CT), Fourier-transformed infrared-spectroscopy (FT-IR), visual evaluation of ultraviolet fluorescence (UV-VS), radiocarbon dating (^{14}C quantification), and historical sleuthing, we were able to identify and sort 161 (83 Baltic amber, 71 Copal and 7 Kauri gum pieces) individually numbered and largely mislabeled pieces of East African Defaunation resin (~145 years old) and copal (~390 years old), as well as Baltic amber (~35 million years old) from the Phyletisches Museum collection. Based on this collection, we define two new species: ‡*Amphientomum knorrei* Weingardt, Bock & Boudinot, **sp. nov.** (Psocodea: Amphientomidae, copal) and †*Baltistena nigrispinata* Batelka, Tröger & Bock, **sp. nov.** (Coleoptera: Mordellidae, Baltic amber). For selected taxa, we provide systematic reviews of the fossil record, including: Amphientomidae, for which we provide a key to all species of *Amphientomum*, extant and extinct, and recognize the junior synonymy of *Am. ectostriolatum* Li, 2002 (an unjustified emendation) under *Am. ectostriolate* Li, 1999 (**syn. nov.**); the fossil ant genus †*Yantaromyrmex* and the clades Dorylinae, Plagiolepidini, *Camponotus*, *Crematogaster*, and *Pheidole* (Formicidae); the Nevrorthidae (Neuroptera); and *Doliopygus* (Coleoptera: Curculionidae: Platypodinae). We synonymize *Palaeoseopsis* Enderlein, 1925 with *Amphientomum* Pictet, 1854, **syn. nov.** and transfer one species from *Amphientomum*, forming *Lithoseopsis indentatum* (Turner, 1975), **comb. nov.** To prevent the uncritical usage of unidentifiable fossils attributed to *Camponotus* for macroevolutionary analysis, we transfer 29 species to the form genus †*Camponotites* Steinbach, 1967, which we consider to be most useful as *incertae sedis* in the Formicinae. We treat †*Ctt. ullrichi* (Bachmayer, 1960), **comb. nov.** as unidentifiable hence invalid **stat. nov.** We also transfer †*Ca. mengei* Mayr, 1868 and its junior synonym †*Ca. igneus* Mayr, 1868 to a new genus, †*Eocamponotus* Boudinot, **gen. nov.**, which is *incertae sedis* in the Camponotini. Concluding our revision of *Camponotus* fossils, we transfer †*Ca. palaeopterus* (Zhang, 1989) to *Liometopum* (Dolichoderinae), resulting in †*L. palaeopterum* **comb. nov.** and the junior synonymy of †*Shanwangella* Zhang, 1989, **syn. nov.** under *Liometopum* Mayr, 1861. Because the type specimens of the genera †*Palaeosminthurus* Pierce & Gibron, 1962, **stat. rev.** and †*Pseudocamponotus* Carpenter, 1930 are unidentifiable due to poor preservation, we consider these taxa unidentifiable hence invalid **stat. nov.** To avoid unsupported use of the available fossils names attributed to *Crematogaster* for divergence dating calibration points, we transfer three species to a new collective taxon that is *incertae sedis* in Myrmicinae, †*Incertogaster* Boudinot, **gen. nov.**, forming †*In. aurora* (LaPolla & Greenwalt, 2015), †*In. praecursor* (Emery, 1891), **comb. nov.**, and †*In. primitiva* (Radchenko & Dlussky, 2019), **comb. nov.** Finally, we transfer †*Ph. cordata* (Holl, 1829) back to *Pheidole*, and designate a neotype from our copal collection based on all available evidence. All new species plus the neotype of ‡*Ph. cordata* are depicted with 3D cybertypes from our µ-CT scan data. We introduce the convention of a

double dagger symbol (‡) to indicate fossils in copal or Defaunation resin, as these may yet be extant. To further contextualize our results, we provide a discussion of amber history and classification, as well as the Kleinkuhren locality, to which multiple specimens were attributed. We conclude with conspecti on key biological problems and increasing potential of μ-CT for phylogenetic paleontology.

Key Words

ants, barklice, best practices, digitization, lacewings, micro-computed tomography (μ-CT), morphology, museomics, phenomics, taxonomy

1. Introduction

> "*Et latet et lucet Phaethontide condita gutta, ut videatur apis nectare clusa suo.*"
> "Caught in a[n] [amber tear] drop of Phaethontide a bee is hidden and shines, so that it may be seen that she is buried in her own nectar."
>
> – (Mart. 4.32), Marcus Valerius Martialis (between 38 and 41 AD – 102 and 104 AD)

The Phyletisches Museum in Jena, Germany, was founded by the famous and notorious zoologist Ernst Haeckel, who laid the foundation stone in 1907 and donated the museum to the University of Jena in 1908. Today, the collection of the *Jugendstil* or Art Nouveau building contains about 750,000 specimens, of which insects represent approximately two thirds, while the remainder is divided among the other animal classes and phyla, with vertebrates forming a large and valuable proportion. Since its founding, the museum has accumulated material from notable scientific figures, including Haeckel's successor Ludwig Plate (1862–1937), Richard Semon (1859–1918), Wilhelm Kükenthal (1861–1922), Jürgen Harms (1885–1956), Otto Wohlberedt (1870–1945), and Dietrich Starck (1908–2001), among others (see Uschmann 1959; von Knorre 1983).

The paleontological collection of the Phyletisches Museum contains more than 30,000 objects, split into historical and contemporary sets. The historical part is marked with the acronym PMJ P and was acquired after the closure of the geoscientific institutes of Jena University in 1968 and represents a "closed collection". All other fossils bear the acronym PMJ Pa, and specimens are still added to this contingent. In addition to type material, these collections also contain other historically valuable objects, such as the so called "*Goethe-Stier*" (the holotype of *Bos primigenius taurus* Bojanus, 1827; von Knorre and Beutel 2018) and an elephant skull that was used by von Goethe for his "*Zwischenkieferstudien*" ("studies on the *os intermaxillare*") (Valentini 1714; Matuschek 2020). The museum also possesses a small amber collection, containing for instance important fossils of Strepsiptera, including members of the stem group and the most ancestral species of the order (Pohl et al. 2005, 2021; Pohl and Beutel 2016).

While reorganizing material and cleaning storage spaces following the closure of the museum in 2020 due to the COVID-19 pandemic, we made a surprising discovery: Another amber collection, which had been lost for several decades. In total, this collection consisted of 161 pieces, of which 76 were unlabeled. The remaining material was labeled as East African copal ("Ost-Afrika"; 3 pieces), amber from Samland (51 pieces from "Bernsteinwerke Königsberg", 14 from Samland, and 1 piece from "Kleinkuhren"), or stated as possibly coming from Samland ("Samland?", 15 pieces), as well as one piece from "Ostseestrand" (Baltic Sea beach). As we processed the material and started making identifications, we found a number of potential new records from specimens directly labeled as Baltic amber, with profound evolutionary implications, particularly for the Formicidae. As the new records accumulated, we became skeptical of the labeling and pursued multiple approaches to resolve the sources of the "amber" pieces in this rediscovered fossil collection of the Phyletisches Museum.

The objectives of our present study, therefore, were to: (1) Identify the source or sources of the fossils; (2) identify the insect inclusions as finely as possible; (3) provide taxonomic treatments within the realms of our expertise; and (4) to contextualize this historically overlooked collection more broadly. Toward these ends, we implemented a battery of qualitative and quantitative tests of the fossil matrices, we investigated the historical records from and associated with the Phyletisches Museum, and we applied synchrotron-radiation micro-computed tomography (SR-μ-CT) and traditional light microscopy methods to interrogate the fine-scale structure of the fossil insects in a comparative framework. Consequently, we report the results of our taphonomic investigation and key historical findings, and we provide revisionary systematic treatments for select taxa of Psocodea, Formicidae, Neuroptera, and Coleoptera.

2. Materials and methods

Note on convention: We introduce the double dagger symbol (‡) to indicate taxa that are known only from copal or Defaunation resin, to distinguish it from the single dagger (†), which is used to indicate taxa known only from amber.

2.1. Fossil specimens

All fossil pieces from the rediscovered *Bernsteinsammlung* (amber collection) of the Phyletisches Museum were provided with unique specimen identifiers. The identifiers are in the "Inv.-Nr. Pa." series, which corresponds to the older accessions of the museum (von Knorre and Beutel 2018). The amber pieces were stored in three drawers in the attic of the museum and have been untouched for around 50 years. Presumably, due to the strong temperature and humidity fluctuations, the overall condition was quite poor with the fossils having brittle, deteriorated surfaces (Bisulca et al. 2012). Some of the pieces were found to be coated with an unknown type of varnish, which emitted a distinct smell during grinding. Other specimens were unconventionally glued to cardstock. We infer that the glue was some sort of epoxy, as this was commercially available in the late 1940s (Chen et al. 2019), and that the pieces were likely glued by E. Uhlmann sometime after acquisition (see section 3.1.1 below). We observed that the epoxy had "eaten" its way into the amber over time, resulting in dissolved surfaces. We removed the epoxy completely through careful grinding.

2.2. Specimen preparation

To facilitate the identification of inclusions, all amber specimens were manually ground and polished. Grinding was done with waterproof single silicon carbide abrasive paper (Robert Bosch GmbH, Robert-Bosch-Platz 1, 70839 Gerlingen, Germany) soaked in water (Sadowski et al. 2021). Initial sandpaper grainsize was chosen for each specimen individually, depending on condition and on the distance of the inclusions to the surface. In general, we used the following grainsize steps: 180, 400, 500, 1000, 1200, and 2000. Whenever possible, we made an effort to generate flat surface windows for viewing. Grinding was performed with sandpaper over a glass plate in one hand and the amber piece in the other hand. Amber pieces and glass plate were cleaned with water between every grain size step.

We experimented with different polishes such as chalk and Peek Polish (Peek Polish International, 51 Waterloo Road London NW2 7TX, United Kingdom). As the latter contains residual petroleum (Peek Premium Polish Paste Safety Data Sheet), it was used very cautiously but produced good results. Finally, we found that excellent results could be achieved by using the toothpaste Colgate® Sensation White Aktivkohle Zahnpasta (Colgate-Palmolive, 300 Park Avenue New York, NY, United States). A dab of toothpaste placed on microfibre cloth with a small amount of water was used to polish the amber pieces on all sides, until most of the remaining small scratches were no longer visible. To finish a single piece took up to three hours, as constant control under a desktop-mounted magnifying glass was mandatory to prevent grinding off inclusions.

To isolate specific inclusions, some amber specimens were cut into smaller pieces using a Dremel® 3000 (Robert Bosch GmbH, Dremel, 1800 W. Central Rd., Mt. Prospect, Illinois, U.S.) with a thin saw blade (0.1 mm) attachment. As the Dremel's minimum speed is 10000/min, which was too fast for freehand amber cutting, we used a defective Proxxon FBS 240/E (Proxxon Inc., 130 US Hwy 321 SW, Hickory, NC 28602 USA) to create guiding cuts. The lowest revolution rate of the Proxxon is given as 5000/min, but the one that we used had a markedly lower speed. With the guiding cuts done, the faster Dremel® could be used safely. This process required very straight cuts to prevent the blade from bending and getting caught in the amber, which would occasionally cause breaking or splintering. Alternatively, we also used a hardwood saw (Heckenrose 3 fein, Augusta-Heckenrose, Werkzeugfabriken GmbH & Co KG, Rudolf-Diesel-Straße 36, 71154 Nufringen, Germany) of 0.3 mm, in this case with the tool fixed in place and the amber pulled over the blade. After polishing and cutting, the specimens were carefully dried using a microfiber cloth.

The final curatorial step was to store the fossils in individually shaped moulds of PE-Foam (SV-Schaumstoffe GmbH, Junkerstraße 10, 82178 Puchheim, Germany) in insect drawers. A slit was cut into the foam above each object, into which the matching label was inserted. A small note was placed under each amber piece (Museumspapier altweiß mit Alkalipuffer, Klug Conservation, Zollstraße 2, 087509 Immenstadt, Germany) with the corresponding inventory number.

2.3. Establishing the material origin of the fossils

As most of the specimens in the three PMJ Pa drawers lacked reliable collection information, we undertook a series of tests to determine whether the fossils had the properties of amber or copal. Specifically, we evaluated melting behavior, autofluorescence, hardness, solubility, and density. All tests were compared between the PMJ Pa material and known samples, which were either from Ethiopian, Baltic, or Burmese ambers. As the Ethiopian pieces were a loan from MAIG (Museum of Amber Inclusions, University of Gdańsk, Gdańsk, Poland), we did not sample these destructively.

To confirm that our specimens were products of plant resin rather than artefacts in plastic material, we heated a needle and attempted to insert it into the test samples to test melting behavior. We checked fluorescence using a handheld LED UV flashlight and a 6 pi LED special UV lamp with a 120° angle of radiation. To test hardness, we scratched the test pieces either against our fingernails or *vice versa*. For the solubility test, we used a Dremel disc saw with a diamond blade to cut small pieces from the test samples, which we then placed in 99.5% Acetone; after a few minutes, we removed the samples and pressed them between our fingers. For the density test, we filled two dishes with fresh water, and added salt to saturation to one of them, after which we placed known and unknown samples in both liquids. Finally, we sent a representative sample of 10 specimens that were either labeled as "copal" or "amber" to the International Amber Association (IAA; Gdańsk, Poland) for UV fluorescence and Fourier-transformed infrared spectroscopy (FT-IR) (Table 1).

Table 1. Specimens tested at the IAA, their expected sources, results of the FT-IR analysis, and the color of each resin piece. Four specimens (**bold**) conformed to expectations based on the provided label data.

PMJ Pa	Expected source	Result	Color	Notable inclusion
5806	Baltic (succinite)	Copal *sensu lato*	Yellow	Mantodea
5807	Baltic (succinite)	Copal *s. l.*	Yellow	Formicidae: *Lepisiota*
5808	Baltic (succinite)	Copal *s. l.*	Yellow	Formicidae: *Dorylus*
5809	Baltic (succinite)	Copal *s. l.*	Yellow	Psocodea: *Amphientomum*
5824	Baltic (succinite)	Copal *s. l.*	Yellow	Formicidae: *Crematogaster*
5825	**Copal**	Copal / (Kauri gum?)[1]	Yellow	Psocodea: Archipsocidae
5827	Baltic (succinite)	Copal *s. l.*	Yellow	Formicidae: *Pheidole*, *Dorylus*
5830	Copal	Succinite	Orange	Brachycera, Auchenorrhyncha
5855	**Baltic (succinite)**	Succinite	Orange	Diptera: Tipulomorpha
5871	**Baltic (succinite)**	Succinite	Orange	Archaeognatha
5858	**Baltic (succinite)**	Succinite	Orange	Diptera: Tipulomorpha
5884	Baltic (succinite)	Copal *s. l.*	Yellow	Formicidae: *Dorylus*
5889	Baltic (succinite)	Copal *s. l.*	Yellow	Formicidae: *Pheidole*

[1] The IAA results suggest that this specimen may be from Kauri gum. Without additional evidence, we provisionally recognize that this specimen is not amber and is of uncertain source.

2.4. Microscopy

Specimens were examined at the Phyletisches Museum primarily with a Zeiss Stemi SV 11 stereomicroscope and a Zeiss Axioskop compound microscope. For the stereomicroscope a maximum magnification of 40× was used. For the light microscope we used the magnifications 50×, 100× and 200×.

2.5. Photography

To remove minute scratches, the amber pieces selected for photography were polished in three successive steps with ST5000, ST7000 wet abrasive paper (Starcke, Melle, Germany), and Peek polish (Tri-Peek International, Saffron Walden, United Kingdom) or Colgate® Sensation White Aktivkohle Zahnpasta (Colgate-Palmolive, 300 Park Avenue New York, NY, United States).

For overview photographs, stacks of partially focused images were taken of the amber pieces with a Canon EOS R5 equipped with a Canon EF 100 mm f/2.8L Macro IS USM lens (Canon, Krefeld, Germany), which was mounted on a Kaiser copy stand. For focus bracketing, the internal camera software was used. The scene was illuminated with a Euromex LE.5211-230 cold light source for stereomicroscopy (Euromex, Papenkamp, Netherlands) equipped with three gooseneck lamps to adjust light conditions and prevent reflections. Underneath the camera a blurred glass plate was positioned over a black sprayed Kapa® box. The amber pieces were placed on the glass plate in a petri dish filled with distilled water as suggested by Sadowski et al. (2021). The amber was held in place with UHU Patafix (UHU, Bühl, Germany). Some pieces were photographed without water to obtain a better spatial impression.

For shots of details from single embedded specimens, a Canon Eos 7D Mark II (Canon, Krefeld, Germany) equipped with a Mitutoyo M Plan Apo 10 microscopic lens (Mitutoyo, Kawasaki, Japan) was used. To perform stack shots, the camera was mounted on a StackShot macro rail (Cognisys, Traverse City, USA). Two flashlights (Yongnuo Photographic Equipment, Shenzhen, China) illuminated the scene. The amber pieces were placed on a cover slip. Plasticine was used to level the surface. A drop of glycerine was placed on the surface of the amber piece, and the glycerine was then covered by an additional cover slip. Additional detail images were taken at the Museum für Naturkunde Berlin (MfN), where manual stacks were taken using a Zeiss Axioscope 5 with a Zeiss Achromat S 1,0 FWD 63 (Carl Zeiss AG, Oberkochen, Germany), mounted with a Canon EOS 80D (Canon, Krefeld, Germany) via a T2-T2 1,6× SLR tube.

All photographs were developed with Adobe Lightroom classic (v.11.5) (Adobe, San Jose, USA). The images (option: standard) were denoised with Topaz DeNoize AI (Topaz Labs, Dallas, USA). Zerene stacker 1.04 (Zerene Systems LLC, Richland, USA) was used to fuse the images (option: align & stack all (PMax).

2.6. Micro-computed tomography

Nine specimens (Table 2) were scanned using synchrotron radiation (SR-μ-CT) at the Imaging Beamline P05 (IBL) (Haibel et al. 2010; Greving et al. 2014; Wilde et al. 2016) operated by the Helmholtz-Zentrum Hereon at the storage ring PETRA III (Deutsches Elektronen Synchrotron—DESY, Hamburg, Germany). A photon energy of 18 keV and a sample to detector distances of 30–50 mm were used. Projections were recorded using a 50 MP CMOS camera system with an effective pixel size of 0.46 μm. 4001 projections were recorded for each tomographic scan at equal intervals between 0 and π, with an exposure time of 350 ms. When specimens were too large to fit into the field of view in the z-axis, we scanned overlapping sections and subsequently stitched them together. Tomographic reconstruction was done by applying a transport of intensity

Table 2. Specimens scanned at DESY; data available as Suppl. material 1.

Specimen ID	Taxon name	Stage/sex
PMJ Pa 5827_a	Coleoptera: Platypodinae: *Doliopygus* cf. *serratus*	Adult male
PMJ Pa 5870	Coleoptera: Mordellidae: †*Baltistena nigrispinata* Batelka, Tröger & Bock, **sp. nov.**	Adult, sex indet.
PMJ Pa 5821[1]	Hemiptera: Auchenorrhyncha: Cixiidae	Adult female
PMJ Pa 5884	Hymenoptera: Formicidae: *Dorylus nigricans molestus* (Gerstäcker, 1859)	Adult worker
PMJ Pa 5809	Psocodea: ‡*Amphientomum knorrei* Weingardt, Bock & Boudinot, **sp. nov.**	Adult female
PMJ Pa 5825	Psocodea: Archipsocidae	Adult female
PMJ Pa 5889	Hymenoptera: Formicidae: ‡*Pheidole cordata* (Holl, 1829)	Adult soldier
PMJ Pa 5874[2]	Neuroptera: †*Palaeoneurorthus* sp.	Adult male
PMJ Pa 5896[3]	Arachnida: Salticidae	Adult, sex indet.

[1] Not analyzed further; no taxonomic expertise.
[2] Not analyzed further; poor preservation.
[3] Not analyzed further; specimen not visible in scan files.

phase retrieval and using the filtered back projection algorithm (FBP) implemented in a custom reconstruction pipeline (Moosmann et al. 2014) using MATLAB (Math-Works) and the Astra Toolbox (Palenstijn et al. 2011; van Aarle et al. 2015, 2016). For further processing, raw projections were binned two times resulting in an effective pixel size of the reconstructed volume of 0.913 µm. For segmentation and visualization, the 32-bit .tif image sequences were converted to 8-bit files and downsampled twofold with Fiji (Schindelin et al. 2012), resulting in an effective pixel (voxel) size of 1.826 µm.

2.7. ^{14}C dating of samples

Two samples, PMJ Pa 5809 (‡*Amphientomum knorrei* Weingardt, Bock & Boudinot, sp. nov.) and PMJ Pa 5884 (*Dorylus nigricans molestus*) were dated using ^{14}C analysis, as recommended by Delclòs Martínez et al. (2020). Amber pieces with a mass of 5 mg (PMJ Pa 5809), 6 mg (PMJ Pa 5884) and 5 mg (PMJ Pa 5889) were cut off and sent to Beta Analytic (4985 S.W. 74th Court, Miami, FL, USA 33155). Dating analyses resulted in estimated age ranges with certain likelihoods. The age range with the highest likelihood was chosen (Table 3). Based on our identifications of the copal inclusions and the history of the collections, East Africa was selected as the geographic reference for dating. We chose the psocodean as taxonomic work on the group is challenged, with presently only a handful of specialists working on them (e.g., Mockford 2018). We also chose the putative Baltic *Dorylus* due to its potential evolutionary and biogeographic implications.

Table 3. ^{14}C-dating results based on the testing by Beta Analytic. The maximum age of the estimated range is listed.

^{14}C-dated	Specimen contained	Results	Maximum age in years
PMJ Pa 5809	‡*Amphientomum knorrei*	390 +/-30 BP	565
PMJ Pa 5884	*Dorylus nigricans molestus*	50 +/-30 BP	145
PMJ Pa 5889	‡*Pheidole cordata*, Lepidoptera indet	720 +/- 30 BP	746

2.8. Data segmentation and rendering

µ-CT-image stacks were segmented and 3D-reconstructed using Amira 6.0.1 (Thermo Fisher Scientific) and Dragonfly 2022.1 (Object Research Systems,). Image (tif) stacks and isosurfaces were exported with the Amira macro "Multi-Export" (Engelkes et al. 2018). The isosurfaces were reduced and smoothed with following parameters: It-Total: 5; smooth: iteration: 4, lambda: 0.6; reduction: 0.7. Tiffs were volume rendered in VGStudio Max 2.0 (Volume Graphics) using the option Phong reflection model. The isosurfaces were further smoothed (modifier: smooth and option shade smooth) with Blender 3.2.0 (Blender Foundation). The 3D-Models were uploaded to the 3D repository Sketchfab (URL: https://sketchfab.com) using the free blender plugin: Sketchfab for Blender 1.5.0 (URL: https://github.com/sketchfab/blender-plugin/releases/tag/1.5.0).

2.9. Image plates

Image plates were compiled using Adobe Photoshop (v. 24.1.0) (Adobe, San Jose, USA). Lettering was added with Adobe Illustrator (v. 27.2).

2.10. Repositories

Specimens evaluated in the present study, and also for the use of comparison to each other, were from the following collections:

BEBC Brendon E. Boudinot research collection, Frankfurt am Main, Germany
MAIG Museum of Amber Inclusions, University of Gdansk, Poland.
PMJ Phyletisches Museum Jena, Germany.
MNHB Museum für Naturkunde Berlin, Germany.
MWC Michael Weingardt research collection, Jena, Germany.
SMNS Staatliches Museum für Naturkunde Stuttgart, Germany.
USNM U.S. National Museum of Natural History, Washington, D. C., U.S.A.

2.11. Data availability

The raw scan data will be made available at MorphoSource upon acceptance.

3. Results

3.1. Fossil sources

3.1.1. Fossil provenance

Collector. Unknown.

Date. Unknown. It is likely that the 161 fossil pieces in the collection were acquired by the Phyletisches Museum in several batches between 1920 and 1930 (see below).

Circumstantial evidence. By the handwriting of the label for specimen PMJ Pa 5827, the date of collection is estimated between 1920 and 1930 (personal communication with Uwe Dathe, Historische Sammlungen ThULB, 15.07.2022 and Alexander Gehler, Geowissenschaftliches Zentrum der Georg-August-Universität, 14.07.2022). The label for specimen PMJ Pa 5827 has two different scripts on each side, which cannot be clearly assigned to any handwriting samples in the museum's archives. Furthermore, the former curator of the museum, Dietrich von Knorre, stated that Eduard Uhlmann (1888–1974) was in charge of the small "Bernsteinsammlung" (amber collection); Uhlmann was a scientific assistant, later conservator at the Phyletisches Museum Jena while it was under the directorship of Ludwig Plate (director from 1909–1935), and later became associate professor (*ao*. [*außerodentlicher*] Professor 1950) and director of the Phyletisches Museum from 1952 till 1954.

In accordance with the statements above, there are handwritten labels on nine specimens (Pa 5828, 5829, 5836, 5871, 5873, 5874, 5875, 5882, and 5885) which can be assigned to E. Uhlmann and his wife Frida Uhlmann (born Preiss, 1894–1981). This assessment is unambiguous as the Uhlmanns re-sorted numerous drawers in the entomology collection, which were labelled by her (Krogmann et al. 2007). Moreover, von Knorre stated (25.07.2022) that Uhlmann (Fig. 1) bequeathed the small amber collection to him after retirement, which von Knorre later added to the museum's collection. We screened the archives of the Friedrich Schiller University (21.07.2022) and the Phyletisches Museum (21–22.07.2022) but did not discover invoices or personal communication of Uhlmann and Plate. In sum, how exactly the small amber collection found its way into the museum cannot be confidently resolved at present.

Listed localities. Of the 161 numbered pieces, 76 lacked locality information and one additional number was associated with human-made beads without further information (Pa 5911; not included in the total count). Of the remaining 85 pieces, 21 have labels indicating a Baltic origin and three are marked as copal from East Africa, such as Pa 5829, which has a handwritten label stating "Kopalinsect Ost-Afrika Diluvium". One of the putative Baltic pieces, Pa 5827, has a handwritten label "Fundstück von Kleinkuhren Samland" (Filino), while 15 are marked with "Samland?" and the derivation of 51 of the other presumptive amber specimens is indicated as Samland Bernsteinwerke Königsberg on the labels, with an authentic invoice from the "Preuß. Bergwerks- und Hütten-Akt.-Ges. Zweigniederlassung Bernsteinwerke Königsberg Pr. for 1 M" for Pa 5863. For a discussion of the Samland and Kleinkuhren localities, see also section 4.2.

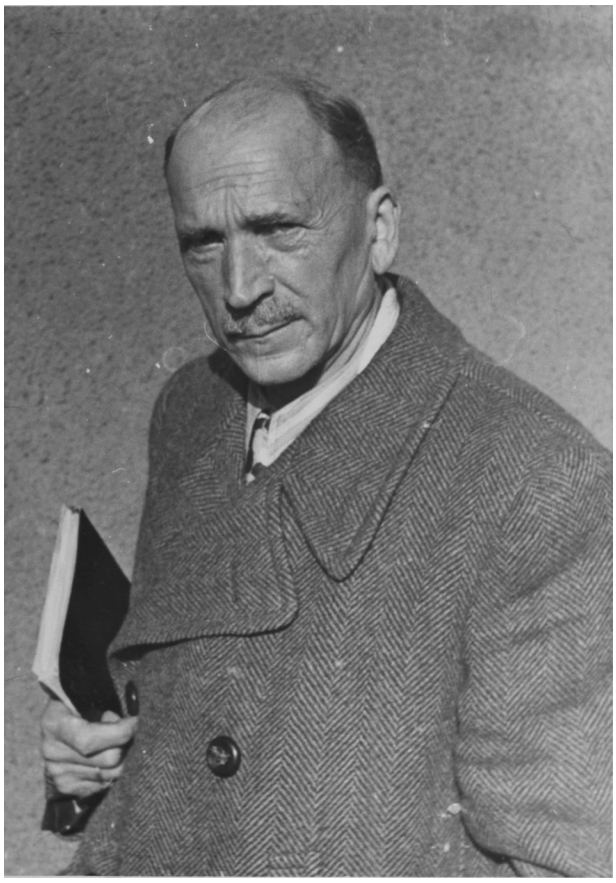

Figure 1. Eduard Uhlmann around 1955. Archive of the Phyletisches Museum XXVII.

Qualitative tests. Despite the labels, the locality or localities of origin are not as clear as the first impression suggested. As it is not possible to discriminate copal and amber reliably based on the visual appearance alone (e.g., Federman 1990), we conducted a series of qualitative tests (see section 2.3), most of them at the Phyletisches Museum. Overall, the qualitative tests were contradictory and inconclusive. All pieces labelled as amber floated in saltwater and all labelled as copal sunk, apparently confirming the original labels. However, not a single piece in the collection emitted

blue light under UV, while amber specimens of known provenance from the BEBC (burmite, succinite) and MAIG (Ethiopian amber) did. By burning the different samples from the PMJ Pa collection, every piece sizzled and produced black smoke, as expected for amber. Only one sample (Pa 5809) showed clear white smoke, but burning a larger piece yielded black smoke. Thus, the expected difference—that amber burns and copal melts—was not observed. When only small pieces were left, both copal and amber melted. Most conspicuous was a sweet odor produced by burning a larger piece of copal (from Pa 5809), which clearly distinguished it from true amber. This scent was not detected with smaller pieces, however.

Quantitative tests. For quantitative testing, additional small pieces were cut off and sent to the International Amber Association (IAA, 1 Warzywnicza Street, 80-838 Gdańsk, Poland) and checked with the UV/VIS and the FT-IR method (Table 1). The results from these analyses contradicted those from the qualitative tests and showed that all light-yellow pieces were copal, including those with *Dorylus*. In contrast, the darker, orange-colored pieces were true succinite (Baltic amber), including the one with †*Yantaromyrmex*. Finally, the ^{14}C dating yielded an age of only ~145 years old for the piece containing the *Dorylus.* Therefore, this and other pieces with similar biotic inclusions are identifiable as Defaunation resin (*sensu* Solórzano-Kraemer et al. 2020), while the estimated age for the *Amphientomum*-bearing specimen is ~390 years old.

Biotic evidence. Ultimately, our final interpretations of the geological source of the putative amber pieces were based on the combined weight of evidence from the IAA results and the insect inclusions themselves. While it was exciting to consider the possibility that the *Dorylus*, *Lepisiota*, *Pheidole*, and *Crematogaster* ants were first records from Baltic amber, our µ-CT scan of the *Dorylus* revealed that it is identifiable as an extant subspecies. Moreover, this subspecies, *Dor. nigricans molestus* (Figs 2A–C, 3, Appendix 1: Fig. A1), was previously recorded from reliably identified Tanzanian copal by DuBois (1998) (see section 4.2.2 below). Another critical element of biotic evidence was the large piece PMJ Pa 5827, which contained another *Do. n. molestus* as well as a distinctive platypodine beetle (Curculionidae; "ambrosia beetles", "pinhole borers"). Based on our µ-CT rendering of the beetle, Bjarte Jordal (01 Nov 2022) identified it as either *Doliopygus serratus* or *Dol.* cf. *serratus* (Figs 4A–C, Appendix 1: Fig. A2), which in either case represents bark beetle populations that are extreme generalists, and presently distributed throughout Southern, Central, and West Africa (Beaver and Löyttyniemi 1985). Several other amber pieces from the PMJ Pa contained sweat bees (Meliponini) that closely resembled specimens from known African copal pieces at the SMNS. All these aforementioned fossil pieces were light yellow, while other specimens—without these distinctive taxa—were dark and of a pinkish red color. Among these darker specimens was an ant definitively identifiable as †*Yantaromyrmex geinitzi*, the type species of a Baltic-amber-endemic genus. In section 3.2, we outline the complete list of taxa that we identified in the PMJ Pa collection, as well as the results of investigations on the origin of material compared to the point of starting our investigations.

3.2. Fossils of the PMJ Pa amber collection and the origin of material

In Table 4 we provide a list of all specimens sorted taxonomically, including reference to the museum accession numbers.

The initial situation of the material, with a rather chaotic sorting, shows that almost half of the material was without evidence of origin. Around 40% were labelled as Baltic amber, while 3 pieces were labeled as copal (Suppl. material 1). Overall, almost 10% were labelled, but with a question mark, which is not reliable information in any case.

Table 4. All identified taxa from the PMJ Pa amber collection.

Taxon	Matrix	PMJ Pa
PLANTAE		
(Trichomes)	Succinite	5872
(Leaf fragments)	first 4 Copal *s. l*, 5886 Copal *s. l*, all others Succinite	5811, 5820, 5826, 5886, 5839, 5840, 5843, 5848, 5849, 5851, 5855, 5856, 5861, 5862, 5867, 5870, 5883, 5885, 5910
CHELICERATA		
Acari		
(Indet.)	Succinite	5798, 5840, 5854, 5876
Araneae		
Linyphiidae	Copal *s. l*	5809
Philodromidae	Succinite	5838
Thomisidae	Succinite	5877
Zodariidae: cf. *Trygetus*	Copal *s. l*	5807
Zodariidae	Succinite	5876
Uncertain: Araneidae, Palpimanidae, Philodromidae, Salticidae, Thomisidae	First two Copal *s. l*, others Succinite	5827, 5890, 5843, 5879, 5878, 5881

Taxon	Matrix	PMJ Pa
Opiliones		
(Indet.)	Succinite	5859
HEXAPODA		
(Indet.)	Succinite	5903, 5908
Collembola		
Symphypleona	Succinite	5908
Archaeognatha		
Machilidae	Succinite	5828
(Indet.)	Succinite	5871, 5872
Dictyoptera		
Blattodea	Succinite	5841
Isoptera	first 11 Copal *s. l*, other Succinite	5794, 5798, 5802, 5803, 5811, 5815, 5818 5819, 5822, 5826, 5827, 5848, 5871
Mantodea	Copal *s. l*	5806
Hemiptera		
Aphididae	Succinite	5860, 5885
Anthocoridae	Copal *s. l*	5827
Cicadellidae	Copal, Succinite, Succinite	5827, 5847, 5852
Cixiidae	Copal *s. l*	5821
Issidae	Copal *s. l*	5821
Psyllidae	Copal *s. l*	5798
Coccoidea	Succinite	5856
Fulgoroidea	Copal *s. l*	5793
Aleyroidea	Copal *s. l*	5822
(Auchenorrhyncha)	Copal *s. l*	5809
Psocodea		
Amphientomidae: ‡*Amphientomum knorrei* **sp. nov.**	Copal *s. l*	5908
Archipsocidae	Kauri gum?	5825
Liposcelididae	Copal *s. l*	5827
Thysanoptera		
(Indet.)	Copal *s. l*	5820, 5822
Hymenoptera		
Anthophila: Apinae	Copal *s. l*	5795, 5807, 5814, 5816, 5817, 5826, 5892
Anthophila: Apinae: Meliponini	Copal *s. l*	5796, 5798, 5800, 5806, 5815, 5822, 5824, 5888, 5893
Anthophila: (indet.)	Copal *s. l*	5793, 5810, 5894
Bethylidae	Copal *s. l*	5823
Braconidae: Cheloninae	Copal *s. l*	5896
Braconidae: (indet.)	Copal *s. l*	5823
Chalcidoidea	Copal *s. l*	5816, 5819, 5820, 5821
Formicidae: *Camponotus*	Copal *s. l*	5829
Formicidae: †*Ctenobethylus*	Succinite	5851, 5874, 5893, 5903
Formicidae: *Crematogaster*	Copal *s. l*	5824
Formicidae: *Dorylus n. molestus*	Copal *s. l*	5808, 5827, 5884
Formicidae: Ponerini: cf. *Hypoponera*	Copal *s. l*	5819
Formicidae: *Lepisiota*	Copal *s. l*	5807
Formicidae: ‡*Pheidole cordata*	Copal *s. l*	5827, 5889
Formicidae: †*Yantaromyrmex geinitzi*	Succinite	5856
Formicidae: Dolichoderinae	Copal *s. l*	5817, 5821
Ichneumonidae	Succinite	5869
Platygastroidea: Platygastridae	Copal *s. l*	5889
Platygastroidea: Scelionidae *sensu lato*	Copal *s. l*, Succinite	5809, 5836
Platygastroidea: (indet.)	Copal *s. l*, Succinite, Succinite	5821, 5846, 5877
(Aculeata)	Copal *s. l*	5822, 5890
(Parasitica)	Copal *s. l*	5808, 5891
(Indet.)	Succinite	5843
Neuroptera		
Nevrorthidae: †*Palaeoneurorthus*	Succinite	5874
Coleoptera		
Cantharidae	Succinite	5863
Chrysomelidae: Bruchinae?	Copal *s. l*	5827
Chrysomelidae: Alticini?	Copal *s. l*	5810
Chrysomelidae?	Copal *s. l*	5892
Curculionidae: *Doliopygus* cf. *serratus*	Copal *s. l*	5827
Curculionidae: Platypodinae	Copal *s. l*	5798, 5805, 5807, 5812, 5814, 5816, 5819
Elateridae	Succinite	5851, 5866

Taxon	Matrix	PMJ Pa
Mordellidae: †*Baltistena nigrispinata* **sp. nov.**	Succinite	5870
Staphylinidae	Copal *s. l*, Succinite	5828, 5861
Bostrichoidea?	Succinite	5836, 5883
Staphylinoidea?	Succinite	5851
(Polyphaga)	Copal *s. l*, Succinite, Copal *s. l*	5819, 5885, 5891
Diptera		
Ceratopogonidae	Succinite, last one Copal *s. l*	5848, 5863, 5864, 5889
Chloropidae	Succinite	5836
Dolichopodidae	Succinite	5837
Mycetophilidae	Succinite, last Copal *s. l*	5848, 5885, 5901, 5890
Sciaridae	Succinite,	5851, 5864
Phoridae	Copal *s. l*	5808, 5823, 5827
Psychodidae	Copal *s. l*	5896
Sciaroidea	Copal *s. l*, Succinite	5809, 5840
(Tipulomorpha)	Succinite	5855, 5858
(Brachycera)	First 7 Copal *s. l* , all other Succinite	5795, 5807, 5811, 5815, 5822, 5827, 5830, 5836, 5839, 5844, 5846, 5849, 5853, 5854, 5857, 5862, 5865, 5867, 5868, 5871
(Muscomorpha)	Copal *s. l*	5797, 5799, 5809, 5891
(Calyptrata)	Copal *s. l*	5586
(Nematocera)	first 5 Copal *s. l*, all following Succinite	5808, 5827, 5830, 5891, 5895, 5836, 5837, 5839, 5844, 5846, 5854, 5857, 5858, 5861, 5862, 5870, 5871, 5872, 5874, 5877, , , 5897, 5902, 5903, 5909
(Indet.)	first three Copal *s. l*, other Succinite	5821, 5892, 5896, 5843, 5882, 5898, 5905
Lepidoptera		
(Indet.)	first 3 Copal *s. l*, last Succinite	5797, 5804, 5889, 5842,
Trichoptera		
Annulipalpia	Succinite	5850, 5875
Integripalpia	Succinite	5863
(Indet.)	Succinite, Copal *s. l*	5845, 5891
Amphiesmenoptera		
(Indet.)	Succinite	5903

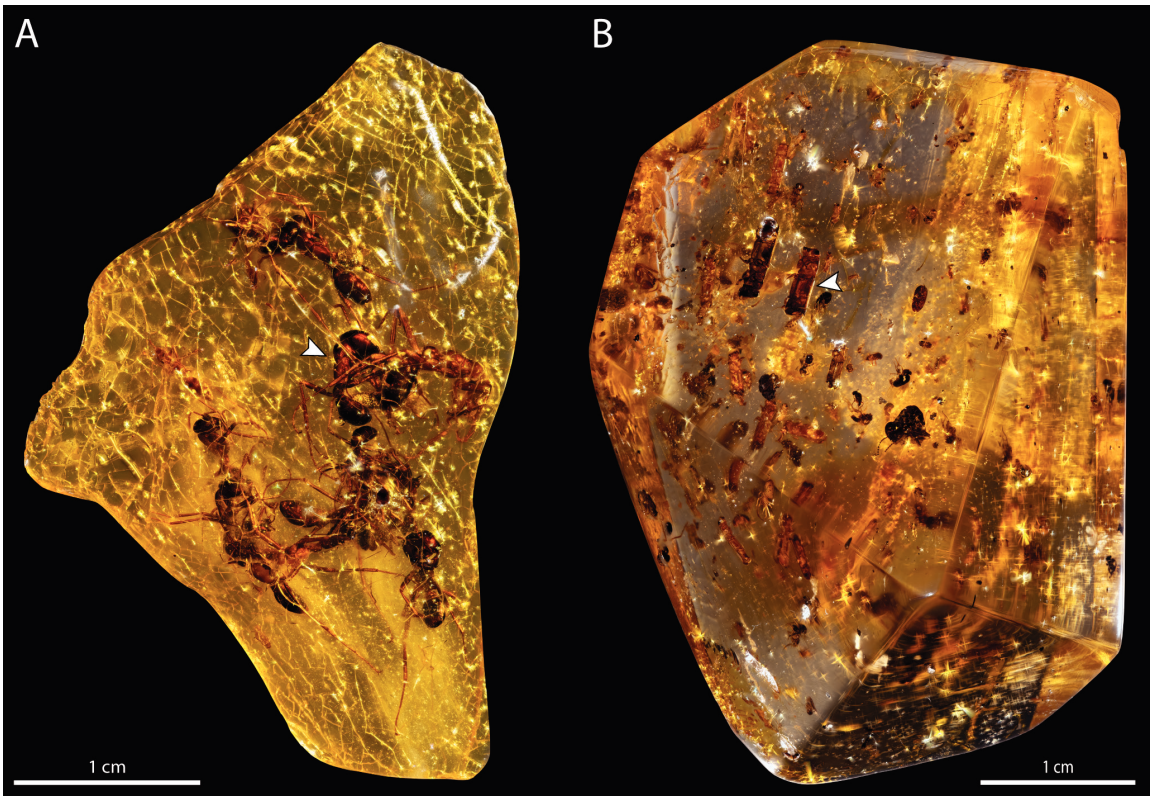

Figure 2. Overview photo of a select piece of Defaunation resin (**A**) and a piece without dating analysis performed (**B**). **A.** Piece PMJ Pa 5884, ^{14}C dated as about ~145 years old, with inclusions of several *Dorylus nigricans molestus* workers; **B.** piece PMJ Pa 5827 with the inclusion of the scanned *Doliopygus* cf. *serratus* as well as another *Do. n. molestus* worker. Arrows mark scanned specimens.

After identification, provenance research and chemical analysis the origin of most of the material could be solved confidently. One of the biggest surprises was that 7 pieces are of Kauri origin. Now, more than half of the material is of clear Baltic origin. The biggest switch was from pieces without evidence and the 3 pieces labelled as copal, as with 44% a sizable number in the collection is indeed East-African copal (Suppl. material 2).

3.3. Systematic entomology

3.3.1. Order Psocodea: Synopsis of higher taxa in the PMJ Pa

Mostly families represented by material in the PMJ Pa are reviewed below. The identification of PMJ Pa material was based on the keys of Smithers (1990), with Taylor (2013) for the amphientomid. Specific details about the fossil deposits and their ages in this and other synopsis header sections are drawn from Paleobio (2022); we have included these for the geological information and to ease future divergence-dating phylogenetic analysis. Taxonomic information was drawn in part from the Psocodea Species File Version 5.0 (Johnson et al. 2023) database.

3.3.1.1. Family Amphientomidae Enderlein, 1903. [Note 1]
Amphientominae Enderlein, 1903 amber species:
I. Genus *Amphientomum* Pictet, 1854. [Note 2].
A. Oise amber [France, Le Quesnoy; Eocene, Ypresian, 56.0–47.8 Mya].
1. †*Am. parisiense* Nel, Prokop, De Ploeg & Millet, 2005.
B. Baltic ambers [Eocene, 37.8–33.9 Mya].
2. †*Am.* (*Amphientomum*) *leptolepis* Enderlein, 1905. [Note 3].
3. †*Am.* (*Amphientomum*) *paradoxum* Pictet, 1854. [Type species!]
4. †*Am.* (*Palaeoseopsis*) *colpolepis* Enderlein, 1905.
C. African resin [ca. 390 ± 30 years].
5. ‡*Am. knorrei* Weingardt, Bock & Boudinot, sp. nov. [Note 4].
II. Genus *Lithoseopsis* Mockford, 1993.
D. Mexican amber [Miocene, 23.0–16.0].
1. †*Li. elongata* (Mockford, 1969).
III. Genus †*Proamphientomum* Vishnyakova, 1975.
E. Taimyr amber [Russia; Cretaceous, 85.8–83.5 Mya].
1. †*Pr. cretaceum* Vishnyakova, 1975.
Amphientomidae amber species *incertae sedis*:
IV. Genus †*Arcantipsocus* Azar, Nel & Néraudeau, 2009.
F. Charentese amber [France; Cretaceous, 105.3–99.6 Mya].
1. †*Ara. courvillei* Azar, Nel & Néraudeau, 2009. [Note 5].

Note 1. As part of our ongoing psocodean revisionary investigations, we provide an extended discussion of *Amphientomum* (see below).

Note 2. A list of all extinct and extant *Amphientomum* species is provided in Table 5. With the addition of the new species described herein, there are 20 species attributed to this genus (Johnson et al. 2023), of which four are extinct; it is unknown if the species described herein is still extant.

Note 3. The species †*Am. leptolepis* might be a variant of †*Am. paradoxum*, as these two taxa are distinguished by only a few characters (Enderlein 1911). Specifically, †*Am. leptolepis* is differentiated from †*Am. paradoxum* by the following: (1) fore wing with very long and slender scales; (2) sides of the scales parallel; and (3) the count of ctenidiobothria on the hind basitarsus is 36 (vs. 29–34 in †*Am. paradoxum*) (Enderlein 1911). It should be noted that the description of †*Am. leptolepis* was based on two specimens (Enderlein 1911, p. 295) and no additional information on this species was published since then, to the best of our knowledge. Overall, we consider the scale shape as not fully reliable, yet we retain the species status of these two taxa pending more detailed study.

Note 4. We describe this new species from African resin in the PMJ Pa collection. See section 3.1.1.1.4 below for our treatment of this taxon.

Note 5. Mockford et al. (2013) synonymized †Arcantipsocidae Azar, Nel & Néraudeau, 2009 with Amphientomidae, arguing that a dark, thickened pterostigma is a homoplastic feature across the order Psocodea, thus cannot be relied upon singly for placement in Psocomorpha. They left †*Arcantipsocus* unplaced within the family but further recognized features that the genus shares with modern Amphientomidae, *i.e.*, the hindwing venation and the shape of maxillary palps, head, and forewings.

3.3.1.2. Family Liposcelididae Broadhead, 1950
Liposcelidinae Broadhead, 1950 amber and copal species:
I. Genus *Liposcelis* Motschulsky, 1852.
A. Baltic ambers [Eocene, 37.8–33.9 Mya].
1. †*Li. atavus* Enderlein, 1911.
B. Mexican amber [Miocene, 23.0–16.0].
2. †*Li.* sp. [Note 1]. [f].
C. Zanzibar copal [Pleistocene?].
3. ‡*Li. resinata* (Hagen, 1865).
Embidopsocinae Broadhead, 1950 amber species:
II. Genus *Belaphopsocus* Badonnel, 1955.
D. Dominican amber [Miocene, 20.4–13.8 Mya].
1. †*Bs. dominicus* Grimaldi & Engel, 2006.
III. Genus *Belaphotroctes* Roesler, 1943.
B. Mexican amber [Miocene, 23.0–16.0].
1. †*Bt. ghesquierei* Badonnel, 1949.
E. Zhangpu amber [Miocene, 16.0–13.8].
1. †*Bt. grimaldii* Engel & Wang, 2022.
IV. Genus *Embidopsocus* Hagen, 1866.
F. Oise amber [France, Le Quesnoy; Eocene, Ypresian, 56.0–47.8 Mya].
1. †*Em. eocenicus* Nel, de Ploëg & Azar, 2004.
A. Baltic ambers [Eocene, 37.8–33.9 Mya].
2. †*Em. pankowskiorum* Engel, 2016.

G. Bitterfeld amber [Eocene, 38.0–33.9 Mya].
3. †*Em. saxonicus* Günther, 1989.
Liposcelididae amber species *incertae sedis*:
II. Genus †*Cretoscelis* Grimaldi & Engel, 2006.
H. Kachin amber [Myanmar; Cretaceous, 99.6–93.5 Mya].
1. †*Csc. burmitica* Grimaldi & Engel, 2006.

Note 1. Mockford (1969) recognized a species of *Liposcelis* from Mexican amber that he left undescribed as insufficient structural detail, *i.e.*, cuticular microsculpture and chaetotaxy, was observable.

3.3.1.3. Family Archipsocidae Pearman, 1936
Archipsocinae Pearman, 1936 amber species:
I. Genus *Archipsocopsis* Badonnel, 1948.
A. Mexican amber [Miocene, 23.0–16.0].
1. †*Ari. antigua* (Mockford, 1969).
II. Genus *Archipsocus* Hagen, 1882.
B. Baltic ambers [Eocene, 37.8–33.9 Mya].
1. †*Aru. puber* Hagen, 1882.

3.3.2. Taxon description (Psocodea)

Family Amphientomidae Enderlein, 1903
Subfamily Amphientominae Enderlein, 1903

Genus *Amphientomum* Pictet, 1854

= *Amphicetomum* Hagen, 1859.
= *Palaeoseopis* Enderlein, 1925 syn. nov. (Type species: †*Am. colpolepis* Enderlein, 1905 *by original designation.*).

Type species. †*Am.* (*Amphientomum*) *paradoxum* Pictet, 1854.

Remarks. Pictet (1854) first described the genus from Baltic amber. Enderlein (1905, 1911) defined several character states that define the genus *Amphientomum*. These include a large body size, a relatively small ocellar area where the distance between the ocelli is short, a lack of spur sensilla on the maxillary palpomeres, an elongated and narrow fourth maxillary palpomere, labial palps with two articles, antennal flagellum with secondary annulation, presence of a complete R1 vein in the hindwing, and perhaps more surprisingly the occurrence of only 13 flagellomeres (Enderlein 1911, p. 333). The number of antennomeres might be an oversight by Enderlein (1911), as Hagen (1882) had already described the number of articles (15) correctly. In his revision of Pearman's (1936) phylogenetic system of Psocoptera, Roesler (1944) provided morphological characters to define previously established groupings including the Amphientomidae. In so doing, Roesler designated the previously established genus *Palaeoseopsis* Enderlein, 1925 as a subgenus of *Amphientomum*. As such, *Am.* (*Palaeoseopsis*) is supposed to differ from *Am.* (*Amphientomum*) by the open basiradial cell, the lack of the basal section of Rs in the hindwing, and the emarginate scale tips (Enderlein 1925; Roesler 1944). Badonnel (1955) went a step further and proposed that the subgenus *Palaeoseopsis* can be removed entirely but did not follow through on this action. It should be noted that an open basiradial cell in the hindwing occurs in all species of the genus that are outside the subgenus *Am*. (*Amphientomum*), as in most species only a short spur vein of the basal section of Rs is present or the basal section of Rs is entirely missing. Phylogenetic studies on this genus are lacking and the monophyly of the subgenera *Am.* (*Palaeoseopsis*) and *Am.* (*Amphientomum*) is therefore questionable, as they are neither supported by morphological apomorphies, nor by molecular data. We therefore formalize the synonymy of *Amphientomum* and *Palaeoseopsis* j. syn., syn. nov. The diagnostic characters of the genus *Amphientomum* are as follows after the identification key by Taylor (2013): presence of wings, the vein M in the hindwing simple, presence of three ocelli, the lateral ocelli closer to each other than to compound eyes, the vein R1 reaching the wing margin in the hindwing, and the distal section of the vein Sc in the forewing present. See also the Remarks section for †*Am. knorrei* sp. nov.

Note. The term sulcus is used here when an external line or furrow corresponds with an internal ridge, i.e., a strengthening ridge (Girón et al. 2023). If no internal ridge is present but a narrow zone of weakness, we use the term suture (e.g., frontal suture). The typical coronal suture (part of the ecdysial suture) of other insects corresponds with an internal ridge in adult psocids and is therefore here classified as a coronal sulcus. The frontal sutures (part of ecdysial suture) are similarly developed as in other insects, without an internal strengthening ridge. The term epistomal sulcus is used as synonym of the frontoclypeal line.

‡*Amphientomum knorrei* Weingardt, Bock & Boudinot, sp. nov.

https://zoobank.org/600FA627-5659-486A-AF36-3F808852EB09

Etymology. We dedicate this species to Dietrich von Knorre, whose lifework was to establish and curate the collection of the Phyletisches Museum. Besides being a natural conservationist and a dedicated teacher of students, von Knorre was the curator of the Museum from 1969 till 2003, during which time he dealt with nearly every item in the entire collection. In addition to his more than 270 publications (Köhler 2019), he has done meticulous research on the history of an immense number of objects and has become the museum's "living archive". With the newly discovered specimen bearing his name, we want to express our gratitude for his continuous support and contributions to the Phyletisches Museum.

Type materials. *Holotype*. PMJ Pa 5809, Copal (East African?). Female. Interactive cybertype: Appendix 1: Fig. A3.

***Paratypes*.** None.

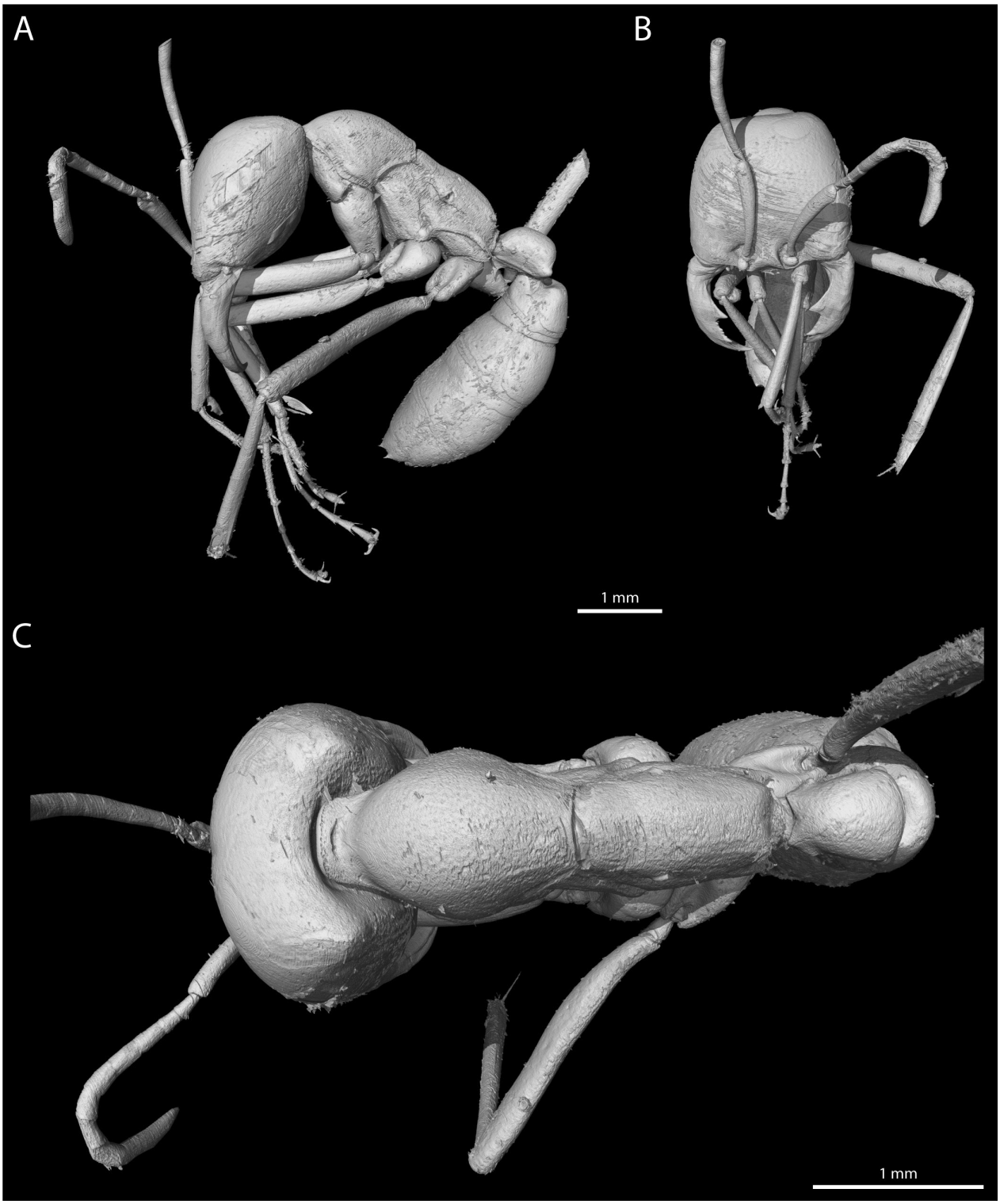

Figure 3. A–C. 3D reconstruction of *Dorylus nigricans molestus* (Formicidae: Dorylinae) preserved in piece PMJ Pa 5884. **A.** Habitus lateral; **B.** Habitus frontal; **C.** Habitus dorsal. See section 4.2.1 below for diagnostic remarks.

Diagnosis. Macropterous. Wings and body covered with scales. Scales apically straight or medially incised. Epistomal sulcus complete and corresponding epistomal ridge wide. Genae long. Vertex narrow and rounded. Three ocelli of similar size present, forming an isosceles triangle. Lateral ocelli closer to each other than to compound eyes. Compound eyes large and their upper margin reaching uppermost margin of vertex. Antenna with 15 articles. Flagellomeres with secondary annulation. Maxillary palps with four articles, a minute basal article and a long and cylindrical last palpomere that is rounded distally. No conical sensillum visible on second maxillary article. Tip of lacinia with long lateral region bearing several rounded denticles, and a shorter truncated median

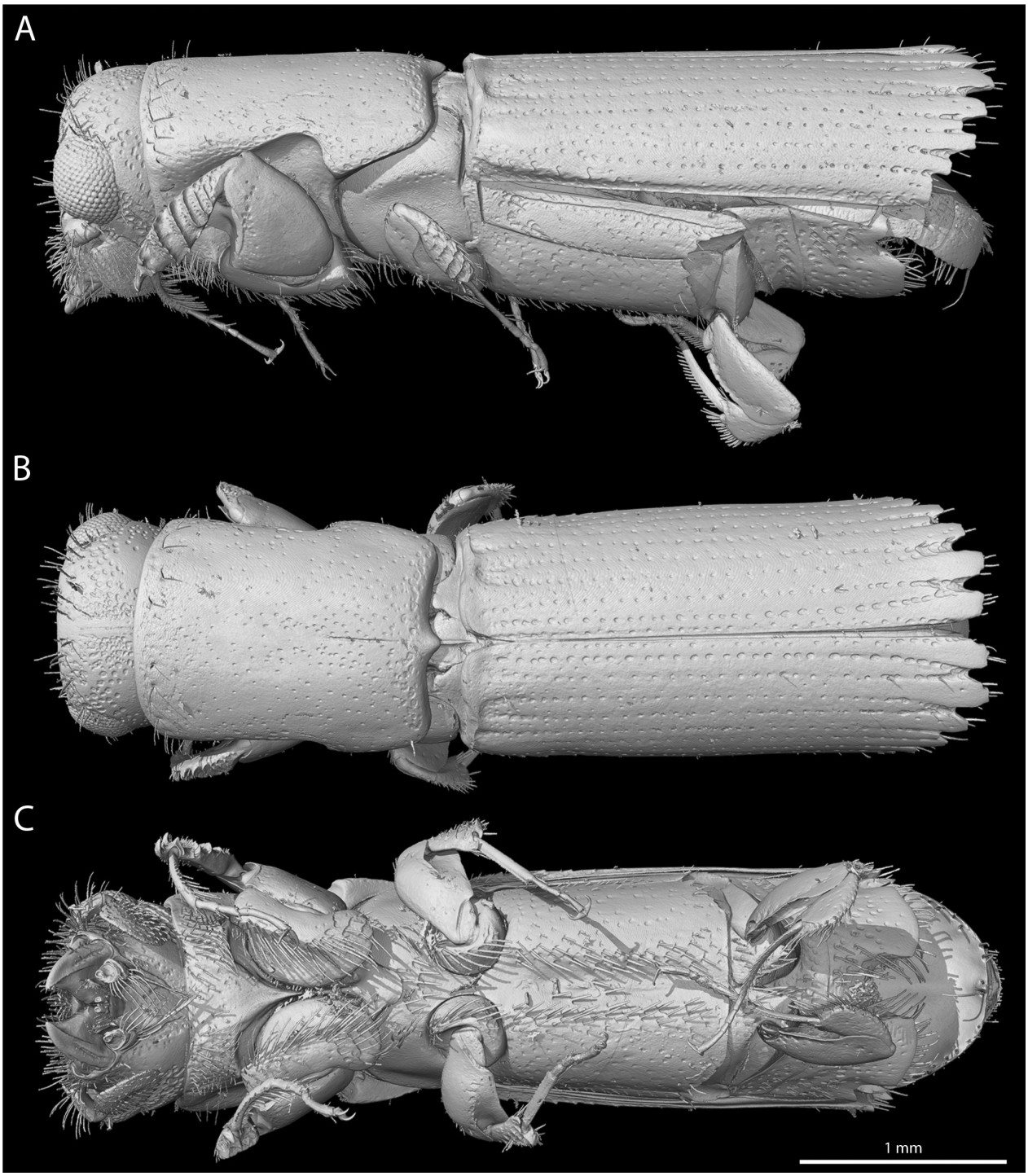

Figure 4. 3D reconstruction of *Doliopygus* cf. *serratus* (Curculionidae: Platypodinae) preserved in piece PMJ Pa 5827. **A.** Habitus lateral; **B.** Habitus dorsal; **C.** Habitus ventral.

tine. Water-vapor absorption-apparatus on hypopharynx present. Labial palps with 2 articles, the basal one short and small, the distal one large, round and flattened. Pronotum strongly reduced, barely visible dorsally as mesonotum exceeds its height. All tarsi with 3 articles. First tarsomere of hind leg very long, with 24 ventral ctenidiobothria. Claws with 1 minute preapical tooth and small ventral subapical microtrichia. Pulvilli absent. Metacoxal interlocking mechanism present. Profemur with at least 27 small spines. Tibiae with horizontal rings of brown scales. Protibia equipped with only 1 distinct apical spur. Mesotibia with 3 long apical spurs. Metatibia with 6 (3 long and 3 short) apical spurs. Unique scale patterning on forewing present, differentiating it from related species. Anteroproximal region of forewing densely covered with dark brown scales. Distal part of Sc in forewing present, closing pterostigma proximally. Rs and M connected by cross vein in forewing. Areola postica of triangular shape

and distinctly longer than high. CuP and A1 do not fuse at forewing margin. Tip of R1 vein of hindwing reaching anterior wing margin. Proximal section of Rs in hindwing absent, basiradial cell open. Hindwing with simple M vein. Conspicuous color patterning on abdomen with pale spots on darker brown patches. Clunium unmodified. Epiproct and paraproct simple, the latter with inconspicuous sensorium. Subgenital plate simple and rounded apically with long setae. T-shaped sclerite not visible. Valvulae largely hidden by subgenital plate, but all three pairs present and external valve bilobed.

Description. ***Measurements*** (in mm): Body length: 3.7. Head length: 1.4 (labrum–vertex). Head width: 1.2 (between compound eyes). Length of antennae: 2.21. Length of scape: 0.10. Length of pedicel: 0.10. Length of flagellomeres: f1 = 0.29, f2 = 0.27, f3 = 0.23, f4 = 0.26, f5 = 0.18, f6 = 0.15, f7 = 0.11, f8 = 0.12, f9 = 0.09, f10 = 0.10, f11 = 0.06, f12 = 0.09, f13 = 0.07. Length of maxillary palpomeres: I = 0.06, II = 0.24, III = 0.14, IV = 0.22. Length of thorax: 0.90. Length of forewings: 3.9. Width of forewings: 1.4 (largest width). Length of hindwings: 2.8. Width of hindwings: 1.0. Length of hindlegs: F = 0.93, T = 1.54, t1 = 1.03, t2 = 0.15, t3 = 0.15. Length of abdomen: 2.2. Length of subgenital plate: 0.78. Length of epiproct: 0.24. Length of paraproct: 0.3.

Note. Different measurements based on photos or renders result from the strong curvature of different body parts. Therefore, we used the 3D reconstructions for most measurements and the photos for measuring the length of metatarsomeres and the forewing.

Indices (measured from dorsal, after Lienhard 1998): IO/D: 1.21. PO/D: 0.73.

***Coloration*.** Head capsule dark brown. Postclypeus with few small darker spots. Labrum brown, slightly darker than rest of head. Antennal flagellum light brown to middle brown, becoming brighter distally. Maxillary palpomeres dark brown with apical regions of articles 2 and 3 lighter in coloration. Labial palpomeres light brown with dark spot on central area of flattened surface of palpomere 2. Compound eyes light brown, with darker circular areas of pigmentation. Ocelli dark brown, but median ocellus slightly brighter. Thorax slightly darker in color than head. Legs brown, less strongly pigmented apically. Forewing membrane of light brown tone, brighter towards apex. Hindwing almost hyaline, slightly more yellowish to brownish towards base. Wing veins in light brown to brownish tone or almost hyaline. Abdomen with conspicuous pattern of pale ocher patches surrounded by dark brown areas. Subgenital plate nearly uniformly dark brown, but lateral base paler. Ovipositor valves light brow with slight yellowish tint. Scales light brown to dark brown, with tips generally darker than base. Color patterns of head, compound eyes and abdomen possibly faded and with artifacts, due to non-ideal preservation in resin and subsequent suboptimal storage.

***Head capsule*.** The head is distinctly higher than wide and anteroposteriorly flattened, thus appearing almost scale shaped. In dorsal view it appears wider than long. The vertex (Figs 5A, 6B, 7A, ve) is narrow and rounded, while the frontal area is relatively large (Figs 5A, 6A, 7A, B, fr). In frontal view, the dorsal margin of the vertex is almost straight with only a very slight concave impression laterad the median line. Three ocelli (Fig. 6A, oc) are placed flat on the frons and vertex without a cuticular elevation, closer to each other than the lateral ocelli to the compound eyes. The median ocellus is slightly smaller than the lateral ones. The ovoid and relatively large compound eyes are not extending over the upper margin of the head, with a wide distance between them. The circumocular ridge (Figs 8A, B, 9, cor) is well-developed and wide, forming an oval that is slightly curved inwards on its posterior side. Externally, a conspicuous coronal sulcus (Fig. 6B, cs) is discernable, corresponding with the well-developed internal median coronal ridge (Figs 8B, 9, cr). The frontal sutures are present but indistinct. The external epistomal sulcus (Figs 5A, 6A, 7A, B, 10A, eps) is complete and semi-oval, with the postclypeus (Figs 5A, 6A, 7A, B, 10A, pcl) extending ventrally over the ventral genal margin. The large postclypeus is not strongly convex or bulging but rather scale-like. It is approximately twice as long as the frons. Two slit-like impressions begin on the ventral end of the postclypeus slightly laterad the midline and run in an acute angle approximately towards the postclypeal midlength where they obliterate. The internal epistomal ridge (Figs 8A, B, 9, epr) is wide (epistomal ridge in sagittal section longer than half of the length of the entire postclypeus, Fig. 8A, B). The anteclypeus (Figs 6A, 7A, B, 10A, acl) is relatively small and more than 4 times as wide as long, wider proximally than the ventral margin of the postclypeus and enveloping parts of it. The anterior tentorial pits (Fig. 7A, B, atp) are visible directly at the ventral margin of the epistomal ridge, almost adjacent to the anterior mandibular articulation. The posterior tentorial pits dorsad the insertion of the maxillary stipes to the head capsule are slit-like (visible in µCT scan). The well-developed tentorium is composed of large anterior (Figs 9, 11I, ata) and posterior arms (Figs 9, 11I, pta), a narrow corpotentorium (Figs 9, 11I, ct) and thin dorsal arms (Figs 9, 11I, dta). The anterior arms are anteriorly twisted and do not fuse with each other posteriorly. The very thin dorsal arms are not entirely preserved. The right dorsal arm is ending before it reaches the antennal insertion, while the left arm is almost completely missing in the specimen. The corpotentorium is compact and short and the posterior arms straight and thick. A well-developed postoccipital ridge (Fig. 9, por) and external postocciput form the posteriormost cephalic region. The head is posteriorly open, i.e., no genal-, hypostomal- or postgenal bridge or gula is developed but the posteroventral closure of the head is formed by the weakly sclerotized postmentum (Fig. 9, pom).

***Head appendages*.** The lobe-shaped labrum (Figs 6A, 7A, B, 10B, 11A, B, lb) is approximately 2-times as wide as long and covered with long setae (likely sensilla) (Fig. 10B). It is narrower at its base and apex and widest at about midlength. A median notch is missing,

and the distal margin evenly rounded. The labral nodes are absent and epipharyngeal sensilla are not visible. A median transverse epipharyngeal fold (Fig. 11B, eptf) is present on the middle region of the epipharynx. The antennal insertions are located in a fovea (Fig. 7A, B, gef), which partly separates the genal region from the frontal region. The genal area is almost twice as long as the frontal area. The internal genal ridge below the fovea is straight (Figs 8A, 9, ger) and increases in thickness posteriorly. It starts shortly behind the posterior end of the ridge enclosing the antennal foramen and ends at the posterior genal region. It corresponds externally with the straight genal sulcus (Fig. 7A, B, ges). The antennae have 15 articles. The barrel-shaped scape and pedicel are approximately as long as wide. All flagellomeres display a secondary annulation (Fig. 5F). The last flagellomere is relatively short and pointed apically. The entire flagellum is very thin and thread-like, with the flagellomeres approximately 1/3 as wide as the pedicellus. The setae on the flagellum are long and thin, slightly thicker and longer on the lateral surface compared to the medial side. The basal portion of the flagellomeres is only faintly differentiated (Fig. 5F), and a proper collar is not developed (see Seeger 1975). The mandibles (Figs 7A, B, 9, 11C, D, md) are subtriangular with similar lengths of the mesal and lateral edges. They are not elongated and of the "outer margin rounded, and posterior margin not hollowed" type (Yoshizawa 2002). The lateral edge is convex over its entire length. The molar region (Fig. 11C, D, mo) is asymmetric, with a distal molar tooth (Fig. 11C, D, mot) on the left mandible. The right mandible has a proximal tooth-like extension (Fig. 11C, D, pmdt). The inner mandibular rim has no distinct features differentiating it from mandibles of other psocids. It is thickest on its median side and becomes narrower laterad. The lateral side of the mandibular rim between the posterior condyle (Fig. 11C, D, pcmd) and anterior socket (Fig. 11C, D, asmd) (primary and secondary mandibular joints) widens. Two apical teeth (incisivi) are present, the apical one (Fig. 11C, D, inc1) longer and wider than the subapical one (Fig. 11D, inc2). Slightly proximad of the incisivi a blade-like projection is present, a convex cutting edge (Fig. 11C, D, mdce). A postmola is not discernible. The apodeme of the mandibular adductor (Fig. 9, amdad), at least partially preserved, inserts on the medial base of mandible. The maxilla lacks a cardo. The stipes (Fig. 7B, st) is oval and represents the main body of the maxilla, together with the apical palpifer (Fig. 7B, ppf). The galeae (Fig. 7A, B, ga) are relatively flat and located between the mandibular concavity anteriorly and the hypopharynx posteriorly (visible in µCT-scan). The tip of the lacinia (Figs 11F, 12I, lc) is long and bears several rounded denticles. It is bent laterad apically. The inner tine is short and bent slightly inwards distally. The outer tine is distinctly longer and higher. The lacinial gland is not preserved or not present. The maxillary palps (Figs 6A, 11E, mxp) consist of four articles. The second article is the longest, ca. 1.3 times as long as the fourth and ca. 2 times as long as the third. The first article is extremely short and only ¼ as long as the third. Several long setae (likely sensilla) are located on each palpomere except for the glabrous first one. The second maxillary palpomere lacks a conical sensillum. The fourth palpomere is conical and has a rounded apex. The hypopharynx (Fig. 9, hy) is equipped with the anterior sitophore (Figs 9, 11G, sit) and the paired posterior salivary sclerites (Figs 9, 11H, sas). A triangular median extension of the sitophore (Fig. 11G, mesit) is present proximad the mortar, which is (Fig. 11G, mor) is oval and embedded in the sitophore like in a sclerotized block. The oral arms of the sitophore are present but indistinct in the µCT-scan. The paired salivary sclerites are lateral elements of the posterior hypopharynx, ovoid and bowl-shaped. They bear a long apodeme (Fig. 11H, asas) which is long and curved inwards at its internalmost apex. A furrow runs longitudinally (Fig. 11H, lfsas) across each salivary sclerite. The tubular filaments between the sitophore and salivary sclerites are not visible (a resolution of 2 µm is not sufficient for visualizing the very thin tubular filaments, which have a diameter of ca. 3 µm in a large psocid (von Kéler 1966) and connect the longitudinal furrow of the posterior salivary sclerites with the anterior hypopharyngeal mortar), but are likely developed, as the water-vapor absorption apparatus functionally depends on their presence. The labium is composed of a thin-walled and weakly sclerotized postmentum (Fig. 9, pom) and a thicker-walled prementum (Fig. 9, prm). A median furrow separates symmetrical premental halves (see Fig. 11J). The labial palps (Fig. 11J, lap) have two articles. Palpomere 1 (Fig. 11, lap1) is short and narrow, and palpomere 2 (Fig. 11, lap2) plate-like, large and rounded, and displays a darkly pigmented field. The second palpomere bears many long setae (likely sensilla), that are concentrated on the margin. The short and rounded paraglossae (Figs 6A, 11J, pgl) are inserted between the palps. The glossae (Figs 6A, 11J, gl) are probably represented by lobe-shaped structures, almost fused medially, with only a faint medial dividing line. Remnants of soft tissue are visible in the head, which are likely vestiges of the central nervous system, retinulae and possibly the mandibular adductor muscle, as well as other cephalic muscles.

Thorax. The cervical region is not exposed. The laterocervical sclerite is indistinctly visible as a thin bar-shaped sclerite, but scarcely discernible from the cervical membrane in the renders. The prothorax is strongly reduced. The pronotum (Fig. 8A, B, prn) is very short and bar-shaped, and the propleurae (Appendix 1: Fig. A3) are continuous with it laterally. The relatively large episternum is located dorsad the small preepisternum (Appendix 1: Fig. A3) and separated from it by an external furrow (Appendix 1: Fig. A3). The mesothorax exceeds the height of the pronotum (Figs 6B, 7A, B, 8A, B). The mesonotum (Figs 6B, 7A, B, 9A, B) is strongly enlarged and dorsally densely covered with scales (Figs 5A, 6B). A prophragma is not developed or extremely reduced. The mesonotum consists of an anterior semicircular part of the scutum,

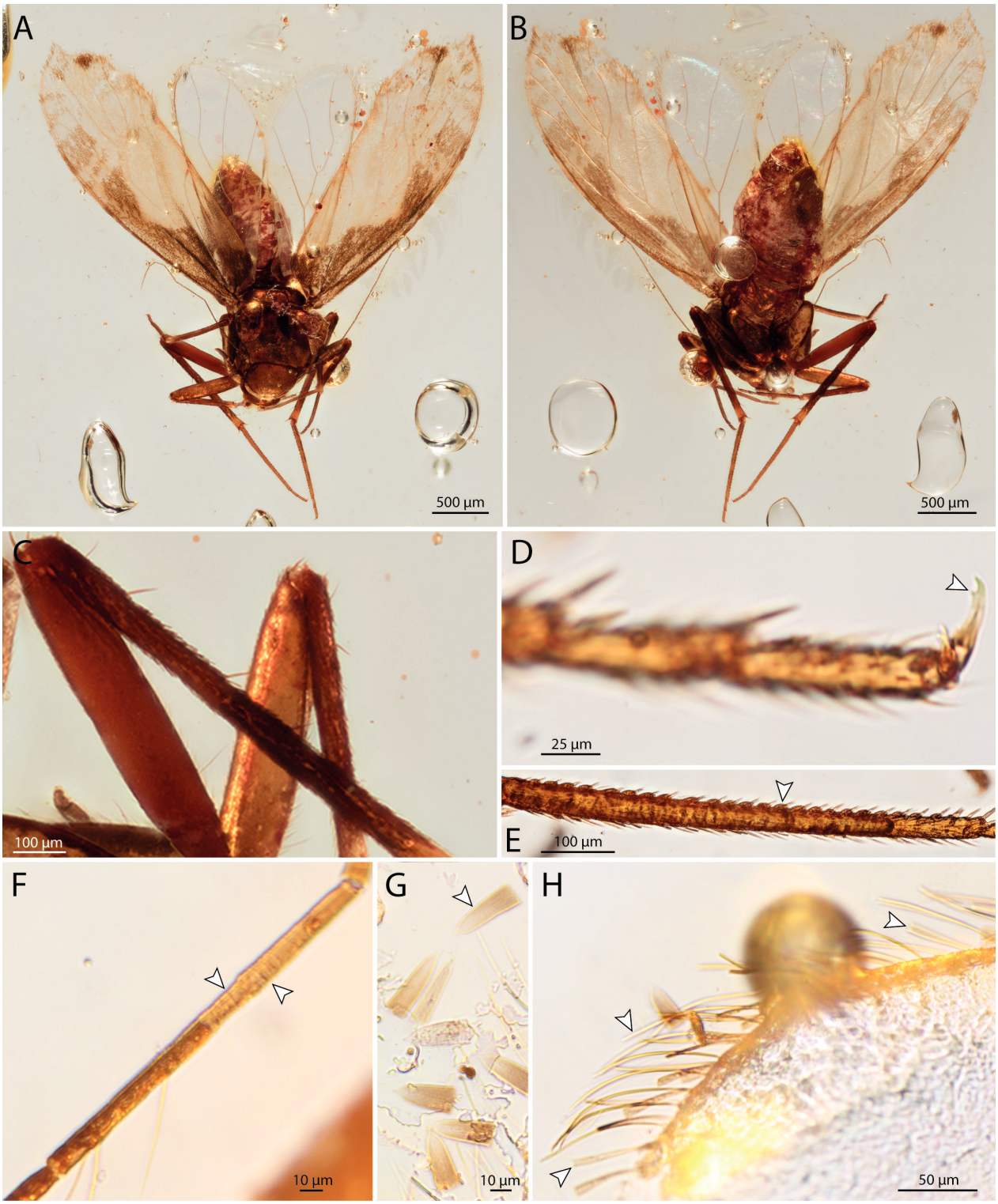

Figure 5. A–H. Photography of ‡*Amphientomum knorrei* sp. nov. preserved in piece PMJ Pa 5809. **A.** Habitus in dorsofrontal view; **B.** Habitus in ventrocaudal view; **C.** Right metafemur and -tibia in posterior view, rings of brown scales on metatibia; **D.** Distal portion of left hindleg with claw, arrow indicates preapical tooth; **E.** Basitarsomere of hindleg, arrows indicate ctenidiobothria; **F.** Right antennal flagellum, flagellomere 5, arrows indicate secondary annulation; **G.** Scales, arrow indicates scale type III; **H.** Tip of right hindwing with scales, arrows indicate scale type I and II.

larger paired lateral scutal lobes, and a posterior triangular scutellum (Fig. 6B). The anterior scutal portion is separated from the lateral lobes by the lateral parapsidial sulci (Fig. 6B), which correspond with internal parapsidial ridges (Fig. 8A, B, parr). The postnotum is located posteroventrad the scutellum as a bar-shaped short sclerite (Fig. 6B). The mesophragma (Fig. 8A, B, msp) is wide and strongly developed. The scutoscutellar suture (Fig. 6B) is present,

Figure 6. A–C. 3D-reconstruction of ‡*Amphientomum knorrei* sp. nov. **A.** Habitus in frontal view; **B.** Habitus in dorsal view; **C.** Habitus in ventral view. Abbreviations: acl = anteclypeus, cs = coronal sulcus, gl = glossa, lap = labial palp, lb = labrum, mxp = maxillary palp, oc = ocellus, pcl = postclypeus, pgl = paraglossa.

albeit somewhat weakly developed. The metathorax is distinctly shorter than the mesothorax. The anterior and lateral lobes of the scutum are not separated by an external furrow, whereas a distinct scutoscutellar line delimits the small, rounded scutellum. The metaphragma (Fig. 8A, B, mtp) is wide but smaller than the mesophragma. As the pleural elements of the specimen appear asymmetric on both sides and as there are many artifacts in the 3D-model, we will not describe this thoracic region in detail. The external sternal elements of each thoracic segment are not discernible from surrounding membranous regions. The profurcae (Fig. 8A, B, prf) are only indistinctly recognizable, whereas the meso- and metafurcae (Fig. 8A, B, msf, mtf) are distinctly visible as distally widened and

flattened arms. Spinae of the meso- and metathorax are absent. The three pairs of coxae are adjacent medially. The profemur bears at least 27 ventral spines (Fig. 10C). The protibia bears one, and the mesotibia three apical spurs. The metatibia displays three short and three long apical spurs. All tarsi are 3-segmented. Metatarsomere 1 bears 24 ctenidiobothria (Fig. 5E). Tarsomere 1 of the foreleg and hindleg are almost 3 times as long as the respective tarsomeres 2 and 3 combined. The very long metarsomere 1 reaches ca. ¾ of the length of the metatibia. Mesotarsomere 1 is approximately twice as long as mesotarsomeres 2 and 3 combined. Two apical ventral spurs are inserted on tarsomeres 1 and 2 of each pair of legs. The symmetrical claws are equipped with a single small preapical tooth (Fig. 5D) and several ventral microtrichia proximad this structure. Pulvilli are absent. The mirror and rasp substructures of the Pearman's organ are absent. A distinct ball-shaped cuticular projection (Fig. 12A, B, hcp) on the inner side of the left metacoxa is visible, fitting with a cup-shaped emargination (Fig. 12A, B, hce) on the inner side of the right metacoxa. The legs, especially the femora and tibiae, are densely covered with scales. Several closely placed somewhat irregular rings of these surface structures are inserted on the metafemur (Fig. 5C).

***Forewing*.** Wing with three types of scales. First type long, parallel-sided, straight and with a straight apex (Fig. 5H). Second type long (slightly to distinctly shorter than type one), parallel-sided to subparallel and straight, emarginate with a median notch (Fig. 5H). Third type short, broad, parallel-sided from 2/5 to apex of scale, and converging in the basal 1/5, with a straight and finely frayed apex (Fig. 5G). The wing scales display a longitudinal striation except for type I where this is not visible. The scale patterning is very distinct, with an increased density at the wing base, differentiating it from related species (Figs 5A, B). The proximal Sc vein is very short and ends freely in the wing membrane. A line of dark scales follows approximately this vein. R1 merges at 2/3 of the wing length with the anterior margin. A short and anteriorly bent distal Sc vein closes the pterostigma. This triangular cell displays a strongly acute angle between Sc and R1 and is wide (600 µm) but very low (110 µm). The base of Rs forms an obtuse angle with the distal portion of this vein. The basal vein of Rs is almost transparent, and dorsally bears a patch of dark scales. The veins R2+3 and R4+5 are convex almost over their whole length, and M1 is curved distally. M2 is almost straight. M3 is concave distally. The origins of all three M veins are placed close to each other, almost forming a fork. The specimen displays a slight asymmetry in the base of the three M veins. On the right forewing, they originate from a common stem, while M1+M2 are connected in left one but both separated from the base of M3. A conspicuous acuminate lobe is present between M1 and M2, and a short cross vein between Rs and M (90 µm). The areola postica is relatively wide and low and forms a triangle with an acute angle between CuA1 and CuA2. CuP and A1 join the posterior wing margin at a distance from each other (Fig. 10D). The course of the very faint vein A1 is almost invisible due to the coupling of the fore- and hindwing on both sides. The vein A2 is indistinct.

***Hindwing*.** Type I and II scales are present (Fig. 5H). No closed cell is present in the hindwing (Figs 5A, B). R1 and CuA are ending at approximately 2/3 of the total wing length, the former on the anterior margin and the latter on the posterior margin. Only one M vein is present. The common veins R2+3 and R4+5 are slightly shorter than half the length of M. R2+3 end anteriorly on the margin in the last 1/5 of the wing length. R4+5 ends almost directly on the wing apex, and M almost at the same length as R2+3 but on the posterior margin. Rs is bent anteriorly where it forms a cross vein with R1 in other *Amphientomum* species, but any trace of this cross vein is lacking. CuA is curved at its distal end. The distance between CuA and CuP is approximately equivalent with the length of Rs. A1 is curved and ends on the basal posterior wing margin. The margin of the apical half is covered with long scales and setae, the latter more densely anteriorly.

***Abdomen*.** The abdomen is strongly bent towards the thorax (Figs 5A, B, 7A, B). The external segmentation of the abdomen is only partially visible, as some segmental borders are very faint or deformed as an artefact. However, it seems to follow the general pattern in Psocodea (Badonnel 1934) without any conspicuous modifications. The clunium (Fig. 10E, clu), the epiproct (Figs 8B, 10E, epp) and the paraproct (Figs 8B, 10E, pap) are unmodified, the latter covered with long setae and bearing an indistinct sensorium. The apex of the subgenital plate is simple and covered by long setae. The subgenital plate largely covers the ovipositor valves, thus only the tips are exposed (Figs 5B, 6C, 7C). The external valve (Fig. 10F, exv) is bilobed, the dorsal portion wider but not as long as the ventral portion, which is pointed apically. The dorsal valve (Figs 7C, 10F, dov) is almost tubular and apically rounded. The ventral valve (Fig. 10F, vev) is barely discernible but present as an elongated tube.

Remarks. "*Die Art und Weise der Lagerung und Erhaltung der Stücke im Bernstein erlaubt den Schluß, daß diese Art wesentlich wilder und beweglicher gewesen sei als die übrigen Psocen, dabei aber zugleich weniger derb gebaut. Daß bei den sichtlich starken Anstrengungen der Thiere, dem Harz zu entgehen, das Schuppenkleid oft stark abgerieben wurde, ist leicht begreiflich und durch mitunter massenhaft danebenliegende Schuppen bewiesen. Aber auch die Endglieder der Fühler sind mitunter beim Vordrängen des Thieres abgetrennt, und die obere Membran der Flügel ist zuweilen von der offenbar fester dem Harz anhängenden unteren Membran getrennt, und beim Vordrängen des Thieres in regelmäßige kleine Querfalten gebracht.*" – Hermann Hagen's (1882) commentary about the preservation of *Amphientomum* specimens in Baltic amber.

‡*Amphientomum knorrei* Weingardt, Bock & Boudinot, sp. nov. (Troctomorpha: Amphientometae: Amphientomidae) represents the first record of this family and genus in East African copal (^{14}C date: ~390 ± 13 years

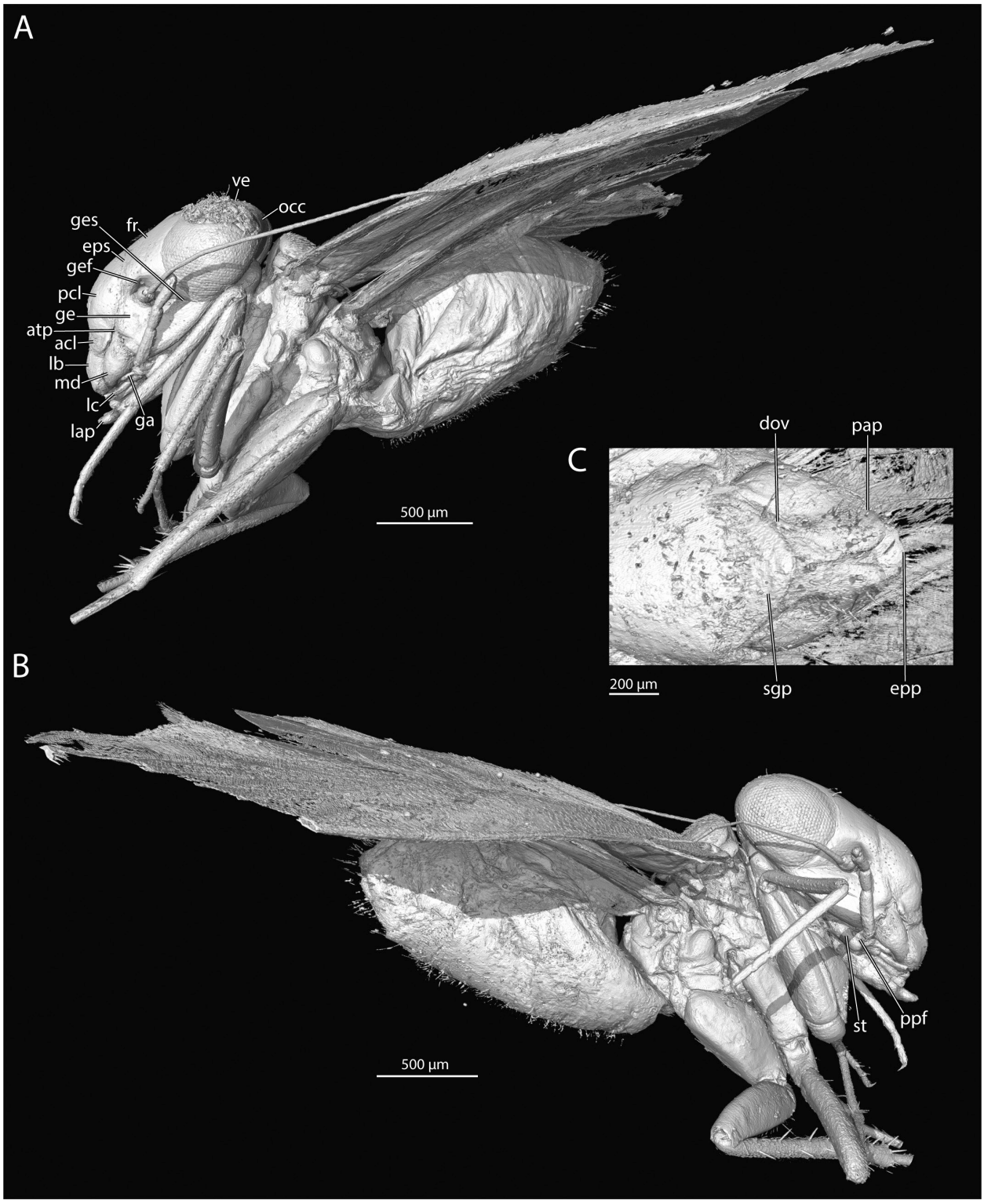

Figure 7. A–C. 3D-reconstruction of ‡*Amphientomum knorrei* sp. nov. **A.** Habitus in left lateral view; **B.** Habitus in right lateral view; **C.** Subgenital plate in ventral view. Abbreviations: acl = anteclypeus, atp = anterior tentorial pit, dov = dorsal valve, epp = epiproct, eps = epistomal sulcus, fr = frons, ga = galea, ge = gena, gef = genal fovea, ges = genal sulcus, lap = labial palp, lb = labrum, lc = lacinia, md = mandible, occ = occiput, pap = paraproct, pcl = postclypeus, ppf = palpifer, sgp = subgenital plate, st = stipes, ve = vertex.

old) and may still be extant in East Africa. The genus *Amphientomum* is known from the lowermost Eocene amber of Oise in France and is at least 56.0–47.8 Mya (Nel et al. 2005) old. In total, 20 species are described including the new one presented here (Table 5). Today they occur in countries of Western (Ivory Coast, Nigeria), Central (Angola, Republic of the Congo) and Eastern Africa (Madagascar, Tanzania) (Lienhard 2016; Johnson et al. 2023), and one additional species is described from China (Li 1999, 2002). Four species are known from the

fossil record, two, as previously listed, were described by Enderlein (1905), and one by Pictet (1854) from Baltic amber. Additionally, one species was described from French Eocene Oise amber by Nel et al. (2005). The subfossil described here is a female, as the subgenital plate and the apical tips of the valvulae are visible. It differs from all other described species of *Amphientomum* by its characteristic forewing scale pattern.

Only one species has been assigned to *Amphientomum* outside of Africa and Eurasia, *Am. indentatum* Turner, 1975, from an extant population in Jamaica. However, this species is definitely misplaced, as several features of it are not compatible with the currently accepted diagnostic character repertoire of *Amphientomum* (see Taylor 2013 for an identification key of the genera of Amphientomidae), *i.e.*, the lateral ocelli are widely spaced and close to the compound eyes, and the hind wing vein R1 does not reach the wing margin. Given these characters, the species in fact matches with *Lithoseopsis* Mockford, 1993 (Mockford 1993; Taylor 2013). Taylor (2013) proposed a smoothly rounded distal forewing margin as a diagnostic character of this genus. In contrast, *Am. indentatum* displays a characteristic indentation at the tip of the forewing, as reflected by the species name. However, the tips are not acuminate as in ‡*Am. knorrei* sp. nov., similar to other species in *Lithoseopsis* (see Taylor 2013). Based on these observations, we propose a new taxonomic combination: *Lithoseopsis indentatum* (Turner, 1975) comb. nov. By excluding *L. indentatum* from the genus *Amphientomum*, this is now restricted to the Afrotropics and Palearctic (see Table 5). The number of described species of *Lithoseopsis* is hereby increased to 12 (Johnson et al. 2023). Broadhead and Wolda (1985) mentioned the occurrence of three different species of the subgenus *Amphientomum* (*Palaeoseopsis*) in Panama. However, they remain undescribed and no details besides the collecting information are known. It is conceivable that these specimens do not belong to *Amphientomum*, similar to the previously stated case.

As the basal section of Rs is absent in the hindwing of ‡*Am. knorrei* sp. nov. (Fig. 13A), the species can be assigned to the subgenus *Amphientomum* (*Palaeoseopsis*) in the system of Roesler (1944). The shape of scales is arguably not a good diagnostic feature, as several types of scale shapes can occur in a single specimen. Emarginate scales are present in ‡*Am. knorrei* sp. nov. (type II scales, Fig. 5H), a diagnostic character of the subgenus *Am.* (*Amphientomum*) after Roesler (1944), but there are also scales with an evenly truncated (type I scales, Fig. 5H) or a frayed (type III scales, Fig. 5G) apical edge, a diagnostic criterium for *Am.* (*Palaeoseopsis*). On the other hand, Enderlein (1911) introduced evenly truncated scales as diagnostic character for *Am.* (*Amphientomum*), while scales with a median notch are characteristic for *Am.* (*Palaeoseopsis*). It is likely that Roesler (1944, p. 138) was mistaken in the characterization of both subgenera. As the polarity of the presence or absence of the basal section of Rs in the hindwing is unknown, the subgenus *Am.* (*Palaeoseopsis*) is possibly not monophyletic. All species except for †*Am. leptolepis* and †*Am. paradoxum*, both described from Baltic amber, have a reduced basal section of Rs in the hindwing (Table 5). Several species, such as *Am. loebli* and *Am. pauliani* (Table 5), also have a vestigial basal section of Rs, but it is never fused with R1. Given these problematic definitions, we synonymize *Palaeoseopsis* under *Amphientomum* syn. nov. and consequently remove the subgeneric rank from *Amphientomum* pending future study.

Table 5. All currently described species of the genus *Amphientomum*. It is uncertain whether ‡*Am. knorrei* sp. nov. is extant. The type species of *Palaeoseopsis* is bolded and that of *Amphientomum* is bolded and in cells with grey shading.

#	Taxon	Authors	Distribution
I	**†*Am. colpolepis***	**(Enderlein, 1905)**	**Baltic amber**
II	‡*Am. knorrei*	Weingardt, Bock & Boudinot, 2024 **sp. nov.**	East African copal
III	†*Am. leptolepis*	Enderlein, 1905	Baltic amber
IV	**†*Am. paradoxum***	**Pictet, 1854**	**Baltic amber**
V	†*Am. parisiense*	Nel, Prokop, De Ploeg & Millet, 2005	French Oise amber
1	*Am. acuminatum*	Smithers, 1964	Madagascar
2	*Am. Aelleni*	Badonnel, 1959	Republic of the Congo
3	*Am. annulicorne*	Badonnel, 1967	Madagascar
4	*Am. annulitibia*	Smithers, 1999	Tanzania
5	*Am. dimorphum*	Badonnel, 1967	Madagascar
6	*Am. ectostriolate*	Li, 1999	China
7	*Am. flexuosum*	Badonnel, 1955	Angola, Nigeria
8	*Am. hieroglyphicum*	Badonnel, 1967	Madagascar
9	*Am. loebli*	(Badonnel, 1979)	Ivory Coast
10	*Am. mimulum*	Badonnel, 1967	Madagascar
11	*Am. montanum*	Badonnel, 1967	Madagascar
12	*Am. pauliani*	Smithers, 1964	Madagascar
13	*Am. punctatum*	Badonnel, 1967	Madagascar
14	*Am. simile*	Badonnel, 1967	Madagascar
15	*Am. striaticeps*	Badonnel, 1967	Madagascar

Several characters of ‡*Am. knorrei* sp. nov. resemble features of *Am. acuminatum*, like the shape of the apex of the lacinia (see Fig. 12 for comparison of all available *Amphientomum* species), the apical lobe of the forewing (see Figs 13, 14 for comparison of all available *Amphientomum* species), as well as the claw with a single preapical tooth. Consequently, this species from Madagascar (Smithers 1964; Badonnel 1967) might be closely related with ‡*Am. knorrei* sp. nov. It differs from it by smaller size (body length = 2.1 mm, forewing length = 2.75 mm), the lower number of ctenidiobothria on the first tarsomere of the hindleg (21–22), the scale pattern on the forewings, and also the facial markings. As the origin of our piece of resin with the psocid inclusion is not fully clarified, the geographical distribution of ‡*Am. knorrei* sp. nov. remains uncertain. That the specimen is enclosed in East African copal imported to Germany during colonial times is suggested by several syninclusions, for instance the *Dorylus* in our present collection. The countries of origin of such pieces of resin are Tanzania, Mozambique, and

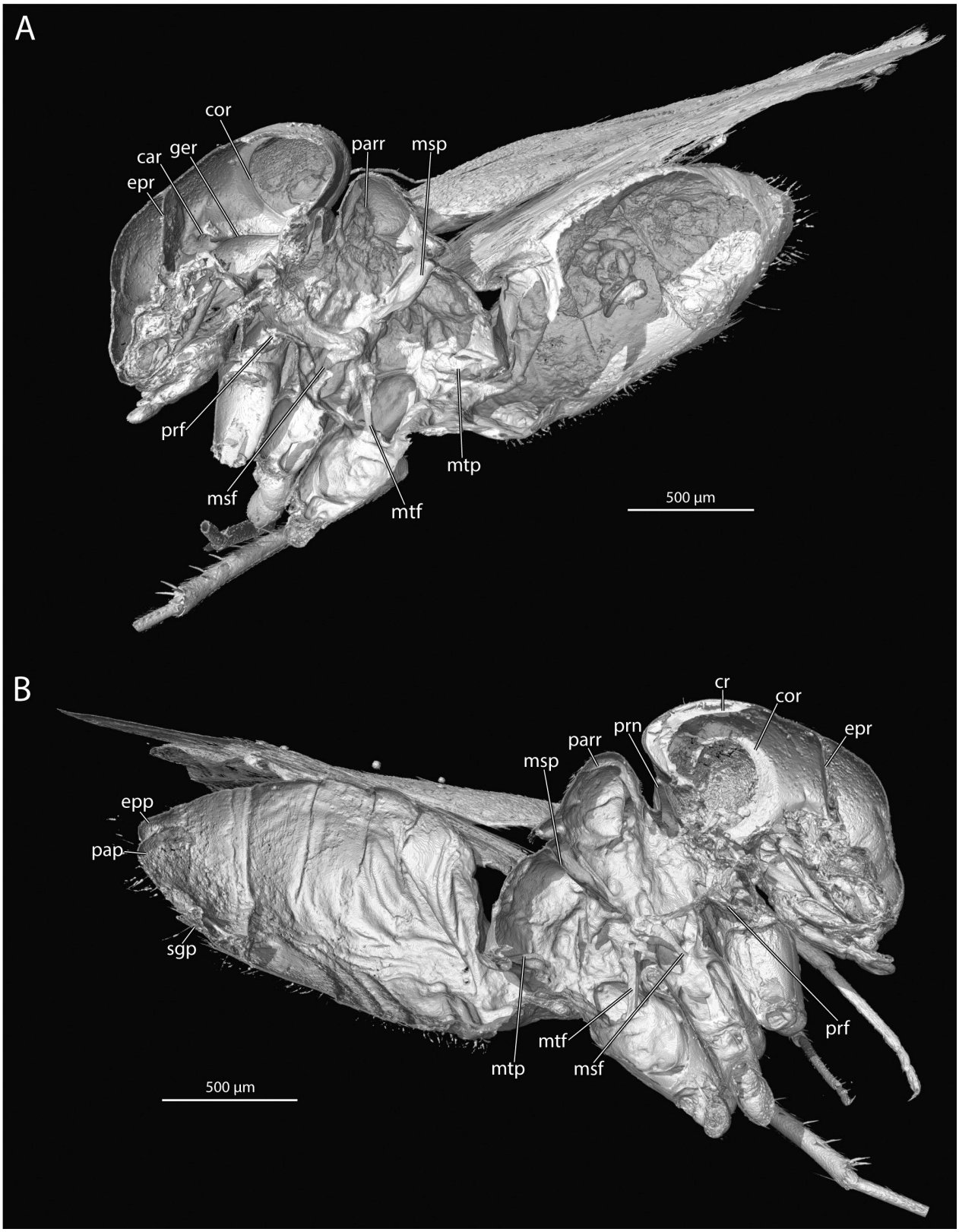

Figure 8. A–B. 3D-reconstruction of ‡*Amphientomum knorrei* sp. nov. **A.** Internal view from left side, sagittal cut; **B.** internal view from right side, sagittal cut. Abbreviations: car = circumantennal ridge, cor = circumocular ridge, cr = coronal ridge, epp = epiproct, epr = epistomal ridge, fl = foreleg, ger = genal ridge, hl = hindleg, lap = labial palp, lc = lacinia, ml = midleg, msf = mesofurca, msp = mesophragma, mtf = metafurca, mtp = metaphragma, pap = paraproct, parr = parapsidial ridge, prf = profurca, prn = pronotum, sgp = subgenital plate.

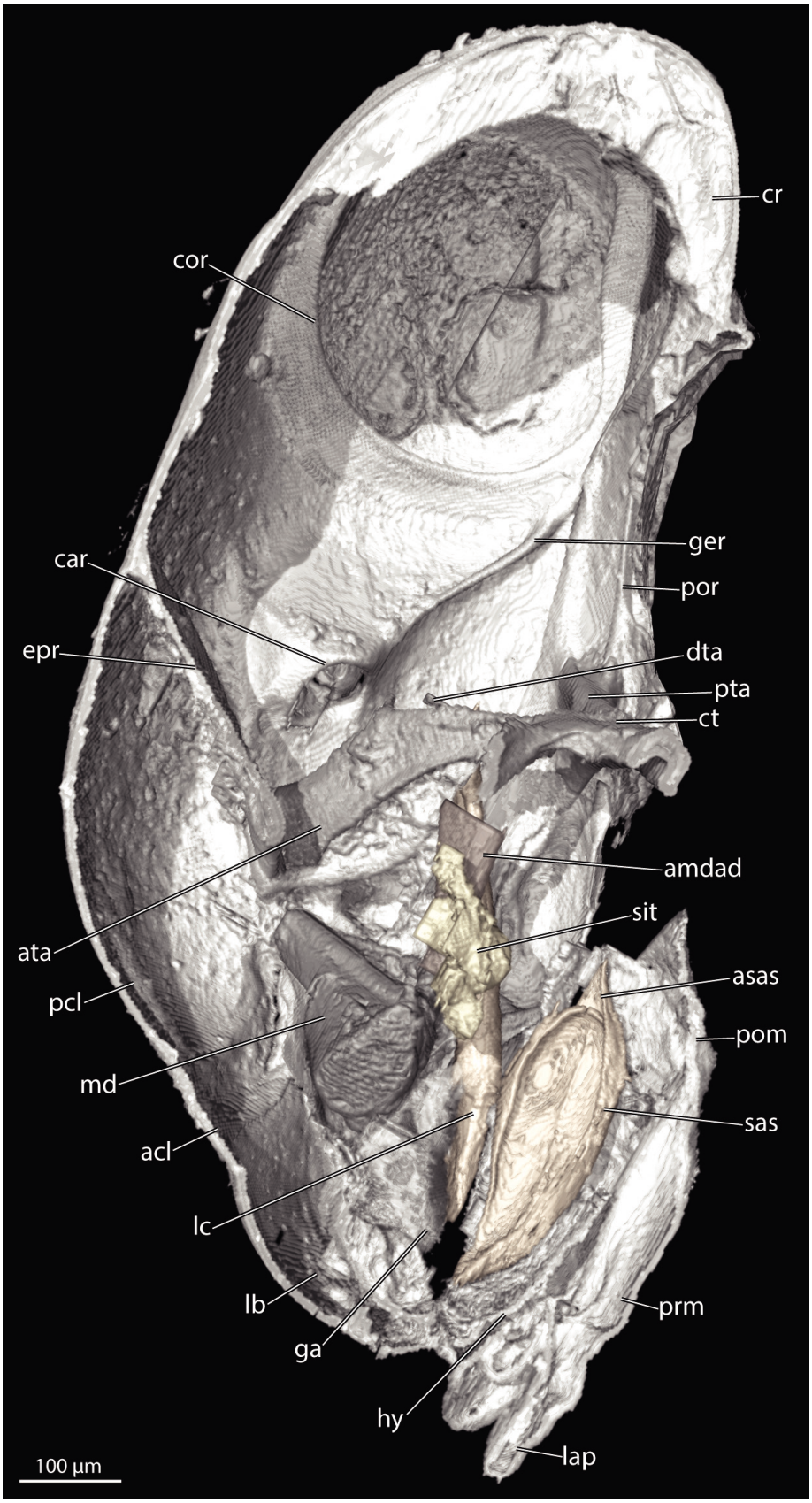

Figure 9. 3D-reconstruction of ‡*Amphientomum knorrei* sp. nov. Internal view of head from left side, sagittal cut. Abbreviations: acl = anteclypeus, amdad = apodeme of mandibular adductor, asas = apodeme of salivary sclerite, ata = anterior tentorial arm, car = circumantennal ridge, cor = circumocular ridge. cr = coronal ridge, ct = corpotentorium, dta = dorsal tentorial arm, epr = epistomal ridge, ga = galea, ger = genal ridge, hy = hypopharynx, lap = labial palp, lb = labrum, lc = lacinia, md = mandible, pcl = postclypeus, pom = postmentum, por = postoccipital ridge, prm = prementum, pta = posterior tentorial arm, sas = salivary sclerite, sit = sitophore.

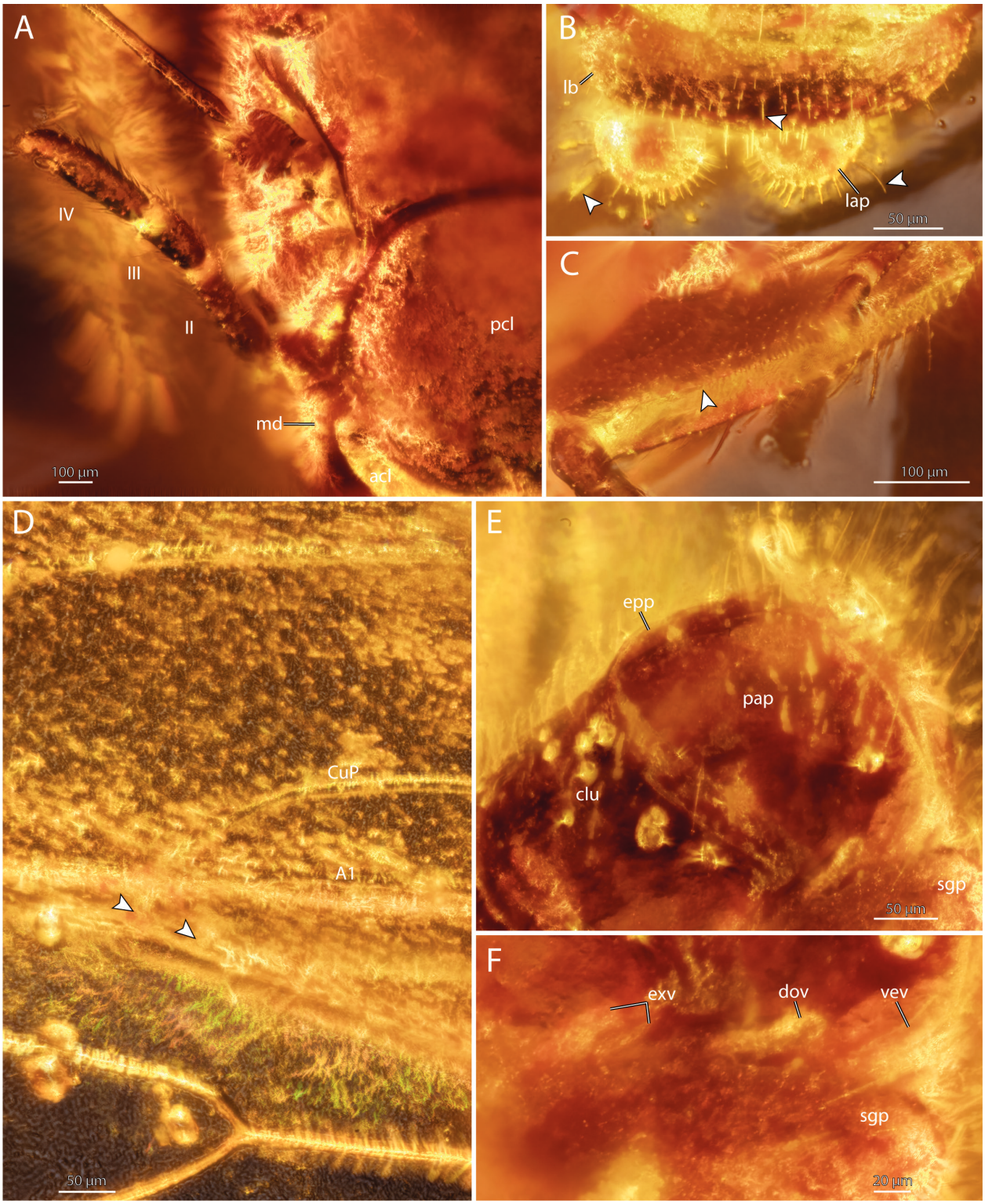

Figure 10. A–F. Photography of ‡*Amphientomum knorrei* sp. nov. **A.** Right maxillary palp and right portion of head in frontal view, numbers indicate maxillary palp article; **B.** Labrum and labial palps in dorsally inclined frontal view; **C.** Right foretibia in frontal view; **D.** Left fore- and hindwing in dorsal view, arrows indicate where the vein CuP and A1 meet the posterior forewing margin; **E.** Details of paraproct and clunium from lateral view; **F.** Details of ovipositor from ventrolateral view. Abbreviations: clu = clunium, dov = dorsal valve, epp = epiproct,. exv = external valve, lap = labial palp, lb = labrum, md = mandible, pap = paraproct, pcl = postclypeus, vev = ventral valve.

Madagascar (Delclòs Martínez et al. 2020). It is therefore likely that *Am. acuminatum* and ‡*Am. knorrei* sp. nov. have a common distribution in East Africa, while the exact distribution of both species is still unclear.

Finally, an unsolved nomenclatorial issue concerning *Amphientomum ectostriolate* Li, 1999 requires clarification. In the Psocodea Species File (Johnson et al. 2023, date: 2023 August 17) the year of publication for this species is incorrectly listed as *Am. ectostriolate* Li, 2002 and the species *Am. ectostriolatis* Li, 1999 mistakenly listed as a valid taxon. We contend that the name should be *Am. ectostriolate* Li, 1999 based on the following reasoning: (1) The protonym, *Am. ectostriolatis*, was established and illustrated in the monograph on the Chinese Psocoptera (p. 199) by Li (2002); (2) the spelling was later emended by Lienhard (2003) to *Am. ectostriolate* Li, 1999, justifiably so by Articles 19 and 34 of the ICZN (1999), with this emendation considered to be the original spelling by section 32.2; and (3) the name *Amphientomum ectostriolatum* Li, 2002 should be considered an unjustified emendation by Article 33, as the author spelled the name this way in the figure legend and twice in the text, indicating an intended name change, hence this name is available but should be a junior synonym of *Am. ectostriolate* syn. nov.

***Amphientomum ectostriolate* Li, 1999**

Am. ectostriolatis Li, 1999; original spelling; justifiably emended to *ectostriolate* by Lienhard, 2003: p. 699.

= *Am. ectostriolatum* Li, 2002 [available unjustified emendation by Li, 2002], syn. nov.

Identification key for all species of *Amphientomum* Pictet, 1854

The present key is modified after Badonnel (1967) using information from Enderlein (1911), Badonnel (1955, 1979), Smithers (1964, 1999), Li (1999, 2002), and Nel et al. (2005). Note that the species *Amphientomum aelleni* Badonnel, 1959 is excluded from the key as only the nymphal stage is described. This species, however, can be identified using an illustration of the unique coloration pattern of the head (Badonnel 1959, p. 763, fig. 1).

1 (A) Species only known from the fossil record. (B) Rs in forewing at a right angle to R1 2
– (A) Extant species or subfossil. (B) Rs in forewing at an obtuse angle (proximal angle) or almost a right angle to R1 5
2 (A) In Eocene French Oise amber. (B) Basal section of Sc in forewing long, more than half the length of R1 ..... †*Am. parisiense* Nel, Prokop, De Ploeg & Millet, 2005
– (A) In Eocene Baltic amber. (B) Basal section of Sc in forewing short, less than half the length of R1..... 3
3 (A) Scales with an apicomedial notch. (B) Basal section of Rs missing in hindwing ..... †*Am. colpolepis* Enderlein, 1905
– (A) Scales apically straight. (B) Basal section of Rs present in hindwing..... 4
4 (A) Scales short and broad, tapering proximally. (B) Tarsomere 1 of hindleg with 29–34 ctenidiobothria ..... †*Am. paradoxum* Pictet, 1854
– (A) Scales long and narrow, parallel-sided over entire length. (B) Tarsomere 1 of hindleg with 36 ctenidiobothria ..... †*Am. leptolepis* Enderlein, 1905
5(1) (A) Rs in forewing almost at right angle to R1. (B) Distributed in China ..... *Am. ectostriolate* Li, 1999
– (A) Angle between Rs and R1 in forewing distinctly obtuse (proximal angle). (B) Recorded from Africa..... 6
6 (A) Proximal half of antennal flagellum with 4 white rings separated by three black-brown rings. (B) Additionally: proximal 2/3 of femora dark brown; tibiae with three dark brown rings; forewings very wide in relation to their length, their posterior margin strongly arched in the apical half ..... *Am. annulicorne* Badonnel, 1967
– (A) Antennal flagellum almost uniformly brown, without alternating white and dark rings. (B) Other characters variable 7
7 (A) Compound eyes elevated or apparently raised above dorsal margin of vertex (frontal view) 8
– (A) Compound eyes on same level as dorsal margin of vertex (frontal view)..... 10
8 (A) Dorsal margin of vertex straight (frontal view). (B) In frontal view, lateral sides of dorsal margin curved downwards, so that compound eyes appear elevated above the rest of the dorsal margin ..... *Am. loebli* (Badonnel, 1979)
– (A) Dorsal edge of vertex distinctly concave (frontal view). (B) In frontal view, compound eyes thus strongly prominent laterally..... 9
9 (A) Legs pale. (B) Proximal halves of fore- and midfemora brown but apices pale; outer margin of proximal halves pale like distal half. (C) Hindfemora with single brown median spot. (D) Tibiae pale, with faint rings. (E) Maxillary palps pale brown, darkening distally. (F) Larger laterodorsal spots on vertex not composed of small dots ..... *Am. montanum* Badonnel, 1967
– (A) Legs dark. (B) Proximal halves of all femora with brown apices; remaining areas yellow. (D) Tibiae with three distinct brown rings. (E) Maxillary palps dark brown. (F) Larger laterodorsal spots on vertex formed by small dots ..... *Am. dimorphum* Badonnel, 1967
10 (A) Vertex and frons divided transversely by three or four parallel brown stripes, which extend across compound eyes. (B) Legs pale with few smaller brown patches..... 11
– (A) No transverse brown stripes on head. (B) Legs brown or pale with extensive brown bands..... 12

11 (A) Forewing strongly convex at level of areola postica. (B) Areola postica smaller, shorter than the next distal section of vein M. (C) Claws with one row of small spines proximad the distalmost preapical tooth ..... *Am. striaticeps* Badonnel, 1967
– (A) Forewing weakly convex at level of areola postica. (B) Areola postica larger, longer than the next distal section of vein M. (C) Claws with one row of distinct teeth proximad distalmost preapical tooth ..... *Am. simile* Badonnel, 1967
12 (A) Forewing almost uniformly brown, apical third paler. (B) Body color chocolate brown 13
– (A) Distinct patterns of contrasting light and dark patches on forewing. (B) Body color variable 14
13 (A) Forewing rounded apically. (B) Forewing posterior margin only slightly flexed distally. (C) Head brown with some diffuse spotting between compound eyes and close to ocelli. (D) Femora uniformly dark brown; scales with double striation. (E) Common base of parameres wide ..... *Am. pauliani* Smithers, 1964
– (A) Forewing apex pointed. (B) Forewing posterior margin distinctly flexuous. (C) Head uniquely patterned with series of darker dots with various size and horizontal stripes. (D) Femora dark brown on proximal 2/3 or 3/4, with yellow brown apex. (E) Common base of parameres very narrow ..... *Am. punctatum* Badonnel, 1967
14 M2 and M3 in forewing strongly curved posteriad at their apical third 15
– M2 and M3 in forewing parallel or only slightly curved 16
15 (A) Frontal area of head crossed by three distinctive transverse chocolate brown bands. (B) Anterior end of phallosome frame close to basal plate more rounded ..... *Am. flexuosum* Badonnel, 1955
– (A) Head without distinctive transverse brown bands. (B) Anterior phallosomal curvature variable .... *Am. annulitibia* Smithers, 1999
16 (A) Hindwing R1 interrupted shortly before costa. (B) Forewing without apical lobe. (C) Forewings with unique pattern: anterior and apical margin with several vertical stripes and patches of scales, and basal half almost completely covered with scales. (D) Tibiae uniformly brown ..... *Am. mimulum* Badonnel, 1967
– (A) Hindwing R1 reaches costa. (B) Forewing with apical lobe. (C) Forewings without this unique pattern. (D) Tibiae with rings of brown scales 17
17 (A) Forewing without large brown patch covering most of anal area. (B) Forewing in its apical 1/3 anteriorly with crescent shaped white patch bordered by brown area. (C) Femora not completely brown. (D) Common base of parameres wide and short ..... *Am. hieroglyphicum* Badonnel, 1967
– (A) Forewing with broad zone of dark scales from distal 1/3 of M + Cu to edge of anal area. (B) Forewing without crescent shaped white patch and brown border. (C) Femora completely brown. (D) Common base of parameres wide and fairly long (unknown for *Am. knorrei*, as no male described!) 18
18 (A) Head yellowish brown. (B) Vertex with irregular vertical lines parallel to compound eyes and coronal sulcus. (C) Metabasitarsus with 21–22 ctenidiobothria. (D) Anteroproximal region of forewing with or without sparse vestiture of scales ..... *Am. acuminatum* Smithers, 1964
– (A) Head dark brown. (B) Vertex without irregular vertical lines. (C) Metabasitarsus with 24 ctenidiobothria. (D) Anteroproximal region of forewing densely covered with dark brown scales ... ‡*Am. knorrei* Weingardt, Bock & Boudinot sp. nov.

3.3.1.3. Further considerations of *Amphientomum*

Several hypotheses on relationships between species of *Amphientomum* have been proposed. According to Badonnel (1979), *Am. flexuosum* and *Am. loebli* are sibling species (= *espèce voisine*), but differ in details of coloration, the reduction of the basal section of Rs in the forewing of *Am. loebli*, and by the presence of a sclerite of the subgenital plate in this species, which is lacking in *Am. flexuosum* (Badonnel 1979). Moreover, both species differ in size and the number of femoral spines (Badonnel 1979), but whether these differences are stable and statistically significant is presently unclear. Both species occur in West Africa and western Central Africa (Angola, Ivory Coast, Nigeria). Additionally, Smithers (1999) proposed that *Am. annulitibia* is likely closely related to *Am. flexuosum*, but noted that it differs in the shape of the anterior margin of the phallosome and in the coloration of the head.

There are few studies on the ecology and faunistics of the East African Psocodea, including for instance the family Amphientomidae (Broadhead and Richards 1982; Georgiev 2022a). One species whose description is based on a single nymph from a Congolese cave might indicate weak troglophilic tendencies (Badonnel 1959). As Badonnel (1959) already discussed, a detailed study on the morphology of nymphal stages of Amphientomidae is needed before the specimen can be reliably placed in a genus. Several genera and the subfamily Tineomorphinae can nevertheless be excluded from the list of potential taxa based on the presence of profemoral spines and the shape of the lacinia (Badonnel 1959), while the genus *Amphientomum* seems to be the most likely taxon based on the few described characters that the nymph shares with species of *Amphientomum*. Several species of the genus are known to be attracted by light traps (Badonnel 1979; Smithers 1999).

A character of special interest is the coxal interlocking device described here for the new species (Fig. 15A, B). It consists of a hemispherical outgrowth on the right metacoxa, which fits into a corresponding cavity on the opposite side. A similar device was described by Pearman (1935) for the amphientomine genera *Syllysis* and *Nephax*, but never before for a species of *Amphientomum*. It is conceivable that the interlocking device is part of a jumping mechanism, but there are no observational data for amphientomids

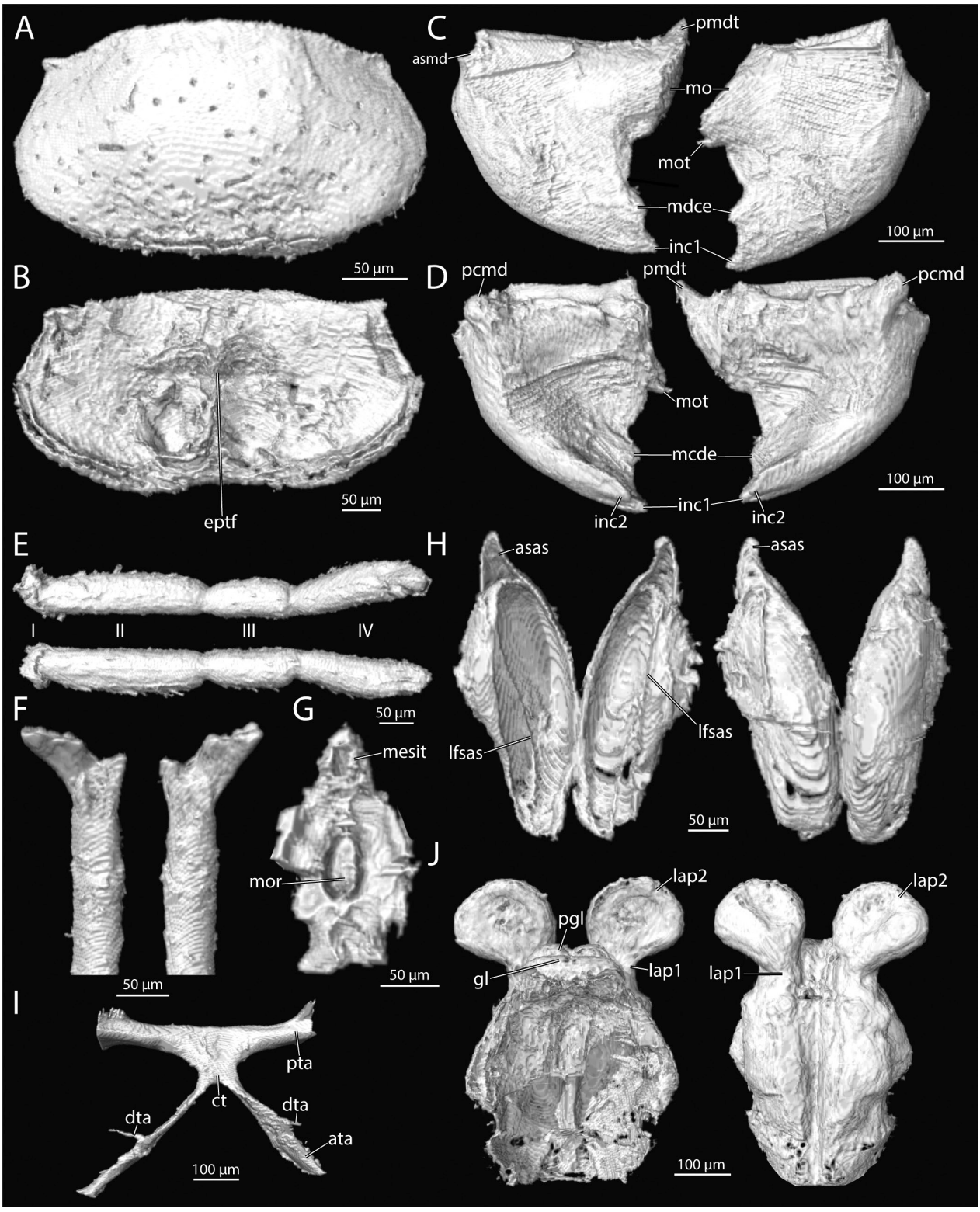

Figure 11. A–J. 3D-reconstruction of ‡*Amphientomum knorrei* sp. nov. **A.** Labrum in anterior view; **B.** Labrum in posterior view; **C.** Mandibles in anterior view; **D.** Mandibles in posterior view; **E.** Maxillary palps, top left palp, bottom right palp, numbers indicate palp article; **F.** Laciniae in anterior view; **G.** Sitophore; **H.** Salivary sclerites in anterior (right) and posterior (left) view; **I.** Tentorium in dorsal view; **J.** Labium in anterior (left) and posterior (right) view. Abbreviations: asmd = anterior socket of mandible, asas = apodeme of salivary sclerite, ata = anterior tentorial arm, ct = corpotentorium, dta = dorsal tentorial arm, eptf = epipharyngeal transverse fold, gl = glossae, inc1/2 = incisivi 1 and 2, lap1/2 = labial palp article 1 and 2, lfsas = longitudinal furrow of salivary sclerite, mdce = mandibular cutting edge, mesit = median extension of sitophore, mo = mola, mor = mortar, mot = molar tooth, pcmd = posterior condyle of mandible, pgl = paraglossa, pmdt = proximal mandibular tooth, pta = posterior tentorial arm.

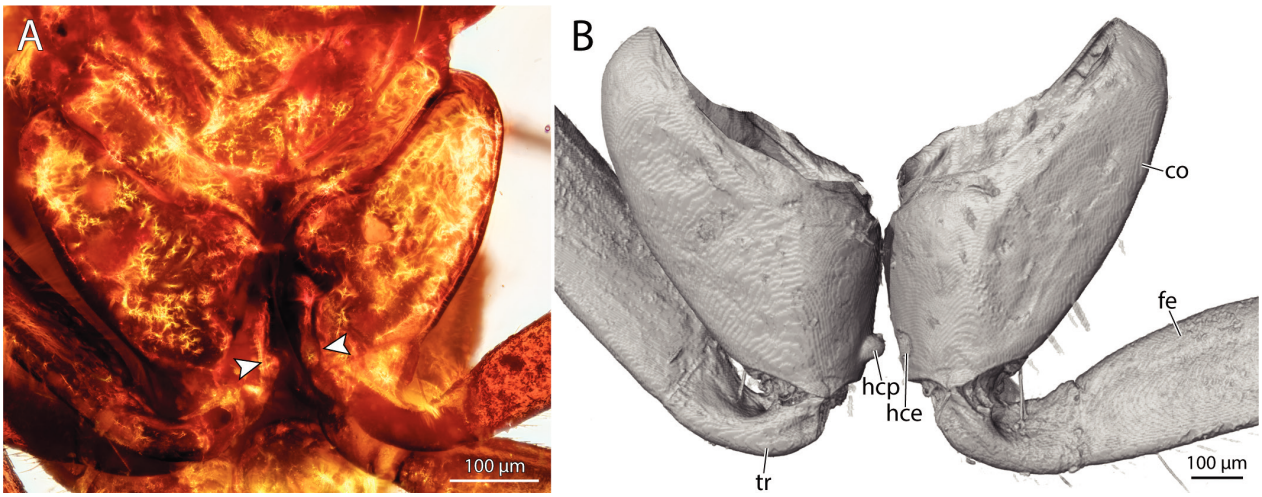

Figure 12. A. Photography of ‡*Amphientomum knorrei* sp. nov., posterior view of hindcoxae, arrows indicate the interlocking mechanism; **B.** 3D-reconstruction of ‡*Amphientomum knorrei* sp. nov., posterior view of hindcoxae. Abbreviations: co = coxa, fe = femur, hce = hindcoxal emargination, hcp = hindcoxal projection, tr = trochanter.

that would support this hypothesis. Interestingly, another interlocking device has been described for species of Lepidopsocidae, in this case on the mesocoxae but with a similar arrangement of a hemispherical protuberance on the right and a cavity on the left side, and involvement in jumping was also suggested in this case (Menon 1938; Ramesh et al. 2020). The occurrence of these devices on different segments represents a remarkable case of parallel evolution in the Psocodea. The evolutionary background still requires clarification.

A candidate homolog for the coxal interlocking devise is the Pearman's organ, a unique structure of Psocodea, which consists of a mirror and rasp on the inner side of the metacoxae in most psocids (Mockford 2018). It can be missing (e.g., Pachytroctidae, Sphaeropsocidae, and likely in Liposcelididae, where the metacoxae are distinctly separated; Yoshizawa and Lienhard 2010; Mockford 2018) or certain substructures can be reduced (e.g., Amphientomidae with only the mirror part; Weidner 1972; but see discussion above and Mockford 1993 for a different view on the presence of the rasp in the family). We were unable to observe any rasping structures on the metacoxae in ‡*Am. knorrei* sp. nov. It is possible that the structure was in fact present but is indistinct due to artifacts and the quality of preservation of our specimen. As the mirror was also not visible in the SR-µ-CT scan and photographs or using light microscopy (maximal resolution 200 ×), it appears plausible that this interlocking device represents a modification of the Pearman's organ, especially due to the functional requirement of intercoxal contact. Pearman (1935) proposed the same hypothesis on the origin of this device in other Amphientomidae. Smithers (1999) described the "tympanum" of the metacoxae of *Am. annulitibia* Smithers, 1999, with a thick and strongly raised edge but without an illustration. Nevertheless, it is conceivable that a similar structure is present in this species (described as inconspicuous by Smithers 1999), and that the device is more strongly developed in ‡*Am. knorrei* sp. nov. In any case, the device described here differs from the mesocoxal interlocking mechanism observed in Lepidopsocidae, which probably represents a non-homologous neoformation.

The lack of a robust phylogeny of Amphientomidae impedes the systematic placement of new species. As many genera are only defined by diagnostic characters and not apomorphies (e.g., Taylor 2013), the possibility of non-monophyly of these groups cannot be excluded and paraphyly may even be widespread in the family. It is therefore important for future research to establish a robust phylogeny of amphientomids, based on molecular data and morphological apomorphies. Badonnel (1967) explicitly mentioned that the use of different characters would lead to different systematic placements of his newly described species. This underlines the lack of morphological support for groupings in the family. Badonnel also commented on the minimal variability of the genitalia in *Amphientomum*, as only the basal common shaft of the parameres and the spermapore sclerite are suitable for diagnostic purposes. Mockford (2018) supported this observation, stating that external genitalia of both sexes are uniform throughout the entire amphientomids, with a y-shaped phallosome and three ovipositor valves, with a bilobed external valve (V3) fused over a part of its length with the dorsal valve (V2). The shape of the forewings can also be used as a diagnostic feature (Badonnel 1967), but sexually dimorphic wing shapes in a single species have to be considered (Badonnel 1967). The shape of the lacinia is an important diagnostic feature (Badonnel 1967) and is displayed together with the wing venation in Figs 13–15 for all species of *Amphientomum* with available data. As a phylogenetic analysis and a detailed study of type material would be beyond the scope of this study, we refrain from providing an updated diagnosis of *Amphientomum* or the subgenus *Amphientomum* (*Palaeoseopsis*). However, our study is a first step towards a phylogenetic investigation of the genus.

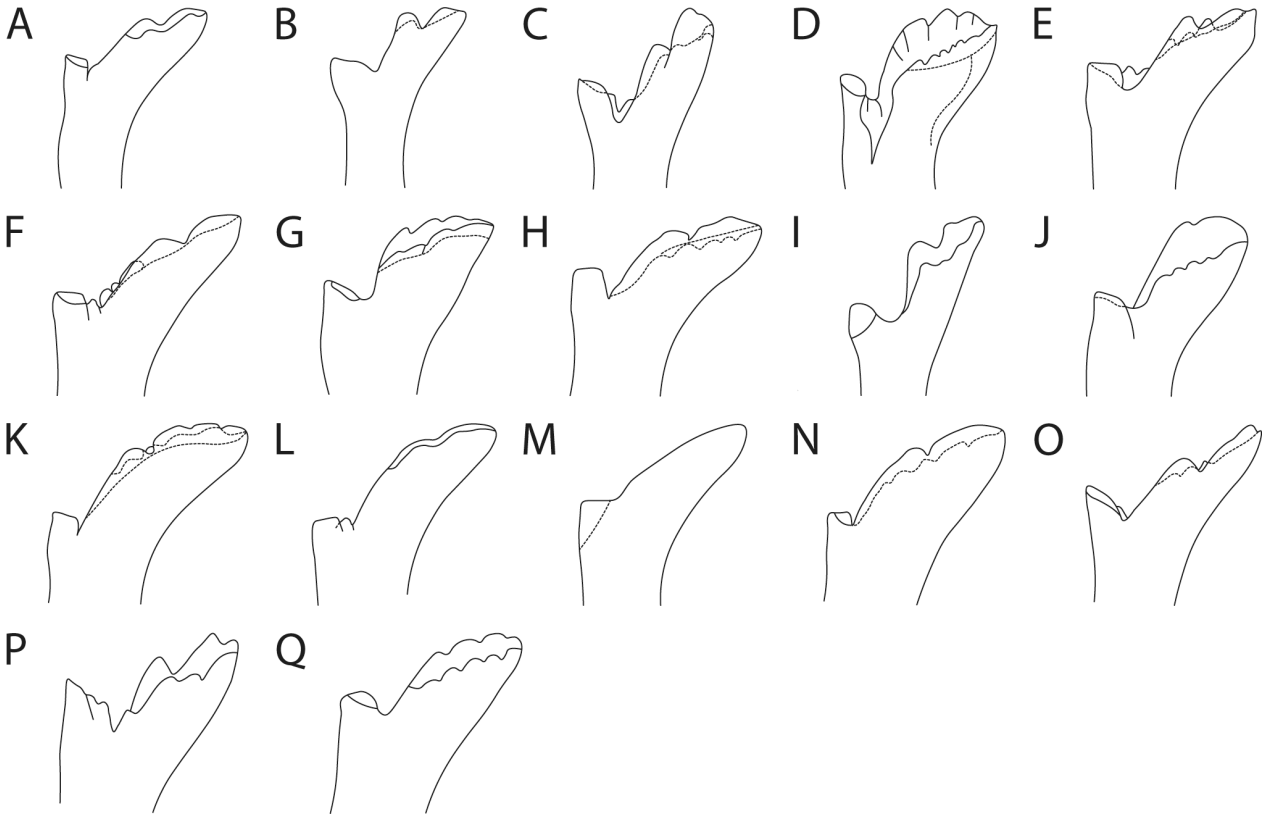

Figure 13. A–Q. Schematized drawings of all available laciniae of *Amphientomum* species from the literature and of ‡*Amphientomum knorrei* sp. nov. (Amphientomidae: Amphientominae) preserved in piece PMJ Pa 5809. The laciniae are not up to scale, and the orientation of the lacinia was flipped at 180° for **C, E, H, J–L, N–P** from the original drawings, only the apical portions of the laciniae are shown. **A.** *Am. acuminatum*, male; **B.** *Am. aelleni*, nymph; **C.** *Am. annulicorne*, female; **D.** *Am. annulitibia*; **E.** *Am. dimorphum*, sex not specified; **F.** *Am. dimorphum*, sex not specified; **G.** *Am. flexuosum*, female; **H.** *Am. hieroglyphicum*; **I.** ‡*Am. knorrei* sp. nov., female, redrawn after 3D render; **J.** *Am. loebli*, female, **K.** *Am. mimulum*, sex not specified; **L.** *Am. montanum*, female; **M.** *Am. pauliani*, male; **N.** *Am. punctatum*, male; **O.** *Am. simile*, female; **P.** *A. simile*, female; **Q.** *Am. striaticeps*, female. Figures modified from the following: **A, C, E, F, H, K, L, N, O, P, Q** after Badonnel (1967); **D** after Smithers (1999); **B** after Badonnel (1959); **G** after Badonnel (1955); **J** after Badonnel (1979); **M** after Smithers (1964).

3.3.1.4. Additional observations and remarks for Psocodea in the PMJ Pa collection

A single apterous liposcelidid trapped in the large piece of resin PMJ Pa 5827 together with many other syninclusions is slightly deformed and almost transparent (Fig. 16C). It is a nymph, as only 8 antennomeres are visible, and the specimen is only ca. 0.9 mm long. As no external metafemoral tubercle is visible, it is likely that the single specimen belongs to the subfamily Embidopsocinae. To assign it to a genus of this subfamily and to make sure that the tubercle on the metafemur is indeed absent, further trimming and cutting of the amber piece would be necessary for higher magnification. However, as many syninclusions could be affected by this we refrained from further processing. As the specimen is miniscule, we could not observe other taxonomically relevant characters (Lienhard 1991), for instance the number of tarsomeres. Even though we do not assign the specimen to a genus, we could verify that the last maxillary palpomere is conical, and not enlarged as in *Belapha* Enderlein, 1917, *Belaphopsocus* Badonnel, 1955, *Belaphotroctes* Roesler, 1943 or *Troctulus* Badonnel, 1955 (Lienhard 1991). This makes a placement in these genera unlikely.

Additionally, one single macropterous specimen of the family Archipsocidae is present in the resin piece PMJ Pa 5825 (see Figs 16A, B, 17A, B, 18A, B, Appendix 1: Fig. A4). The presence of large wings indicates that this individual is a female (Mockford 1993). As the genital region is deformed and blocked by a large air bubble, it is unclear whether ovipositor valvulae are present or not. The visible, apically flattened and very wide subgenital plate resembles the homologous structure of *Archipsocopsis* (Mockford 1993, fig. 248; Georgiev 2022b, fig. 30). The results of the FT-IR analysis (IAA) suggest that the resin containing the archipsocid belongs to a kauri-type (see SI: Report No 41995_17022023), a tree species today only occurring in New Zealand (Steward and Beveridge 2010). This suggests that the specimen might be part of the fauna of this country and the first possible record of the family in this region (Lienhard 2016). That

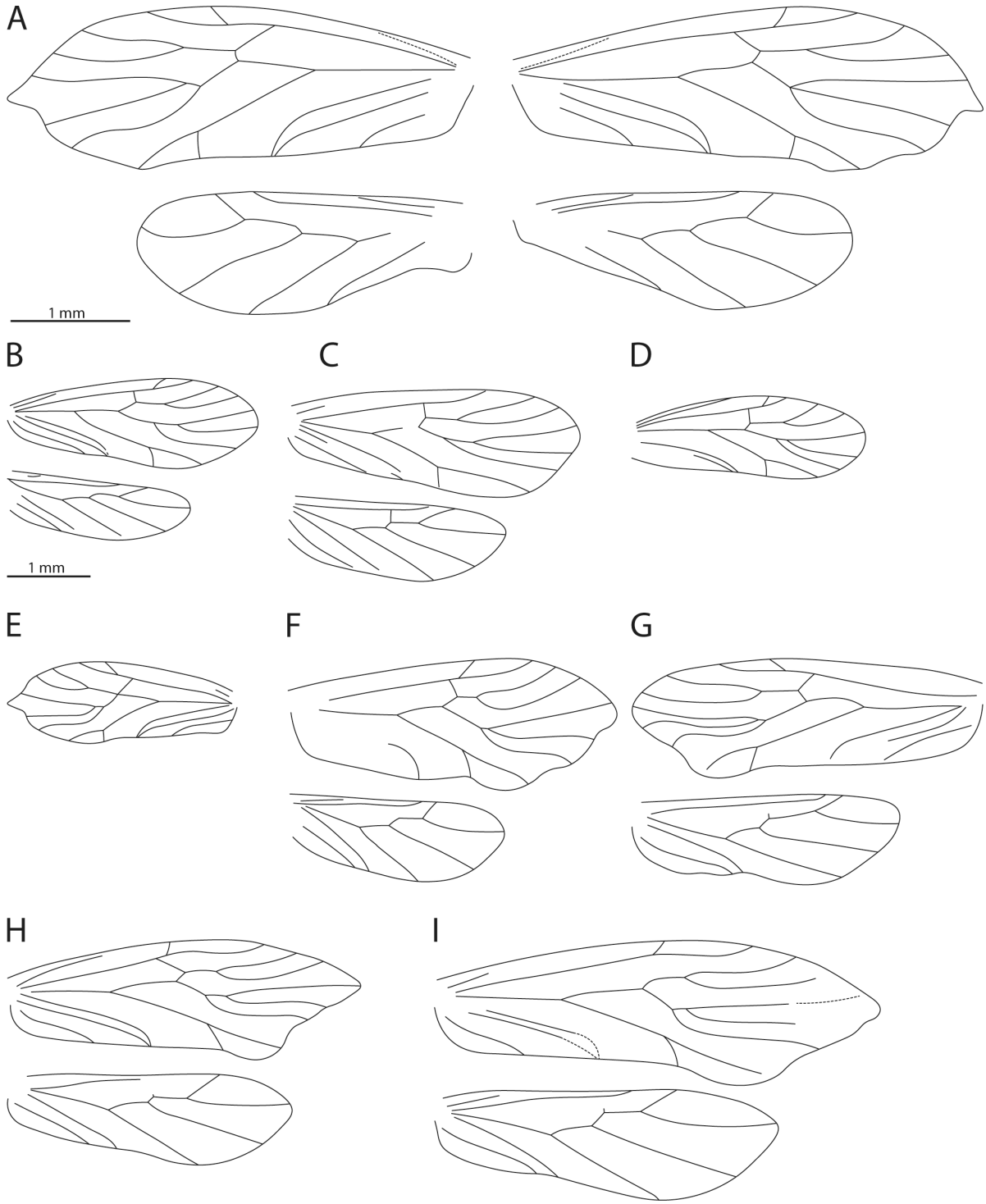

Figure 14. A–I. Schematized drawings of all available fore- and hindwings of *Amphientomum* species from the literature and of ‡*Amphientomum knorrei* sp. nov. (Amphientomidae: Amphientominae) preserved in piece PMJ Pa 5809. The same scale bar was used for **B–I. A.** ‡*Am. knorrei* sp. nov., female; **B.** †*Am. colpolepis*; **C.** †*Am. paradoxum*, female; **D.** †*Am. parisiense*; **E.** *Am. acuminatum*; **F.** *Am. annulicorne*, female; **G.** *Am. annulitibia*, male; **H.** *Am. dimorphum*, female; **I.** *Am. dimorphum*, male. Figures modified from the following: **B**, **C** after Enderlein (1911); **D** after Nel et al. (2005); **E** after Smithers (1964); **F, H, I** after Badonnel (1967); **G** after Smithers (1999).

the specimen belongs to the genus *Archipsocopsis* is tentatively suggested by the shape of the subgenital plate. As further confirmation is required, we treat it here as Archipsocidae gen. et sp. indet. We briefly characterize this specimen as follows: Female. Head large and globular, with comparatively small compound eyes. Antennae relatively short and with relatively thick flagellum. Three ocelli present but indistinct. Macropterous. Fore

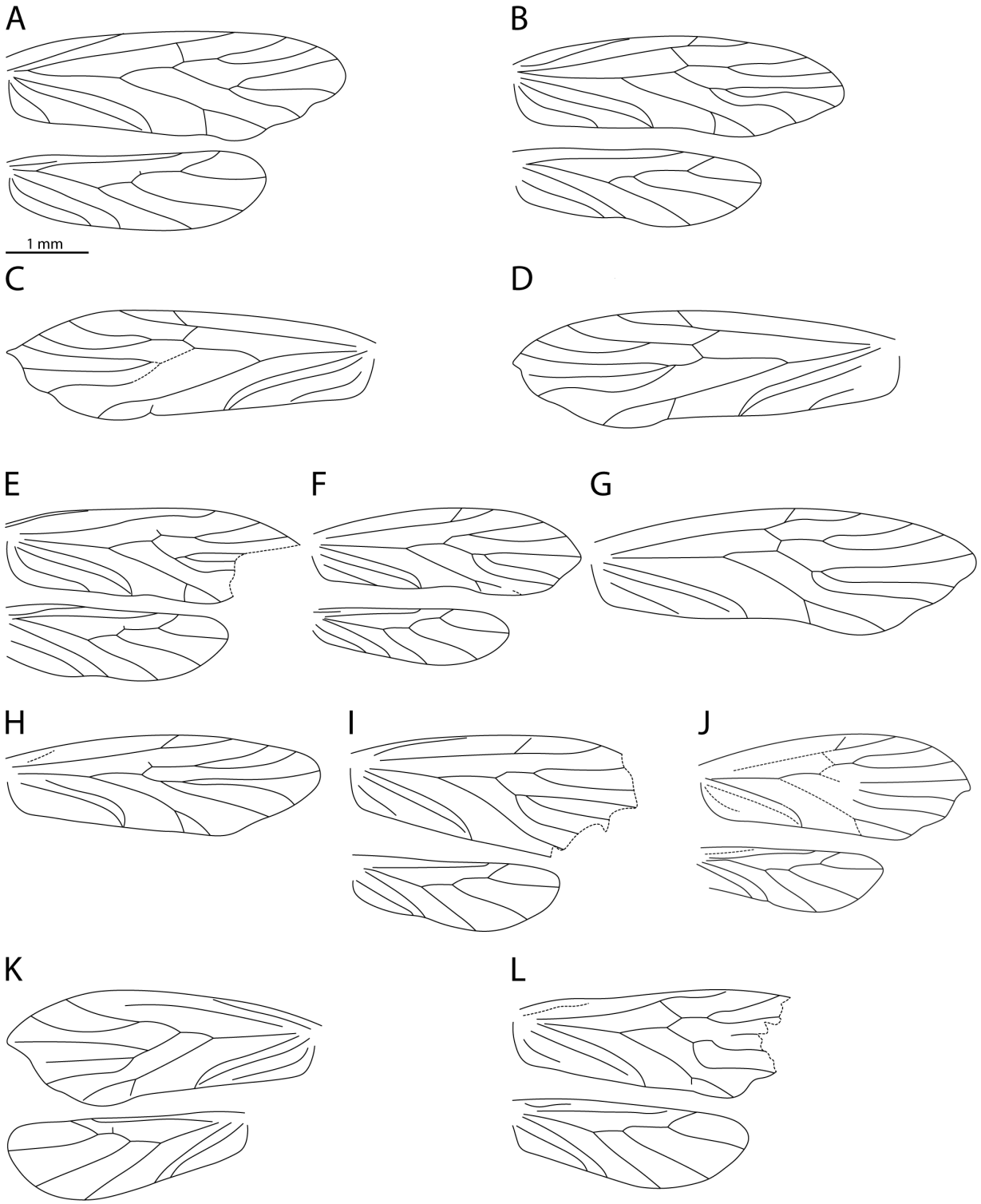

Figure 15. A–L. Schematized drawings of all available fore- and hindwings of *Amphientomum* species from the literature. The same scale bar was used for **A–L. A.** *Am. ectostriolate*, **B.** *Am. flexuosum*; **C.** *Am. hieroglyphicum*, female; **D.** *Am. hieroglyphicum*, male; **E.** *Am. loebli*, female; **F.** *Am. mimulum*, male; **G.** *Am. montanum*, female; **H.** *Am. pauliani*; **I.** *Am. punctatum*, male; **J.** *Am. punctatum*, female; **K.** *Am. simile*, female; **L.** *Am. striaticeps*, female. Figures modified from the following: **A** after Li (2002); **B** after Badonnel (1955); **C, D, F, G, I, J, K, L** after Badonnel (1967); **E** after Badonnel (1979); **H** after Smithers (1964).

wings and hind wings completely developed. Tarsi with two articles. Ovipositor seemingly entirely missing. Subgenital plate wide and flattened posteriorly. Body length: 1.46 mm. Forewing length: 1.71 mm. Hindwing length: 1.45 mm.

3.3.2. Order Hymenoptera: Subfamilial and tribal synopsis of fossil Formicidae in the PMJ Pa collection

In this section, we review the fossil record of each subfamily of ants that occurs in the Phyletisches Museum

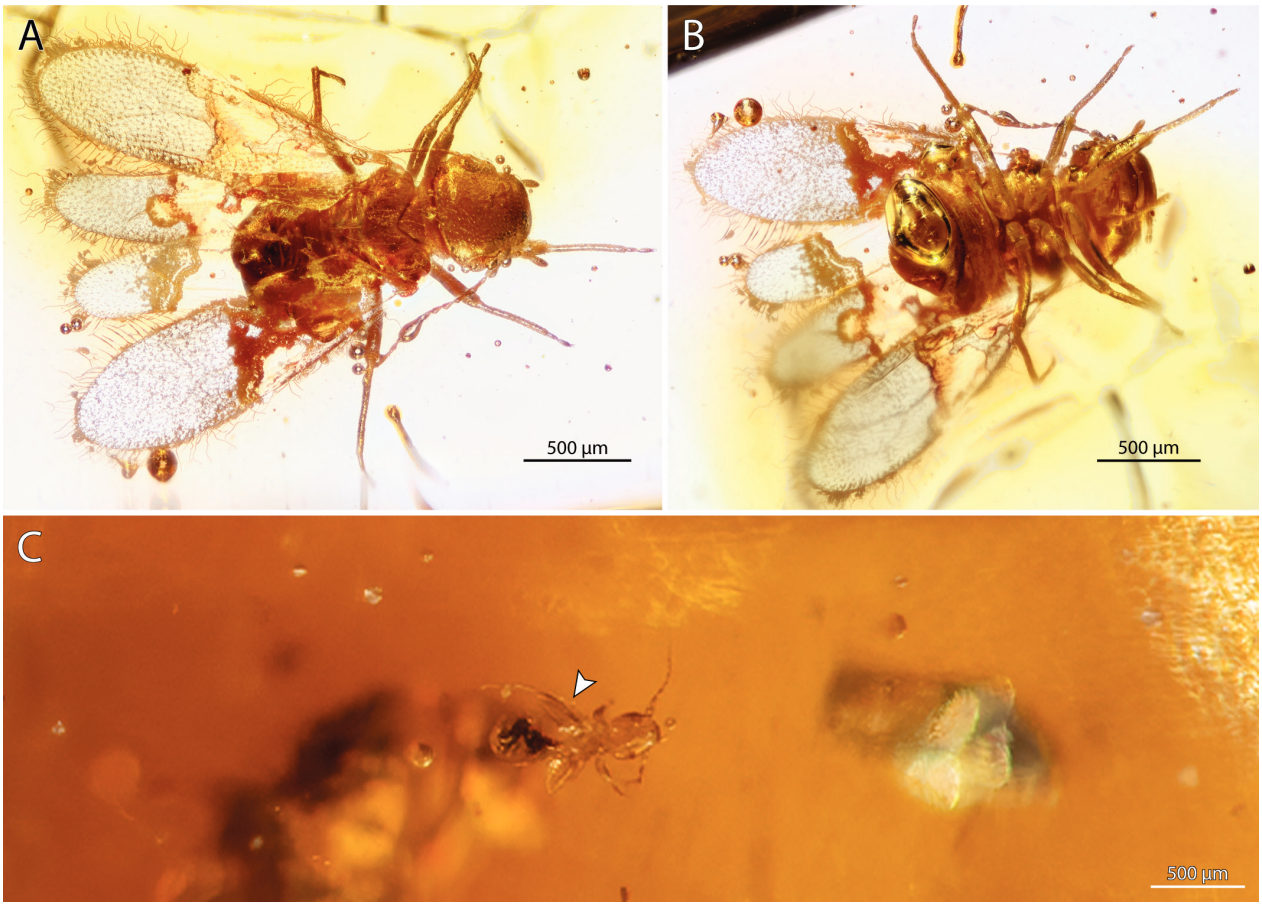

Figure 16. A, B. Photography of Archipsocidae gen. et sp. indet. preserved in piece PMJ Pa 5825. **C.** Photography of Liposcelididae gen. et sp. indet. Preserved in piece PMJ Pa 5827. **A.** Habitus in dorsal view; **B.** Habitus in ventral view; **C.** Habitus in ventral view, arrow indicates right hindfemur.

amber collection, with the exception of Formicinae, for which our review is restricted to the tribes Plagiolepidini and Camponotini. See section 3.3.1 for details about deposit and age source information.

3.3.2.1. Subfamily Dorylinae Leach, 1815
Amber fossils: Identifiable to species:
A. Baltic ambers [Eocene, 37.8–33.9 Mya].
I. Genus †*Procerapachys* Wheeler, 1915. [Note 1].
1. †*Pr. annosus* Wheeler, 1915. [w, m]. [Type species of genus].
2. †*Pr. favosus* Wheeler, 1915. [w].
3. †*Pr. sulcatus* Dlussky, 2009. [w].
B. Dominican amber [Miocene, 20.4–13.8 Mya].
II. Genus *Acanthostichus* Mayr, 1887.
5. †*A. hispaniolicus* de Andrade, 1998b. [w].
III. Genus *Cylindromyrmex* Mayr, 1870.
6. †*Cy. antillanus* de Andrade, 1998a. [q].
7. †*Cy. electrinus* de Andrade, 1998a. [q].
8. †*Cy. inopinatus* de Andrade, 1998a. [q].
IV. Genus *Neivamyrmex* Borgmeier, 1940.
9. †*N. ectopus* Wilson, 1985. [w]. [see Wilson 1985b].
Copal fossils: Identifiable to species:
C. East African copal [Holocene, 145 years based on our ^{14}C analysis; < 36 Kya more generally, based on Solórzano-Kraemer et al. 2020].
V. Genus *Dorylus* Fabricius, 1793.
10. *D. nigricans molestus* (Gerstäcker, 1859). [w]. [See section 4.2.1; Fig. 3].
D. Colombian copal [Pleistocene(?); DuBois 1998].
VI. Genus *Neivamyrmex* Borgmeier, 1940.
11. *N. iridescens* Borgmeier, 1950. [w].

Note 1. After the morphological and phylogenomic revision of the Dorylinae by Borowiec (2016, 2019), the generic identities of the species attributed to †*Procerapachys* are uncertain. Ongoing work by multiple research groups will resolve at least some of these questions. At least one specimen in the BEBC is meaningfully identifiable as *Lioponera* (unpubl. data).

3.3.2.2. Subfamily Dolichoderinae Forel, 1878
3.3.2.2.1. Genus †Yantaromyrmex Dlussky & Dubovikoff, 2013 [Note 1]
Amber fossils: Identifiable to species:
A. Baltic ambers [Eocene, 37.8–33.9 Mya].
1. †*Y. constrictus* (Mayr, 1868). [w].
2. †*Y. geinitzi* (Mayr, 1868). [w, q, m]. [Note 2].
3. †*Y. intermedius* Dlussky & Dubovikoff, 2013. [w].
4. †*Y. mayrianum* Dlussky & Dubovikoff, 2013. [w].
5. †*Y. samlandicus* (Wheeler, 1915). [w].

Note 1. †*Yantaromyrmex* is an extinct genus of ants that is endemic to ambers from Baltic sources. The genus is of unknown phylogenetic affiliation with other Dolichoderinae, although it has been hypothesized to be close to the so-called "DNAPPTOFI" clade of the Leptomyrmecini (sensu, Ward et al. 2010; Boudinot et al. 2016), more specifically, as an ancestor of the clade containing *Anonychomyrma* and *Iridomyrmex* (Dlussky and Dubovikoff 2013). Addressing this hypothesis is outside the scope of the present study, so we retain the placement of this fossil in Leptomyrmecini and note explicitly that this is an uncertain and untested relationship.

Note 2. The PMJ Pa specimen identified as †*Y. geinitzi* (PMJ Pa 5856) was identified using the key of Dlussky and Dubovikoff (2013).

3.3.2.3. Subfamily Formicinae Latreille, 1802

3.3.2.3.1. Tribe Plagiolepidini Forel, 1886

Amber and copal fossils: Identifiable to species:

I. Genus *Lepisiota* Santschi, 1926.
  A. African copal [Holocene, < 36 Kya (Solórzano-Kraemer et al. 2020)].
    1. †*Le.* cf. *canescens* [w]. [Note 1].
II. Genus *Plagiolepis* Mayr, 1861.
  B. Baltic amber [Eocene, 37.8–33.9 Mya].
    2. †*Pl. klinsmanni* Mayr, 1868. [w].
      • Wheeler, 1915: 101 (m); Dlussky, 2010a: 65 ("ergatoid" q).
    3. †*Pl. kuenowi* Mayr, 1868. [w].
      = †*Pl. balticus*: Dlussky, 2010a: 69.
      • Dlussky, 2010a: 70 (q).
    4. †*Pl. singularis* Mayr, 1868. [q].
    5. †*Pl. solitaria* Mayr, 1868. [m].
    6. †*Pl. squamifera* Mayr, 1868. [w].
    7. †*Pl. wheeleri* Dlussky, 2010. [w].
  C. Rovno amber [Ukraine; Eocene, 38.0–33.9 Mya].
    8. †*Pl. minutissima* Dlussky & Perkovsky, 2002. [m].
  D. Saxonian (Bitterfeld) amber [Germany; Eocene (Priabonian), 38.0–33.9 Mya].
    9. †*Pl. paradoxa* Dlussky, 2010. [m].
  E. Sicilian amber [Italy; Oligocene, 11.6–5.3 Mya].
    10. †*Pl. labilis* Emery, 1891. [w].
III. Genus *Acropyga* Roger, 1862.
  F. Dominican amber [Miocene, 20.4–13.8 Mya].
    11. †*Acropyga glaesaria* LaPolla, 2005. [q, m].

Species inquirendae:

II. Genus *Plagiolepis*.
  G. Uncertain [Cenozoic?].
    (1.) †*Pl. succini* André, 1895. [Note 2].

Note 1. This specimen (PMJ Pa 5807) may be the first fossil or sub-fossil *Lepisiota* recorded to date. The specimen is dark, has the bituberculate form of the propodeum associated with *L. canescens*, and lacks spines on the petiolar node. *Lepisiota* is also the third genus (of nine) from the Plagiolepidini to be recovered from fossil-bearing sediments, the other two being *Acropyga* and *Plagiolepis*. Ants of this tribe were formerly lumped with the *Prenolepis* genus group of the Lasiini (see Bolton 2003; Boudinot et al. 2022a).

Note 2. As reported by Dlussky (2010a, b), there is considerable uncertainty about the generic identity and geological origin of the fossil(s) described as †*Pl. succini* by André (1895). In André's own words (paraphrased, p. 83), "despite its great size for [*Plagiolepis*], this species resembles [*Anoplolepis*] *custodiens* [F. Smith]", with the following diagnostic note (also paraphrased): "but it is distinguished by its size and the thicker and less elongate antennae". Dlussky (2010a, b) was unable to find the specimen(s) originally described by André and speculated that the taxon may be from East African copal, *i.e.*, misidentified as Baltic amber. This species should, therefore, be continued to be considered of uncertain status until the original or additional material becomes available.

3.3.2.3.2. Tribe Camponotini Forel, 1878

Overview. The Camponotini is a comparatively diverse tribe of Formicinae with > 1950 valid species attributed to eight extant genera (Bolton 2023), which have received revisionary attention subsequent to the major phylogenomic study of Blaimer et al. (2015) (see Ward et al. 2016; Ward and Boudinot 2021). Because this clade represents a major radiation of ants (e.g., Rafiqi et al. 2020), fossils are particularly important for understanding and modeling the tempo and mode of formicine evolution. The diversity of fossils attributed to this tribe, moreover, necessitates this overview. Prior to the present study, Camponotini contained two monotypic and valid fossil genera (†*Chimaeromyrma brachycephala* Dlussky, 1988, †*Pseudocamponotus elkoanus* Carpenter, 1930), one monotypic fossil genus that is a synonym of *Camponotus* Mayr, 1861 (†*Palaeosminthurus juliae* Pierce & Gibron, 1962), one fossil species attributed to *Polyrhachis* (†*Po. annosus* Wappler et al., 2009), and 29 valid and 5 invalid fossil species placed in *Camponotus* itself (Bolton 2023).

Based on our assessment of all 38 of these fossil species plus the three species attributed to the *Camponotus*-like form taxon †*Camponotites* Steinbach, 1967, we propose the following revision to the fossil record of Camponotini below. In brief, we transfer one species out of the subfamily Formicinae to *Liometopum* (I), we recognize one as-yet unidentified copal specimen of *Camponotus* (II) and one fossil species of *Polyrhachis* (III), we leave †*Chimaeromyrma* and †*Pseudocamponotus incertae sedis* in Camponotini (IV, VII), we transfer one Baltic fossil species from *Camponotus* to †*Eocamponotus* gen. nov. (V), we revive †*Palaeosminthurus* and consider it unidentifiable while transferring it out of Camponotini as *incertae sedis* in Formicinae (VI), and finally, we transfer 29 fossil species from *Camponotus* to the form genus †*Camponotites*, which we treat as a catch-all that is *incertae sedis* in Camponotini (VIII). We also provide detailed annotations for our synopsis of fossil Camponotini (see the "Notes").

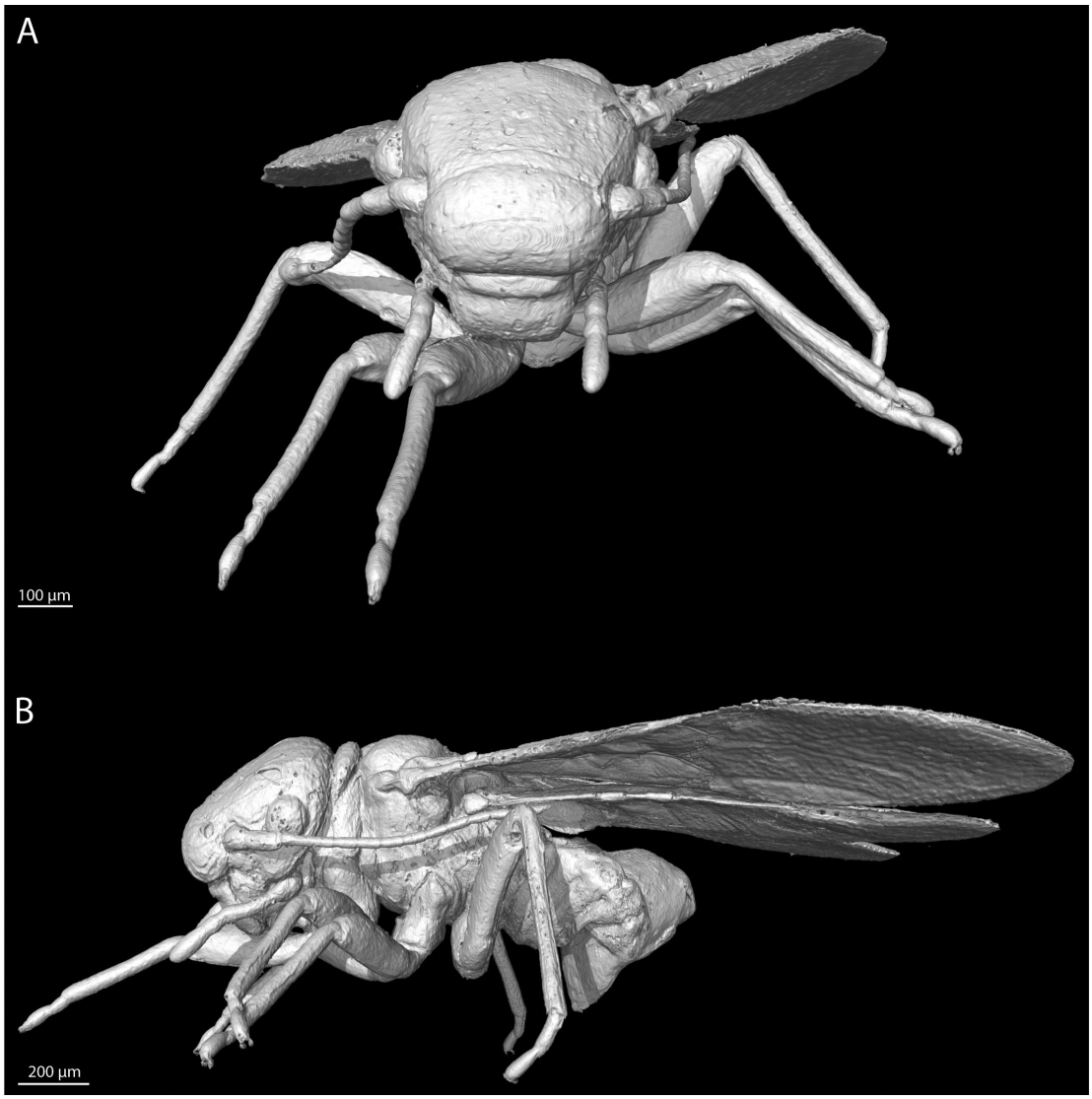

Figure 17. A, B. 3D-reconstruction of Archipsocidae gen. et sp. indet. **A.** Habitus in frontal view; **B.** Habitus in lateral view.

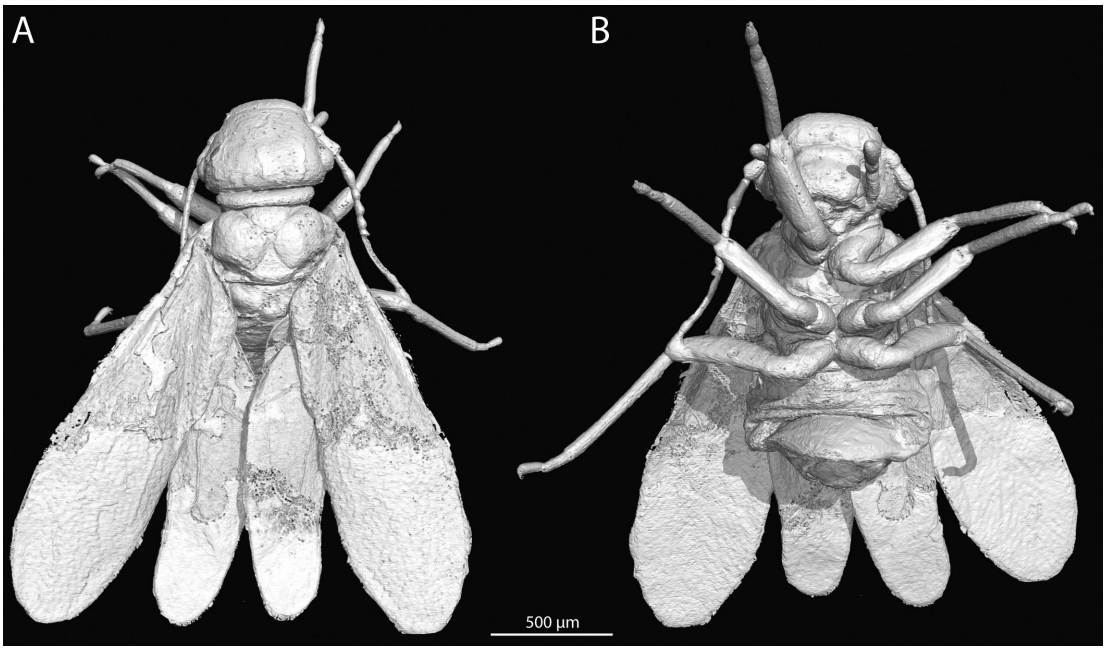

Figure 18. A, B. 3D-reconstruction of Archipsocidae gen. et sp. indet. **A.** Habitus in dorsal view; **B.** Habitus in ventral view.

Finally, we point out that all future studies on fossils that may possibly be associated with *Camponotus* or Camponotini should critically evaluate the morphological evidence for placement in any of the extant genera particularly in reference to Ward et al. (2016) for workers and Ward and Boudinot (2021) for workers and alates (the wing venation characters apply equally to males and queens). A recent work which ignored these studies is Takahashi and Aiba (2023), which misidentified multiple specimens as *Camponotus*. If a species name must be given to a fossil that cannot be placed in any of the extant genera of Camponotini based on synapomorphies, we strongly encourage authors to place these fossils in the form genus †*Camponotites* so that uncertainty is explicitly recognized and to prevent the propagation of errors in macroevolutionary analysis.

I. Transferred to *Liometopum* (Dolichoderinae):
Compression fossil:
A. Shanwang formation [China, Linqu County; Miocene (Burdigalian), 20.4–16.0 Mya].
a. *Liometopum* Mayr, 1861.
= †*Shanwangella* Zhang, 1989. Syn. nov.
(1.) †*L. palaeopterum* (Zhang, 1989). Comb. nov. [q]. [Note 1].
= †*S. palaeoptera* Zhang, 1989.
• Combination in *Camponotus*: Hong and Wu 2000: 19.

II. Genus *Camponotus* Mayr, 1861, subgenus indet. [Note 2].
Copal fossil: Identifiable to species:
B. East African copal [Holocene, < 36 Kya (Solórzano-Kraemer et al. 2020)].
1. *Ca.* sp. THIS STUDY. [w]. [Note 3].

III. Genus *Polyrhachis* Smith, F., 1857.
Compression fossil:
C. Varvara formation [Miocene, 7.2–5.3 Mya].
1. †*Po. annosus* Wappler et al., 2009. [Note 4].

IV. Genus †*Chimaeromyrma* Dlussky, 1988, *incertae sedis* in tribe.
Amber fossil:
D. Sakhalin amber [Eocene, 47.8–41.3 Mya].
1. †*Ch. brachycephala* Dlussky, 1988. [Note 5].

V. Genus †*Eocamponotus* Boudinot, gen. nov. [Note 6].
Type species: †*Eo. mengei* (Mayr, 1868) by original designation.
Amber fossils: Identifiable to species:
E. Baltic ambers [Eocene, 37.8–33.9 Mya].
1. †*Eo. mengei* (Mayr, 1868). [w]. Comb. nov. [Note 7].
= †*Eo. igneus* (Mayr, 1868). Comb nov.
• Synonymized by Wheeler (1915): 138.

VI. Genus †*Palaeosminthurus* Pierce & Gibron, 1962 stat. rev., *incertae sedis* in Formicinae, unidentifiable hence invalid stat. nov.:
Phosphatized fossil:
F. Barstow formation, Calico member [USA, California; Miocene (Hemingfordian), 20.4–16.0 Mya].
(–.) †*Pa. juliae* Pierce & Gibron, 1962. [m]. Comb. rev.; unidentifiable, hence invalid, stat. nov. [Note 8].
= Formerly unresolved junior homonym of *Camponotus juliae* Emery, 1903.
• Transferred to Formicidae: Najt, 1987: 152.
• Status as species: Bolton, 1995b: 311.
• Transferred to *Camponotus*: Snelling, R.R. pers. comm. to Bolton, B. 2004, in Bolton (2023).

VII. Genus †*Pseudocamponotus* Carpenter, 1930, *incertae sedis* in tribe, unidentifiable hence invalid stat. nov.
Compression fossil:
G. Elko formation [Eocene, 37.2–28.4 Mya].
(–.) †*Ps. elkoanus* Carpenter, 1930. [q]. Unidentifiable, hence invalid, stat. nov. [Note 5].

VIII. Genus †*Camponotites* Steinbach, 1967, *incertae sedis* in Formicinae. [Note 9].
Amber fossil: Unidentifiable at neontological genus level:
H. Fushun amber [China, Liaoning, Jijuntun formation; Eocene (Lutetian), 47.8–41.3 Mya].
(1.) †*Ctt. tokunagai* (Naora, 1933). [q?]. Comb. nov. [Note 10].
Compression fossils: Unidentifiable at neontological genus level: [Note 11].
I. Green River formation [USA, Colorado; Eocene, 50.3–46.2 Mya].
(2.) †*Ctt. vetus* (Scudder, 1877). [q?]. Comb. nov. [Note 12].
J. Bouldnor formation, Bembridge Marls member [Great Britain; Eocene (Priabonian), 38.0–33.9 Mya].
(3.) †*Ctt. cockerelli* (Donisthorpe, 1920). [m]. Comb. nov.
= †*Leucotaphus cockerelli* Donisthorpe, 1920.
• Combination in *Camponotus*: Dlussky and Perfilieva 2014: 417.
K. Florissant formation [USA, Colorado; Eocene, 37.9–33.9 Mya].
(4.) †*Ctt. fuscipennis* (Carpenter, 1930). [q]. Comb. nov.
(5.) †*Ctt. microcephalus* (Carpenter, 1930). [q]. [Note 13]. Comb. nov.
(6.) †*Ctt. petrifactus* (Carpenter, 1930). [w]. Comb. nov.
L. Brunstatt, horizon d2 [France; Early Oligocene, 33.9–28.4 Mya].
(7.) †*Ctt. compactus* (Förster, 1891). [q]. Comb. nov.
(8.) †*Ctt. vehemens* (Förster, 1891). [m]. Comb. nov.
• Théobald, 1937: 218 (w, q, m).
= Senior synonym of †*Ca. miserabilis* Förster, 1891: Théobald, 1937: 218.
M. Creek near Bechlejovice [Czechia; Oligocene (Rupelian), 33.9–28.1].
(9.) †*Ctt. novotnyi* (Samšińák, 1967). [q]. Comb. nov.
N. Rott formation [Germany, Orsberg; Oligocene: 28.4–23.0 Mya].
(10.) †*Ctt. lignitus* (Germar, 1837). [q]. Comb. nov.
= †*Formica lignitum* Germar, 1837.
• Combination in *Camponotus*: Mayr, 1867: 51.

O. Niveau du gypse d'Aix Formation [France; Oligocene (Chattian), 28.1–23.0 Mya].
(11.) †*Ctt. longiventris* (Théobald, 1937. [q, m]. Comb. nov.
(12.) †*Ctt. theobaldi* (Özdikmen, 2010). [m]. Comb. nov.
• Replacement name for †*Ca. saussurei* Théobald, 1937.
(13.) †*Ctt. penninervis* (Théobald, 1937). [m]. Comb. nov.

A. Shanwang formation (see above).
(14.) †*Ctt. ambon* (Zhang, 1989). [q?]. Comb. nov.
(15.) †*Ctt. ampullosus* (Zhang, 1989). [q?]. Comb. nov.
(16.) †*Ctt. curviansatus* (Zhang, 1989). [q]. Comb. nov.
(17.) †*Ctt. gracilis* (Zhang, 1989). [m?]. Comb. nov.
(18.) †*Ctt. longus* (Zhang, 1989). [q]. Comb. nov.
(19.) †*Ctt. microthoracus* (Zhang, 1989). [q]. Comb. nov.
(20.) †*Ctt. plenus* (Zhang, 1989). [q]. Comb. nov.
(21.) †*Ctt. shanwangensis* (Hong, 1984). [q]. Comb. nov.
(22.) †*Ctt. pictus* (Zhang et al., 1994) [q]. [Note 14]. Comb. nov. • Previously junior primary homonym of *Ca. ligniperda pictus* Forel, 1886.
(23.) †*Ctt. xiejiaheensis* (Hong, 1984). [m]. Comb. nov.
• TYPE SPECIES of †*Rabidia* Hong, 1984.
• Combination in *Oecophylla*: Zhang, 1989: 297.
• Combination in †*Camponotites* Dlussky et al., 2008: 616.

P. Radoboj [Croatia; Miocene (Sarmatian), 12.7–11.6 Mya].
(24.) †*Ctt. heracleus* (Heer, 1849). [m]. Comb. nov. = †*Formica heraclea* Heer, 1849.
• Combination in *Camponotus*: Mayr, 1867: 52.
• Also described as new by Heer, 1850: 116.
(25.) †*Ctt. induratus* (Heer, 1849). [m]. Comb. nov. = †*Formica indurate* Heer, 1849.
• Dlussky and Putyatina 2014: 249 (m, q).
• Combination in *Camponotus*: Mayr, 1867: 52.
• Also described as new by Heer, 1850: 116.
(26.) †*Ctt. oeningensis* (Heer, 1849). [q]. Comb. nov. = †*Formica obesa oeningensis* Heer, 1849.
• Combination in *Camponotus* and raised to species: Cockerell, 1915: 486.

Q. Joursac [France; Miocene, 11.6–7.2].
(27.) †*Ctt. obesus* (Piton, 1935). [q?]. [Note 15]. Comb. nov.

R. Montagne d'Andance Saint-Bauzile, Privas [France, Ardèche; Miocene (Turolian), 8.7–5.3 Mya].
(28.) †*Ctt. crozei* (Riou, 1999). [q]. Comb. nov.

S. Brunn-Vösendorf [Austria; Miocene (Messinian), 7.2–5.3 Mya]
(–.) †*Ctt. ullrichi* (Bachmayer, 1960). [wing]. Comb. nov.; unidentifiable, hence invalid, stat. nov. [Note 16].

T. Willerhausen clay pit [Germany; Pliocene (Piacenzian), 3.6–2.6 Mya].
(29.) †*Ctt. silvestris* Steinbach, 1967. [q].
• †*Camponotites* Steinbach, 1967 TYPE SPECIES.
• Redescribed: Dlussky et al. 2011: 452.
(30.) †*Ctt. steinbachi* Dlussky et al., 2011. [q].

Note 1. The species †*Ca. palaeopterus* (Zhang, 1989) was originally attributed to its own genus, †*Shanwangella* Zhang, 1989 before being placed in *Camponotus* by Hong and Wu (2000). The fossil cannot be attributed to Formicinae at all, however, due to the presence of cross vein 2rs-m, which never occurs in Formicinae; this crossvein encloses the second submarginal cell of the wing. Because the specimen has 2rs-m, lacks postpetiolation of abdominal segment III, and does not have cinctation of abdominal segment IV (= presence of transverse sulci), we transfer the species to Dolichoderinae. Therein, the specimen is recognizable as an alate of *Liometopum* given its large size (discal and submarginal cells ~ 1 mm long), its massive gaster, and details of the venation. †*Liometopum palaeopterum* comb. nov. was discovered in Shanwang in the Shandong Province, reasonably within the current distribution of the extant species *L. sinense* Wheeler, 1921 (Del Toro et al. 2009). Moreover, it is plausible that the fossil represents an ancestral population given that *L. sinense* is the only species currently known from China, at least to present knowledge. Unfortunately, gynes and males are unknown for the extant species. The unusual head and antennae of †*L. palaeopterum* comb. nov. are here interpreted as preservational artefacts.

Note 2. *Camponotus* and the tribe Camponotini more broadly is one of the most challenging taxonomic puzzles in the Formicidae, and not merely due to the massive size of these taxa (1084 valid species and 411 valid subspecies are currently attributed to *Camponotus* at the date of writing, Bolton 2023). Although some genera in the tribe are reasonably identifiable based on external morphology (e.g., Ward et al. 2016), others, such as the fundamental distinction between *Colobopsis*—which is sister to all other Camponotini—and the hyperdiverse *Camponotus* is challenging even with extant material in hand and under the microscope (Ward and Boudinot 2021). For these reasons, we substantially revise the fossil system of *Camponotus* in order to meet the twin aims of: (1) cleaning up the useless species names attributed to *Camponotus*, and (2) discouraging uncritical use of these fossils for macroevolutionary analysis (e.g., Klimeš et al. 2022). Toward these aims, we have: (a) provided a new genus name for †*Camponotus mengei*, †*Eocamponotus* gen. nov., as this fossil cannot be confidently placed in *Camponotus* yet; (b) transfer red 29 fossil taxa from *Camponotus* to the form genus †*Camponotites*, which we treat as *incertae sedis* in Formicinae; and (c) transfer red one species out of the Formicinae altogether.

Note 3. The minor worker specimen (PMJ Pa 5829) is difficult to identify, given the limited resources available. We attempted to identify the specimen using Emery's (1925) key to Old World *Camponotus* subgenera, Brian Taylor's

Ants of Africa website (Taylor 2022), and AntWeb (2022). Ultimately, we were unable to obtain a satisfying identification. In mesosomal form and postcephalic setation, the specimen resembles *Camponotus* (*Myrmacraphe*) *furvus* Santschi, 1911 but it differs in head shape and by having shorter palps. In Taylor's key, the specimen runs to *C. acvapimensis* Mayr, 1862, yet it differs in mesosomal form. We therefore conservatively consider the specimen unidentified.

Note 4. †*Polyrhachis annosa* neatly meets the expectations for *Polyrhachis* as it clearly has lateral petiolar spines, which is synapomorphic condition of the genus. Based on the limited preservation, we do not have confidence that this species will be placeable either in the stem or crown of the genus based on morphology. However, given that the Varvara formation is young, being dated at between 7–5 Myo, we do not think that it is defensible to place this fossil in a separate genus. We therefore leave this species in *Polyrhachis* with the hope that future phylogenetic work will resolve the polarity of petiolar spines within the genus.

Note 5. The monotypic genera †*Chimaeromyrma* and †*Pseudocamponotus* have been treated as *incertae sedis* in Camponotini, for which we see no specific morphological evidence to question these otherwise harmless placements. We choose to retain †*Chimaeromyrma brachycephala* Dlussky, 1988 as a valid genus and species as it is possible that the identification of this amber fossil may be refined through the application of μ-CT at some point in the future. As for †*Pseudocamponotus elkoanus* Carpenter, 1930, we doubt that this fossil will ever be identifiable given the lack of wing venation and very limited preservation of the single known specimen. Given that there is insufficient preservation to confidently place the species to tribe, we consider †*Ps. elkoanus* to be unidentifiable, hence invalid stat. nov. We do not synonymize †*Pseudocamponotus* with †*Camponotites*, however, as the former would take priority and we prefer the latter name as the form genus, given that it has the proper suffix (-tites) to indicate paleontological uncertainty.

Note 6. We erect the genus †*Eocamponotus* gen. nov. for †*Camponotus mengei* and its junior synonym †*Ca. igneus* as, although these fossils are sufficiently preserved for species diagnosis, formal combined-evidence analysis failed to support a relationship with any particular genus of the Camponotini (Boudinot et al. 2022a). In so doing, we aim to preclude the usage of this fossil in macroevolutionary analysis as a calibration point for the genus *Camponotus*. At most, this fossil species can be used as a calibration for the Camponotini; whether as a stem or crown calibration point, however, is much less certain, and a conservative approach would be for the stem of the tribe.

Note 7. We briefly note that †*Ca. mengei* was described alongside †*Ca. igneus* by Mayr (1868), and that the latter was accepted in a number of articles until Wheeler (1915) concluded that the latter is a subjective synonym of the former based on an examination of 103 *Camponotus* specimens and Mayr's types of †*Ca mengei*. Wheeler reported that the type specimens of †*Ca igneus* were in the collection of Franz Anton Menge, which is presumably in Gdańsk, Poland. The valid species was originally considered to be a *Ca.* (*Tanaemyrmex*) but was recently suggested by Radchenko and Perkovsky (2021) to be *Ca.* (*Camponotus*) due particularly to the form of its clypeus, and the shapes of the head and mesosoma, without further specification. Reevaluation of the morphological affinities of this species is necessary.

Note 8. †*Ctt. juliae* (Pierce & Gibron, 1962) comb. nov. is represented by a single male that was phosphatized in a calcareous nodule in the Calico member of the Miocene-aged Barstow formation in the Mojave Desert of California. The taxonomic history of this fossil is unusual. In its original description in Pierce and Gibron (1962), the fossil was classified as a new species of a new genus representing a new family of symphypleonan Collembola: †*Palaeosminthurus juliae* (†Palaeosminthuridae). These names went unnoticed for more than two decades, until the collembolist Dr Judith Najt (see Deharveng et al. 2017) observed that the preserved head, scape, thorax, and leg remnants of the fossil belong to a hymenopteran, which she identified as *Camponotus* (see Najt 1987). Subsequently, Roy R. Snelling examined the fossil, presumably at the Los Angeles County Museum, and concluded that the taxon is a junior synonym of *Camponotus festinatus* (Buckley, 1866) (Snelling 2006), an identification that was communicated to Barry Bolton in 2004 but went unpublished by the time of Roy Snelling's death in 2008. Bolton provisionally accepted this hypothesis in his taxonomic catalog (Bolton 2023). Here, after critical consideration of the available morphological evidence, we exclude the species from *Camponotus*, and revive the genus †*Palaeosminthurus* stat. rev., which we consider to be *incertae sedis* in Formicinae and unidentifiable hence invalid stat. nov. Specifically, we attempted to run the specimen through the male-based key to all Nearctic genera of Smith (1943) and that of Boudinot for all New World formicine genera (see section 3.7.H of Boudinot 2020); there is simply too little structural detail preserved to render a meaningful identification of this fossil. Unless a method like laminar μ-CT may be applied successfully, we anticipate that this fossil will remain unidentifiable at the genus and tribal levels among the Formicinae.

Note 9. Here, we recognize the form taxon †*Camponotites* to which we transfer 29 species. †*Camponotites* should be categorically precluded from usage as calibration points for macroevolutionary analysis of the Formicinae or Formicidae. A balance for retaining and actively using this form genus is that the fossils in this taxon may be useful for paleogeographic study, so invalidation of this name may result in loss of paleostratigraphic information. Future work involving direct re-examination of these fossils is necessary to determine some of the taxa now placed in †*Camponotites* may perhaps be placed with more confidence among the genera of Camponotini—such as †*Ctt. novotnyi* (Samšińák, 1967) comb. nov. as this fossil is quite well preserved and clearly displays the major synapomorphy of the Camponotini, namely that the antennal sockets are separated posteriorly from the posterior clypeal margin. For this example, however,

the remainder of the specimen is too poorly preserved to allow the fossil to be meaningfully associated with any extant genus of the Camponotini.

Note 10. From the illustration provided in the original description, it is not possible to confidently identify the specimen as a member of *Camponotus*. We retain this species as *incertae sedis* in the genus to encourage future work on the fossil, if possible.

Note 11. All of these fossils could be considered unidentifiable to species, hence invalid, but are here treated as *incertae sedis* in *Camponotus* to highlight their existence. Critically, because of the lack of morphological information, it is possible that a number of these taxa belong to other genera of Camponotini (see Ward et al. 2016 and Ward and Boudinot 2021). Reexamination of the original material is necessary in all cases.

Note 12. While it may be tempting to use †*C. vetus* as a calibration for *Camponotus* or the Camponotini, it cannot be confidently attributed to any living genus, subgenus, or species group due to insufficient morphological information.

Note 13. The generic placement of †*Ca. microcephalus* is dubious and should be confirmed through direct examination of type and additional material.

Note 14. Although †*Camponotus pictus* Zhang et al., 1994 is a junior primary homonym of *Ca. ligniperda pictus* Forel, 1886, we transfer this species to the form taxon †*Camponotites*, rendering a *nomen novum* unnecessary.

Note 15. The compression-fossil taxon †*Ca. obesus* is represented by fragments of the mesosoma, legs, and metasoma, all of which are preserved in a dorso-anterolateral oblique view. These remains are suggestive of *Camponotus* but otherwise cannot be identified meaningfully. Identification, in this case, is primarily driven by the rough similarity and absence of other ~14 mm long ants with an apparently rounded mesosoma in modern Western Europe.

Note 16. Bachmayer (1960) described †*Ctt. ullrichi* based on a single forewing from a Miocene-aged deposit in Austria. This ~10.3 mm long wing cannot be attributed to *Camponotus* or the Camponotini because free M diverges from Rs+M proxi‹mad 2r-rs by more than twice the length of that cross vein. In Camponotini, free M diverges at or distad 2r-rs (see Char. 499 on p. 293 of Boudinot et al. 2022b; also, Ward and Boudinot 2021). Because only Myrmelachistini in Formicinae have the split of Rs+M well proximad 2r-rs, and as these ants are miniscule, we would prefer to consider the taxon *incertae sedis* in Formicidae. However, as this would necessitate the recognition of another "trashbin" form taxon, we elect to place the fossil in †*Camponotites* and to consider it unidentifiable, hence subjectively invalid stat. nov.

Genus †*Eocamponotus* Boudinot, gen. nov.

https://zoobank.org/031A69F6-4431-4C53-9898-73728761C2C6

Type species. †*Eo. mengei* (Mayr, 1868) by original designation.

Note. *Incertae sedis* in Camponotini.

3.3.2.4. Subfamily Myrmicinae Lepeletier de Saint-Fargeau, 1835

3.3.2.4.1. Genus *Crematogaster* Lund, 1831

I. Species retained in *Crematogaster*.

Copal fossil: Identifiable to species:

A. African copal [Holocene, < 36 Kya (Solórzano-Kraemer et al. 2020)].

1. *Cre.* sp. THIS STUDY. [w].

II. Fossils excluded from *Crematogaster*:

Genus †*Incertogaster* Boudinot, gen. nov., *incertae sedis* in Myrmicinae. [Note 1].

Type species: †*Inc. primitiva* (Radchenko & Dlussky, 2019), by original designation.

B. Kishenehn formation [USA, Montana; 47.8–41.3 Mya].

(1.) †*In. aurora* (LaPolla & Greenwalt, 2015). [q]. [Note 2]. Comb. nov.

C. Rovno amber [Ukraine; Eocene, 38.0–33.9 Mya].

(2.) †*In. praecursor* (Emery, 1891). [m]. [Note 3]. Comb. nov.

D. Sicilian amber [Italy; Oligocene, 11.6–5.3 Mya].

(3.) †*In. primitiva* (Radchenko & Dlussky, 2019). [m]. [Note 3]. Comb. nov.

Note 1. We erect the explicit catchall taxon †*Incertogaster* gen. nov., into which we place †*In. aurora* comb. nov., †*In. praecursor* comb. nov., and †*In. primitiva* comb. nov. We do so in order to recognize that these latter two species are not meaningfully placeable in *Crematogaster* based on their preserved morphologies, and that †*In. aurora* requires renewed attention. We choose †*In. primitiva* as the type species as the specimen of †*In. praecursor* examined by Emery is likely lost (see, e.g., Boudinot et al. 2016), and as the compression fossils require revised scrutiny and may be placeable in other genera, whether extant or extinct.

Note 2. †*Crematogaster aurora* is the oldest fossil attributed to the genus and is the most difficult to critique due to its highly suggestive but incomplete preservation. While we are uncertain about the placement of the fossil in *Crematogaster* due to the apparently axial postpetiolar helcium (*i.e.*, located at about mid-height of AIV rather than atop AIV) and the unknown antennomere count, the specimen does indeed lack a vertically oriented petiolar node, at least as preserved. To prevent the use of this fossil for divergence dating analysis while the preserved anatomy is reevaluated, we transfer the species forming †*In. aurora* comb. nov. We hope that additional specimens may be found, or the known specimens are subjected to documentation using advanced techniques. One of the authors (BEB) examined both the type and the paratype of †*In. aurora* at the USNM and observed that the paratype differed substantially, having (possibly) antennal scrobes but more importantly a lateromedially narrow postpetiole that was anteriorly attached to abdominal segment IV (metasomal III). Additionally, this specimen possibly had a 2–3-merous antennal club. Altogether, this raises doubt about the attribution of the paratype to †*In. aurora*, which remains of uncertain identification at present.

Note 3. The amber-preserved males described by Emery as †*In. praecursor* comb. nov. and Radchenko & Dlussky as †*In. primitiva* comb. nov. are unlikely to be representatives of either the stem or crown of the genus *Crematogaster* and are *incertae sedis* in the Myrmicinae within †*Incertogaster*. Both specimens have 13-merous antennae, while all *Crematogaster* males examined by the lead author have antennae that are 10–12-merous (Bolton 2003, p. 286; BEB, unpubl. data). Other diagnostic features include the short scape, which is ≤ 2 × the length of the pedicel, the pedicel shape, which is globular rather than cylindrical, and the mandibles, which are reduced or otherwise vestigial; the anterodorsal position of the postpetiolar helcium on abdominal segment IV can be difficult to discern. Unfortunately, Emery did not illustrate the wings or the face of †*Cr. praecursor*, so the fossil may need to be considered unidentifiable, hence subjectively invalid, if the specimen does not resurface. †*Crematogaster primitiva*, on the other hand, is well illustrated; its scapes are about 4 × the length of the pedicels, and the pedicels are not swollen or globular in shape. The mesosoma of this fossil (PMJ Pa 5824) is large and the mesoscutum is impressed, as in many *Crematogaster*, but the long and strongly nodiform petiole also contradict placement in that genus. At present, we cannot confidently attribute †*Cr. primitiva* to any valid generic taxon.

Genus †*Incertogaster* Boudinot, gen. nov.

https://zoobank.org/C309774E-AD72-4AD1-81D5-A13DDA867614

Type species. †*Inc. primitiva* (Radchenko & Dlussky, 2019), by original designation.

Note. *Incertae sedis* in Myrmicinae.

3.3.2.4.2. Genus *Pheidole* Westwood, 1839

Amber/copal species: Identifiable to species:

A. Mexican amber [Miocene, 23.0–16.0 Mya].
1. †*Ph. pauchil* Varela-Hernández & Riquelme, 2021. [w].

B. Dominican amber [Miocene, 20.4–13.8 Mya].
2. †*Ph. anticua* Casadei-Ferreira et al., 2019. [w].
3. †*Ph. primigenia* Baroni Urbani, 1995. [w].
4. †*Ph. tethepa* Wilson, 1985. [w]. [see Wilson 1985a].

C. East African copal *sensu lato* [Holocene, < 36 Kya (Solórzano-Kraemer et al. 2020)].
5. ‡*Ph. rasnitsyni* Dubovikoff, 2011. [w]. [Note 1].

D. East African copal or Defaunation resin [Holocene, < 36 Kya (Solórzano-Kraemer et al. 2020)].
6. ‡*Ph. cordata* (Holl, 1829). [w, s]. [Note 2].
= †*Formica cordata* Holl, 1829.
• Neotype here designated (specimen Pa 5889).

Compression fossil species: *Species inquirenda*.

E. Florissant formation [USA, Colorado; Eocene, 37.9–33.9 Mya].
(1.) †*Ph. tertiaria* Carpenter, 1930. [q]. [Note 3].

Note 1. Similar to the recent description of a *Dorylus* from putative Baltic amber (see section 4.2.1), the species ‡*Ph. rasnitsyni* was initially interpreted as an Eocene fossil (Dubovikoff 2011) but later reidentified as copal based on reevaluation of the material (Dubovikoff pers. comm. in Perkovsky 2016).

Note 2. We designate one soldier (= major) from the PMJ Pa collection (PMJ Pa 5889, copal, ^{14}C-dated: ~700 years old) as the neotype of the ‡*Ph. cordata*, and tentatively associate a minor worker (PMJ Pa 5827) with this name although we do not recognize this as a secondary type. See section 3.3.2.6.1 for elaboration and Casadei-Ferreira et al. (2019) for a recent review of this taxon.

Note 3. Given the single photograph available for this species, which is otherwise reported from two specimens (Carpenter 1930), we consider †*Ph. tertiaria* in need of revised study, and strongly recommend against its use in divergence dating analysis until definitive synapomorphies of *Pheidole* may be documented. Most notably would be the occurrence of cross vein 2rs-m, which encloses the second submarginal cell and is otherwise absent from other Myrmicinae with the exception of various Myrmicini and Pogonomyrmecini.

3.3.2.4.2.1. Pheidole taxon treatment

‡*Pheidole cordata* (Holl, 1829)

Figs 19–21, Appendix 1: Fig. A5

Neotype. PMJ Pa 5889, *designated here*. Figs 19A–D, 20A–D, 21B, D, F.

Locality and horizon. East African copal (IAA results for PMJ Pa 5889: copal (Table 1); ^{14}C-dating for PMJ Pa 5889: ~700 years old).

Syninclusions. Platygastridae, Ceratopogonidae, and Lepidoptera.

Preservation. The cuticle is preserved as a distinct layer as seen in the SR-µ-CT scan data. Most of the soft tissues are absent, except for parts of the digestive tract and some musculature, such as parts of the mandibular adductor (0 md1) and some muscles of the legs. The endoskeleton of the head and mesosoma is distinctly preserved and can be meaningfully used for future comparative anatomy.

Paraneotypes. None.

Diagnosis. The species, represented by the major worker, is identifiable as a member of the *Ph. megacephala* species group by (1) the presence of the conspicuous ventral convexity of the postpetiolar sternum (Fig. 19A; e.g., Salata and Fisher 2020). It differs from *Ph. megacephala* (Fabricius, 1793), *Ph. megatron* Fischer & Fischer, 2013, and *Ph. spinosa* Forel, 1891 by (2) the well-developed inner hypostomal teeth (Fig. 20B; e.g., Salata and Fisher 2022). Among the *megacephala* group species more broadly (e.g., Fischer et al. 2012), it differs in having (3) facial rugosity that extends to the posterior margin of the occipital lobes (Fig. 20A, note: among type specimens of the group imaged on AntWeb, this condition also occurring in *Ph. megacephala impressifrons* Wasmann, 1905, which has a

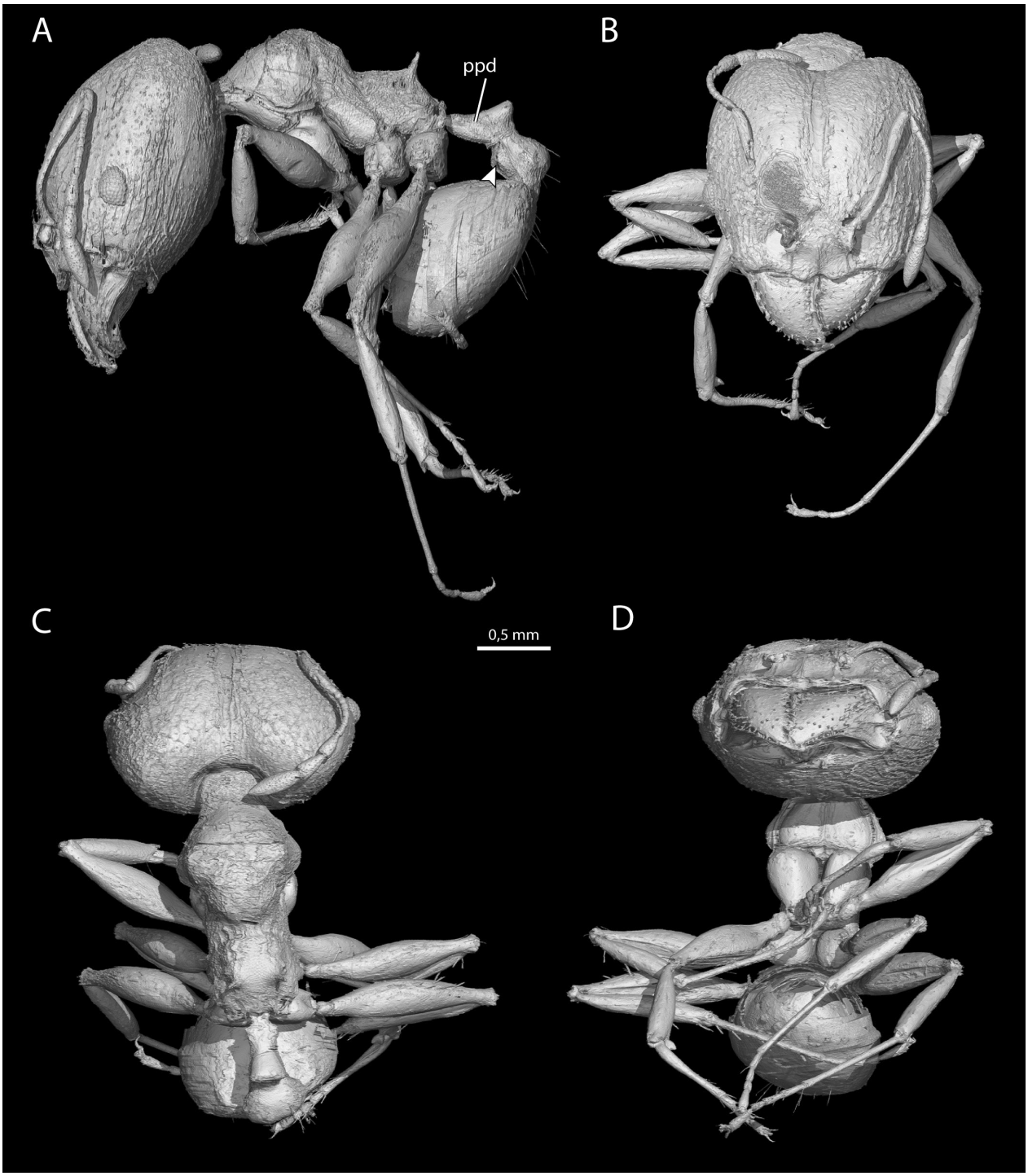

Figure 19. A–D. 3D-reconstruction of the neotype of ‡*Pheidole cordata* **A.** Habitus in lateral view; **B.** Habitus in frontal view; **C.** Habitus in dorsal view; **D.** Habitus in ventral view. Abbreviation: ppd = propodeum.

more angular bulge of the postpetiolar sternum). See the description below for further conditions.

Description. ***Measurements*** (in mm; abbreviations follow Salata and Fisher 2022): EL = 0.152; HL = 1.290; HW = 1.230; MTL = 0.673; PNW = 0.618; PPW = 0.324; PSL = 0.202; PTW = 0.172; SL = 0.714; WL = 1.110.

Indices (also following Salata and Fisher 2022): CI = 95.3; MTI = 54.7; SI = 58.0; PNI = 50.2; PPI = 26.3; PSLI = 16.4. Note: Measurements taken from cross-sectional projections in DragonFly using the reregistration and ruler tools.

Head. In full-face view (Figs 19B, 20A), the head is subcordate, with the lateral margins widest somewhat beyond head midlength and with the posterior portions of the lateral margins converging posterad to the occipital lobes. In lateral view (Fig. 19A), the head is subovate. The antennal scrobes are indistinct. The occipital lobes are rugose, with shagreened interspaces. The inner hypostomal teeth are well-developed; they are distant from the outer teeth, which are also well-developed (Fig. 20B). The median hypostomal tooth is indistinct.

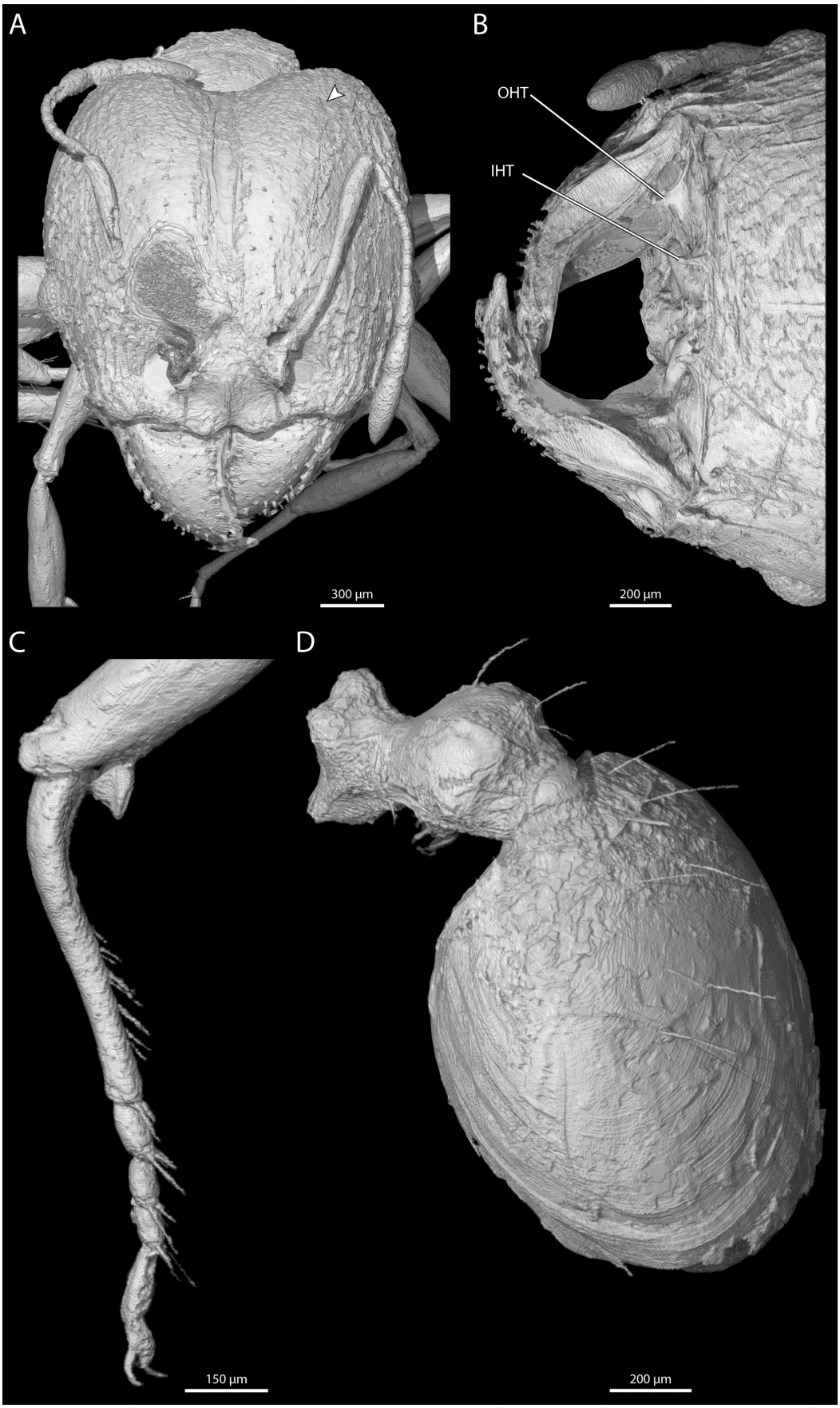

Figure 20. A–D. 3D-reconstruction of the neotype of ‡*Pheidole cordata* preserved in piece PMJ Pa 5889. **A.** Details of head in frontal view, arrow indicates occipital lobe; **B.** Detail of mouthparts in ventral view; **C.** Details of foreleg in lateral view; **D.** Details of metasoma in dorsolateral view. Abbreviations: IHT = inner hypostomal tooth, OHT = outer hypostomal tooth.

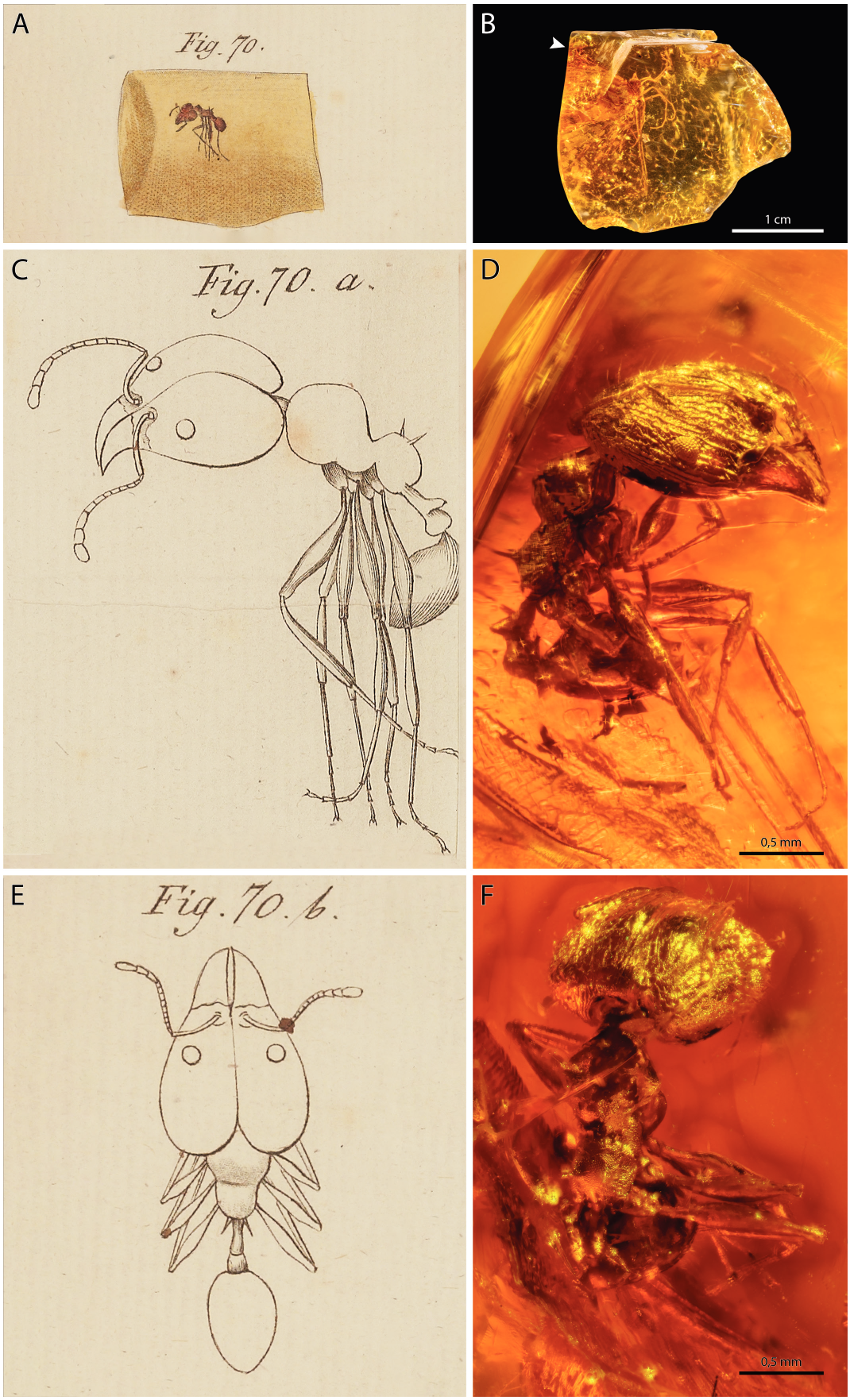

Figure 21. A, C, E. Copper lithographs by Schweigger (1819), which Holl (1829) named †*Formica cordata*. **B, D, F.** Photographs of the neotype of ‡*Pheidole cordata* **A.** Overview of the amber piece; **B.** Overview of the amber piece, arrow indicates the inclusion; **C.** Habitus in lateral view; **D.** Habitus in ventrolateral view; **E.** Habitus in dorsal view; **F.** Habitus in dorsolateral view.

Mesosoma. The humeral tubercle of the pronotum is weakly developed. The mesonotal bulge is distinct but not pronounced. The metanotum is only weakly indicated by a slight angularity of the promesonotal profile in lateral view. The propodeal spines are moderately long, with a wide base and acute tip (Fig. 19A).

Metasoma. The bulge of the postpetiolar sternum is rounded anteriorly. The first gastral tergum (ATIV) appears to be shagreened at its base (Fig. 20D).

Setation. Length and stature of setation uncertain, although density measurable in the scans based on the distinct occurrence of the setiferous punctation.

Coloration. Not clearly visible; appears brownish/reddish.

Remarks on the neotype. Designation of the soldier in piece PMJ Pa 5889 as the neotype of ‡*Ph. cordata* meets the requirements of article 75 of the ICZN (1999), as follows. 75.3.1. The identity of this taxon is in severe need of clarification, as it has vexed systematists for nearly two centuries (e.g., Mayr 1868; Casadei-Ferreira et al. 2019) and may mistakenly be used for evolutionary inference, such as an Eocene-aged calibration for divergence dating based on the assumption that it is from Baltic amber, as recorded by, e.g., Bolton (1995, p. 319) and Bolton (2003). 75.3.2, –.3. Diagnostic remarks and description are provided above. 75.3.4. The original material is known to be lost (Casadei-Ferreira et al. 2019). It is unclear if the material sent by Schweigger ever made it to the MfN Berlin in the first half of the 19th century; see p. 111 of Schweigger (1819) and elsewhere for his stated intent to have the specimens identified there. Further, Holl (1829, p. 140) indicates that he defined his species †*Formica cordata* based on the observations of Schweigger and Mayr (1868, p. 18) explicitly states that he had not seen the material referred to by Holl. 75.3.5. The neotype matches the best available evidence. More specifically, the first author of the present work directly examined a physical print of the original illustrations by Schweigger (1819, figs 70, 70a, 70b on plate 8 therein; Fig. 21A, C, E), which were used by Holl (1829) to designate the species. Based on this, that author observed clearly illustrated 3-merous antennal clubs, which would rule out other Afrotropical Myrmicinae (Fisher and Bolton 2016). The illustrations further show attributes of *Pheidole*, including a massive head, high and domed promesonotum, low and spined propodeum, and long petiolar peduncle with a short node. Mayr (1868) was uncertain about the size of the original material, which is unknowable at this point and irrelevant for the present designation. Therefore, we interpret the fossil as *Pheidole* based on the available evidence (Fig. 21B, D, F), which is restricted to the examined copper plate due to loss of the original material. 75.3.6. The designated neotype does come from the original type locality and horizon as much as is practicable, given that Schweigger (1819): (a) knew about copal (pp. 103, 104 therein) and East African copal was available around that time (e.g., Smith 1868, see section 4.3.2 below); (b) he was uncertain about the provenance of the two specimens eventually named ‡*Ph. cordata* by Holl (1829), as stated in the text; and (c) he pointed out that the species he examined resembled a taxon possibly from Africa (“Diese Bildung findet sich an Ameisen südlicher Länder.”, pp. 119 therein). Regarding the type locality further, although we cannot be absolutely certain that the specific fossil is from East African or Malagasy copal *sensu lato*, the syninclusion of a *Pheidole* minor from the PMJ Pa collection with *Dorylus* (PMJ Pa 5827), which has never been recorded from Madagascar, strongly implies that the material was from the mainland of the African continent. 75.3.7. The neotype is permanently preserved in and available for study at the Phyletisches Museum, Jena.

We have taken this action to resolve a suite of problems associated with the name ‡*Ph. cordata*, as recently reviewed by Casadei-Ferreira et al. (2019), who, after much consideration, concluded by placing this fossil *incertae sedis* in Myrmicinae. We fully agree with Casadei-Ferreira et al. (2019) that this fossil needs to be disposed of in order to avoid its uncritical use in systematic or evolutionary study and inference. By placing the name ‡*Ph. cordata* back in *Pheidole*, we alleviate the need for treating this taxon in the next revision of the fossil record of Myrmicinae, particularly as the specific epithet will be paired with the genus *Pheidole*, unless it were returned to *Formica*, to which it certainly cannot belong. Further, by designating a neotype we permanently fix this name to a known specimen that is both preserved in perpetuity in the PMJ Pa collection and is available for global evaluation via the cybertype data. Finally, there is no possibility beyond egregious error for this taxon to be used as an Eocene calibration for *Pheidole* as the neotype is from ^{14}C-dated copal. (copal *sensu lato*).

Remarks on Afrotropical *Pheidole*. It is widely appreciated among myrmecologists working on *Pheidole* that the genus is in severe need of revision both globally and in the Afrotropical region (Wilson 2003; Fischer et al. 2012; Sarnat et al. 2015), which is also the particular case for the *megacephala* species group (Fischer et al. 2012; Salata and Fisher 2022). While we would strongly prefer to not provide a one-off description of a *Pheidole* due to this complicated problem, we accept this as necessary and acceptable only in order to resolve the problem of ‡*Ph. cordata*, which is otherwise an irksome thorn-in-the-side bestowed upon generations of us by the well-meaning cataloging work of Holl (1829).

Although ‡*Ph. cordata* as typified here cannot be included in barcoding or phylogenomic datasets given its poor soft tissue preservation, it is our hope that the SR-μ-CT data may allow the confident and quantitative placement of this species among the species allied to *Ph. megacephala* via a dedicated revision of this species group. As noted in our diagnosis above, the neotype of ‡*Ph. cordata* (PMJ Pa 5889) is most similar to *Ph. megacephala impressifrons*, being most starkly distinguished from this form by the form of the postpetiolar sternum in lateral view. Notably, the form of the medial hypostomal teeth has not been recorded for the various forms of *Ph. megacephala* and similar species (e.g., Fischer et al. 2012). Whether the newly typified

species ‡*Ph. cordata* is extant is an open question; it is plausible that the historical habitat has been destroyed, hence this species may be considered a candidate Lazarus taxon. Further exploration of known Afrotropical copal *sensu lato* and extant myrmecofauna will be of considerable value.

3.3.3. Order Neuroptera: Synopsis of Nevrorthidae

3.3.3.1. Family Nevrorthidae Nakahara, 1915. [Note 1]

I. Genus †*Balticoneurorthus* Wichard, 2016.
  A. Baltic ambers [Eocene, 37.8–33.9 Mya].
    1. †*Ba. elegans* Wichard, 2016. [m].

II. Genus †*Cretarhopalis* Wichard, 2017.
  B. Kachin amber [Myanmar; Cretaceous, 99.6–93.5 Mya].
    1. †*Crh. patrickmuelleri* Wichard, 2017. [f].

III. Genus †*Electroneurorthrus* Wichard, Buder & Caruso, 2010.
  A. Baltic ambers [see above].
    1. †*El. malickyi* Wichard, Buder & Caruso, 2010. [f].

IV. Genus †*Girafficervix* Du, Niu & Bao, 2023.
  C. Daohugou shale [China; Jurassic, 166.1–157.3 Mya].
    1. †*G. baii* (Du, Niu & Bao, 2023). [l].

V. Genus †*Palaeoneurorthus* Wichard, 2009.
  A. Baltic ambers [see above].
    1. †*Pa. bifurcatus* Wichard, 2009. [m].
    2. †*Pa. eocaenus* Wichard, 2016. [m].
    3. †*Pa. groehni* Wichard, Buder & Caruso, 2010. [m].
    4. †*Pa. hoffeinsorum* Wichard, 2009. [m]. [Type species!].

VI. Genus †*Proberotha* Krüger, 1923.
  A. Baltic ambers [see above].
    1. †*Pr. dichotoma* Wichard, 2016. [f].
    2. †*Pr. eocaenus* Krüger, 1923. [m, f]. [Type species!].

VII. Genus †*Rhopalis* Pictet, 1854.
  A. Baltic ambers [see above].
    1. †*Rh. relicta* Pictet, 1854. [f, m]. (See also: Wichard et al. 2010.)

VIII. Genus †*Sisyroneurorthus* Nakamine, Yamamoto, Takahashi & Liu, 2023.
  B. Kachin amber [see above].
    1. †*S. aspoeckorum* Nakamine et al., 2023. [f].

Note 1. Six of the eight fossil genera of Nevrorthidae are monotypic. For those two genera that have more than one species attributed to them, the type species is indicated.

3.3.3.2. Genus *Palaeoneurorthus* Wichard, 2009

Genus Palaeoneurorthus Wichard, 2009

Type species. †*Palaeoneurorthus hoffeinsorum* Wichard, 2009.

Diagnosis. This genus can be characterized by the forewing with costal cross veins almost all simple, the cross veins 3rp3+4-rp2 present in forewings and absent in hindwings, the flattened male sternum 9 with tongue-like tip and the needle-like male gonapophyses 9.

Note. One male specimen in the amber collection (PMJ Pa 5874) is a member of Nevrorthidae. It was assigned to the genus *Palaeoneurorthus* based on our examination (Fig. 22A). We briefly characterize this specimen below:

†*Palaeoneurorthus* sp.

Description. Body length ca. 3.0 to 4.0 mm; forewing length 7.5–7.8 mm, hindwing length 6.4–6.8 mm.

Head. Ocelli absent. Antenna slenderly filiform, with slightly enlarged scapus, smaller pedicellus, and 30 flagellomeres. Maxillary palps and labial palps not visible.

Wings (Fig. 22B, C). Elliptical, translucent. Forewing venation with trichosors present among marginal forks of RA, RP, MA, MP, CuA and CuP; all costal cross veins simple. Sc and RA almost parallel to margin, connected basally and subdistally by two and one cross veins, respectively. RP with three main branches. MA fused with RP at proximal 1/3 of wing, distally branched. MP proximally separated into two main branches, with each branch bifurcated distad. Cu branching near wing base; CuA with seven pectinate branches; CuP sinuate, simple, forked distad. A simple. Most cross veins present at base, middle and distal 1/3. Hindwing venation: Basal part of the hindwing not visible. Trichosors present among marginal forks of RA, RP, MA, MP, CuA and CuP; costal cross veins on proximal 2/3 not visible, distal 1/3 simple. Sc and RA almost parallel to margin, subcostal cross veins absent. RP with two main branches. MA fused with RP at wing proximal 1/3, distally forked. MP with two main branches, one branch bifurcated distally and the other proximally, respectively. Cu branching near wing base; CuA with ten pectinate branches, CuP straight, simple. A not visible. Only two rows of cross veins visible, present at middle and distal 1/3, respectively. In forewings the cross vein 3rp3+4-rp2 present; in hindwings cross vein rp3+4-rp2 absent.

Abdomen (Fig. 22D, E). Visible part of abdominal segment 9 annular. Sternum 9 not visible. Robust gonocoxites 9 (= "gonocoxa" in Boudinot 2018) strongly incurved, with broad base, apically tapering, with strongly sclerotized, claw-like gonostyli 9 (= "stylus" in Boudinot, 2018), which are directed ventromedially. Ventrolateral lobes (= gonapophyses 9, "penital sclerites" in Boudinot 2018) consist of two needle-shaped projections, which are distinctly spaced; dorsal projection slightly longer than ventral one, both pointed apically. Ectoproct (= "proctiger" in Boudinot 2018) broad, slightly convex at middle and distinctly protruding on both sides in dorsal view.

Remarks. There are four described species belonging to *Palaeoneurorthus*, which are all known from Baltic ambers (Wichard 2009, 2016, Wichard et al. 2010). Among the four species of *Palaeoneurorthus* with males described our collection shares similarities with *P. eocaenus* in having the set of two needle-like projections of gonapophyses 9, and the ventral projection of gonapophyses 9 being shorter than the dorsal one longer. However, based on our examination, the ventral projection of gonapophyses 9 is slightly

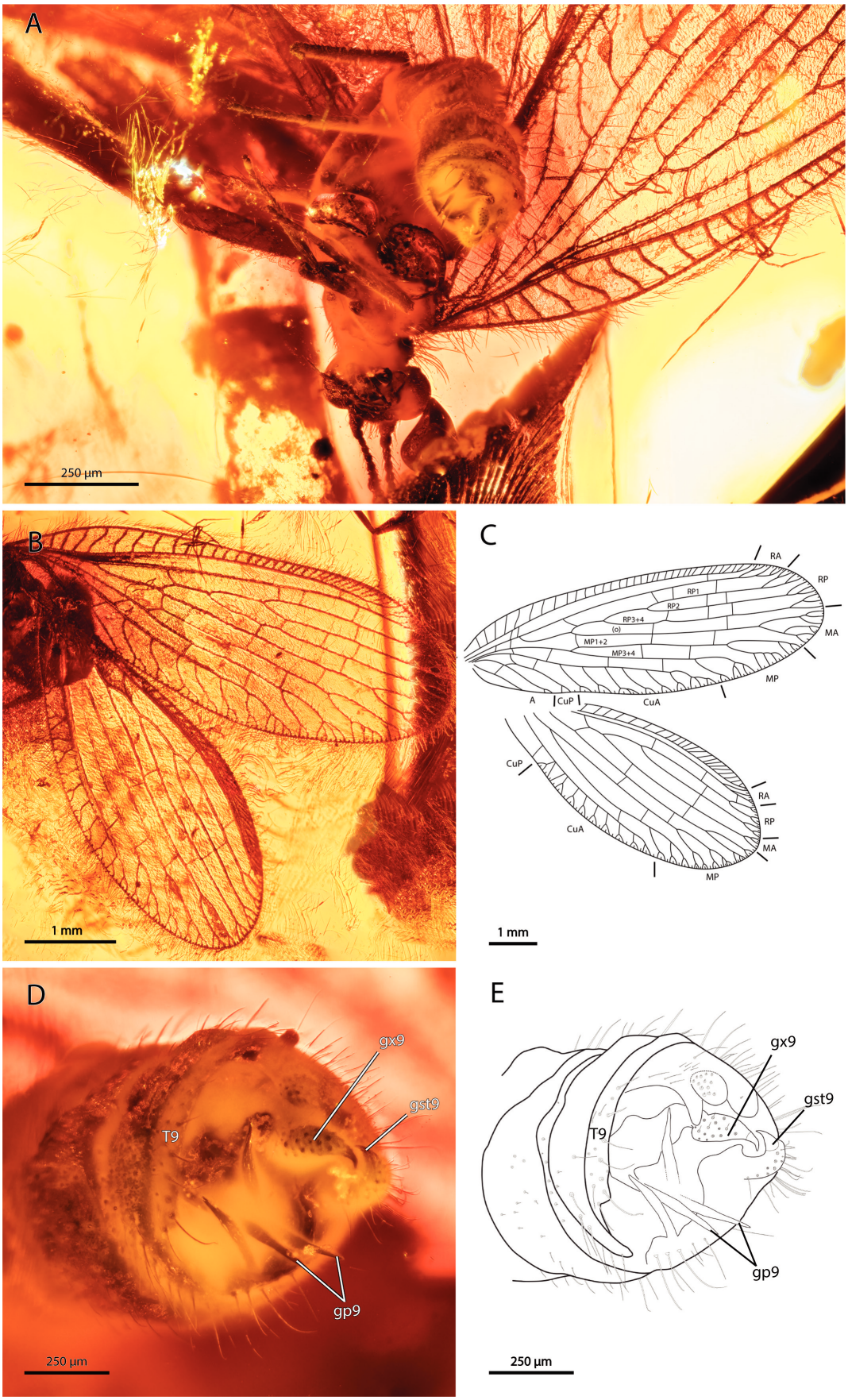

Figure 22. †*Palaeoneurorthus* sp. (Nevrorthidae) preserved in piece PMJ Pa 5874. **A.** Overview; **B.** Wing venation; **C.** Wing venation drawing; **D.** Genitalia; **E.** Genitalia drawing. Abbreviations: e = ectoproct, gp9 = gonapophyses 9, gst9 = gonostyli 9, gx9 = gonocoxites 9, T9 = tergum 9.

shorter than the dorsal one (Fig. 22C), whereas the dorsal projection is almost five times longer in *P. eocaenus* (Wichard 2016: fig. 6f). That the sternum 8 and the base of gonapophyses 9 are not visible impedes a further comparison. Thus, we currently treat this amber as *Palaeoneurorthus* sp.

3.3.4. Order Coleoptera

3.3.4.1. Synopsis of fossil *Doliopygus* (Platypodinae)

3.3.4.1.1. Genus *Doliopygus* Schedl, 1939
Copal taxa:

A. East African "copal" [Holocene, 0.0–0.0 Mya].
1. *D. crinitus* Chapuis, 1865. [Note 1].
2. *D. tenuis* Strohmeyer, 1912. [Note 1].

B. Defaunation resin or copal (possible East African) [Holocene, 0.0–0.0 Mya].
3. *D.* cf. *serratus* HERE. [Note 2].

Note 1. *Doliopygus crinitus* and *D. tenuis* were identified by Schedl (1939) from East African copal as species of *Crossotarsus*, with this original material presumably associated with the material misidentified as Baltic amber by F. Smith (e.g., Smith 1868; Grimaldi et al. 1994; O'Hara et al. 2013; see Note 2 of *Dorylus* above).

Note 2. We do not have the expertise to confidently identify the µ-CT scanned specimen to species level, thus we appreciate the identification suggested by Bjarte Jordal. *Doliopygus* is known to be paraphyletic (Jordal 2015), with *D. serratus* being close to *D. chapuisi* (B. Jordal, pers. comm. 9 Nov 2022). Given the objective of the present manuscript, the tentative species identification is sufficient to resolve our uncertainty about the age of the resin matrix.

3.3.4.2. Family Mordellidae Latreille, 1802

Family Mordellidae Latreille, 1802

Note. We do not provide a taxonomic synopsis of Mordellidae here as the fossil record of the family has been recently treated by Batelka et al. (2023).

3.3.4.2.1. †*Baltistena* (a collective group name established by Batelka et al. 2023)

†*Baltistena nigrispinata* Batelka, Tröger & Bock, sp. nov.

https://zoobank.org/CF6A27EB-FACD-482C-81B1-ECDD3130B529

Etymology. The species name *nigrispinata* refers to distinctly black combs on metatibia and tarsomeres contrasting with orange surface of the cuticle.

Type materials. *Holotype*. PMJ Pa 5870, Baltic amber. Sex indeterminable. Cybertype: Appendix 1: Fig. A6.

***Paratypes*.** None.

Differential diagnosis. The species belong to the subgroup of Mordellistenini with emarginated or dilated penultimate pro- and mesotarsomere *sensu* (Ermisch 1950). To this possible clade belong twelve of fourteen of Baltic Mordellistenini so far described (Batelka et al. 2023). In †*B. nigrispinata* sp. nov. the eyes are glabrous without interfacetal (= interommatidial) setae as in †*Palaeostena eocenica* Kubisz from which it differs by lower number of combs on metatibia and metatarsomeres I and II, and by the shape of palpomere IV which is type C1 *sensu* Franciscolo (1957) in †*Palaeostena*. The ultimate maxillary palpomere is securiform as in †*Baltistena korschefskyi* (Ermisch) from which †*B. nigrispinata* sp. nov. differs by the absence of combs on metatarsomere III and by the comb formula. The ring of short black scale-like setae on the tip of pygidium is similar to that in †*Baltistena brevispina* Batelka, Rosová & Prokop and in †*Palaeostena eocenica.* The metakatepisternum is fused early with the metaventrite in the middle of its posterior edge, which has so far only been observed in †*Palaeostena eocenica* among the Eocene Mordellistenini, while the other four species described by Batelka et al. (2023) have a separate and discernible metakatepisternum that is elongate and extends to the metanepisternum. Based on the shape of the body, the glabrous eyes, the shape of the metakatepisternum, and the setae on the cauda, †*B. nigrispinata* sp. nov. most closely resembles †*Palaeostena eocenica*. Also, while adding the species into the key provided by Batelka et al. (2023) it is coupled with †*Palaeostena eocenica* and †*Baltistena amplicollis* (Ermisch). From the last species, †*B. nigrispinata* sp. nov. differs by the comb formula, the shape of the ultimate maxillary palpomere, and the length of antennomeres III and IV, combined compared to antennomere V.

This set of characters observed for †*B. nigrispinata* sp. nov. supports the hypothesis that the species of Baltic Eocene Mordellidae formed a characteristic fauna that was much different from extant European representatives (Batelka et al. 2023).

Description. Head subglobular, frons continuously convex, hind margin of eye at posterior margin of head, elytra convex, pygidium long, metacoxa broad, comb formula 3//2/1/0/0. Habitus in lateral view (Fig. 23A, Fig. 24A).

Main diagnostic characters as defined by Franciscolo (1967) and Batelka et al. (2023): Right antenna well visible, left antenna (Fig. 23B) visible from basal part of antennomere II, antennomeres subcylindrical, slightly compressed, without any lateral projections, antennomeres III–IV slightly widening towards apex (Fig. 24B), length ratios of antennomeres as follows: ?-1.4-1.0-1.25-1.6-1.4-?-?-?-1.6-2.0; antennomere XI regularly rounded at apex; antennae densely covered by erect or semierect sensilla from antennomere III. Maxillary palpomere I small, palpomere II prolonged, widest at apex, palpomere III short, triangular, palpomere IV long, securiform of *Mordella*-type (Franciscolo 1957: fig. 6_A1) (Fig. 24C). Eyes finely faceted; Eyes glabrous without interfacetal setae. Scutellar shield continuously rounded (Franciscolo 1957: fig. 9_type10) (Fig. 24D). Basal side of pronotal disc widely convex in central part (Fig. 24E). Elytra 3.2 × as long as pronotal disc. Form of protarsi indiscernible. Structure of

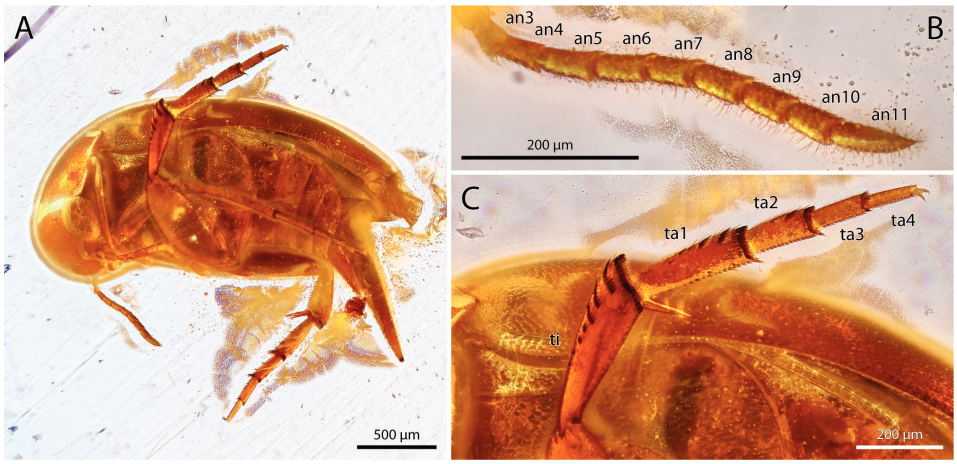

Figure 23. A–C. Holotype of †*Baltistena nigrispinata* Batelka, Tröger & Bock, sp. nov. (Mordellidae) preserved in piece PMJ Pa 5870. **A.** Habitus; **B.** Left antenna; **C.** Right metathoracic leg. Abbreviations: an3–an11 = antennomeres 3–11, ta1–4 = tarsomeres 1–4.

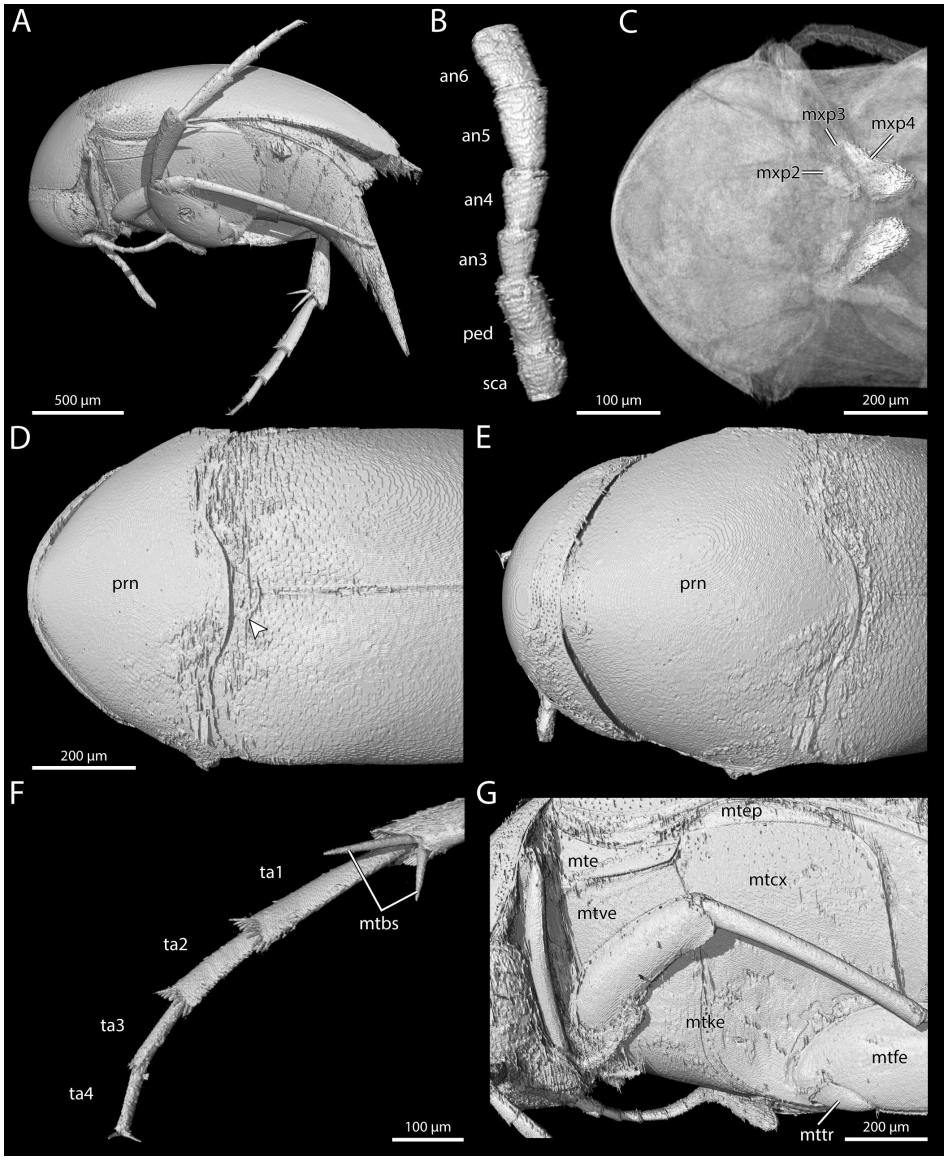

Figure 24. A–F. 3D reconstruction of the holotype of †*Baltistena nigrispinata* Batelka, Tröger & Bock, sp. nov. (Mordellidae). **A.** Habitus in lateral view; **B.** Antennomeres I–VI; **C.** Maxillary palpomeres; **D.** Habitus dorsally (scutellar shield pointed by arrow); **E.** Pronotal disc; **F.** Metatibial spurs; **G.** Thorax laterally. Abbreviations: an3–an6 = antennomeres 3–6, mtbs = metatibial spurs, mtcx = metacoxa, mtfe = metafemur, mte = metanepisternum, mtep = metepimeron, mttr = metatrochanter, mtke = metakatepisternum, mtve = metaventrite, mxp2–4 = maxillary palpomeres 2–4, ped = pedicel, prn = pronotum, sca = scape, ta1–4 = tarsomeres 1–4.

protibia indiscernible. Mesotarsomeres I – III cylindrical, tarsomere I 6.1 × as long as wide; tarsomeres II and III 5.0 × as long as wide; tarsomere IV excised almost to middle region; tarsomere V about 3.0 × as long as wide. Mesotibia very slightly shorter than metatarsomeres combined. Metatibia (Fig. 23C) with three distinct lateral combs of scale-like setae including preapical comb, combs do not reach middle of metatibia; preapical comb runs parallel with apical fringe of setae, remaining two combs slightly oblique; few isolated patches of scale-like setae inserted posterior to last dorso-lateral comb. Metatibia with two spurs, outer spur shorter than inner one (Fig. 24F). Metatarsomeres (Fig. 23C) I–IV with row of spiniform setae consisting ventrally of 12 to 17 short, strong setae, formula: 17/14/12/15; metatarsomere I with two black and short lateral combs of scale-like setae and three isolated patches of black setae; metatarsomere II with one short lateral comb of scale-like setae and one black isolated seta, metatarsomeres III – IV without combs; length ratio of metatarsal segments 2.2-1.2-1-1. Pygidium long and straight, 2.4 × as long as hypopygium. Metanepisternum long and narrow, lower corner of posterior edge rounded, anterior edge 3 × as long as posterior edge, ventral edge 7.5 × as long as posterior edge (Fig. 24G). Metakatepisternum restricted to ventral part of thorax, fused with median portion of posterior edge of metaventrite (Fig. 24G). Pretarsal claws long and straight, with 2 indistinct teeth on ventral edge. Tip of pygidium with ring of short black scale-like setae. Lengths in mm: pronotal disc = 0.46, elytra = 1.29, mesotibia = 0.46, metatarsomere I = 0.38, pygidium = 0.73, body without head = ca. 2.

4. Discussion

4.1. Geological provenance of the rediscovered PMJ Pa amber collection

Between the taxonomic and color qualities of the resin pieces, coupled with the IAA results (Table 1), we were able to sort the fossils into Baltic amber and African copal categories to our satisfaction. Initially, the conflict among the qualitative tests and the results from the IAA confounded us. After considering these results, the true significance of the biotic inclusions, however, became clear, resolving the conundrum of fossil source. From our perspective, it was deeply surprising to find specimens interpreted as copal from the IAA tests that were directly labelled as from "Samland Kleinkuhren" in the PMJ Pa collection, especially as there are no reports, to our knowledge, that copal has been found in the Samland Peninsula (See also 4.2.2.). While we were initially skeptical that labels and objects might have been mixed in the small PMJ Pa collection, this seems to be the most likely scenario. We note that von Knorre kept the collection as it was given to him, thus the collection has not been seen and processed until now. The evidence from the PMJ Pa amber collection clearly shows a shift in source, especially from "without" to a confidently assigned one and simply false labeling could be resolved, and thus presents in a small scale what it might look like in another, larger collection.

At the bottom line, the scenario we encountered with this collection illustrates two critical points: (1) the importance of the correct labeling of any specimen, further underscoring the value of accurate corresponding information for contemporary and future research (King 1975; Corado 2005; Donovan and Riley 2013); and (2) the necessity of skepticism for fossils, even when having label data, as it was only the combination of biotic and chemical data that allowed us to draw confident conclusions about "amber" provenance in the present study. While the chemical or biotic evidence alone may have been sufficient, our uncertainty was not resolved until we had both lines of evidence, which clearly showed the inadequacy of the qualitative tests that have been supposed to differentiate between amber and copal.

4.2. Historical conspectus

To arrive at a more comprehensive understanding of the Phyletisches Museum amber collection and the materials contained therein, it was necessary to review the historical literature on amber in general (section 4.2.1) and on the Kleinkuhren locality in particular (section 4.2.2).

4.2.1. From the amber road to the 19th century

In antiquity, Tacitus (circa 56–120 AD) correctly concluded that amber was a tree resin: "*sucum tamen arborum esse intellegas, quia terrena quaedam atque etiam volucria animalia plerumque interlucent, quae implicata humore mox durescente materia*" (that it is a tree sap, however, can be seen from the fact that some crawling, but also flying animals are often visible between, which get into the liquid and are then trapped when the material hardens) Tac. Ger. 45.6 The Baltic Sea has been a source of amber well before the time of Tacitus, as amber from this region has been found in neolithic burial sites (Singer 2016). There exists much older evidence for the use of amber, such as in the cave of Isturitz, dating back to 34,000 years ago (King 2022), but only a brief outline with a focus on Baltic amber shall be given here as full-length books have been published on the subject from various perspectives (e.g., Brost and Dahlstrom 1996; Grimaldi 1996; King 2022).

Through the so called "Amber Road", an ancient trade route, amber was exported from Europe to Asia, the Mediterranean Sea and Egypt (Singer 2008, 2016). Amber might have reached Egypt directly by sea or via Syria, of which the famous Quatna lion would be proof (Mukherjee et al. 2008). In the neolithic era the first use of amber was certainly due to superstition and so the transparent, flammable and, when rubbed, fragrant material was attributed with protective properties. It was worn by the living as jewels or donated as precious grave goods (Andrée 1951; Frondel 1968; Larsson 2010; Vijande Vila et al. 2015). The scientific use of inclusions played a subordinate role during antiquity, despite a few correct inferences that amber is a

tree resin and is originally liquid, for example, Tacitus (see above), Aristotle (*Meteorology* 4.10), or Pliny the Elder (Plin. Nat. 37.11). Nevertheless, the "amber effect" was already known by Plato, which is the oldest mention of the fact that rubbed amber attracts lightweight objects placed near it (Assis 2010). With this only applying to amber, our present terms "electric" and "electricity" are derived from the Ancient Greek ἤλεκτρον (ēlektron) (Andrée 1951).

Considerable time passed until inclusions became demonstrably more important for science, from the Bronze Age via ancient scholars up to the 16th century. As early as in the beginning of 14th century, the paternoster makers used amber for their necklaces (Buchholz 1961; Hinrichs 2007). Amber as jewellery and art is still widely appreciated today (Pileckaitė 2001; Goldenberg 2004; Sado 2022) and one of the most famous goldsmiths in the last century was Toni Koy (1896–1990). Written evidence for the beginning of a scientific use was provided by scholars, such as medical doctors and pharmacists, or affluent persons interested in natural history.

One of the first scientific records, found in Gessner (1565)[-1566], is about the mineral collection of Johannes Kentmann (p. 22–24), who listed in his order "Succina gravida" few insects in amber, for example "*5. Eiufdem coloris, in quo formica*. *Darin ein omeiß*.", *i.e.*, an ant is within. In his work he used the system of minerals published by Agricola (1546) and was in fact one of the first scholars to put it into practice. A comparable scientific collection of that time was owned by Michele Mercati, an Italian polymath (cf. Hinrichs 2007), whose work was published posthumously in 1717 (Mercati 1717; King 2022). Amber was an attractive object in the so-called *Wunderkammern* (cabinets of curiosities), where it was valued more for its beauty than for scientific reasons. Probably one of the best-known wonder chambers is the famous "*Grünes Gewölbe*" in Dresden (Germany), while the most famous and mysterious is the *Bernsteinzimmer* of Königsberg, which was established by the Prussian king Frederick I in 1701 and the following years, and vanished in 1944, in the turmoil of war. The possible survival and whereabouts of this assembly of amber remain a mystery.

In 1742 Nathanael Sendel published his "*Historia Succinorum*" on the Dresdner amber collection of Augustus the Strong (Augustus II, "August der Starke") and his son Friedrich August II. In this remarkable work, which largely deals with animals enclosed in amber as shown in part one "*Historia insectorum succino conditorum*" (Sendel 1742), he laid the foundation of modern amber research (Wichard and Wichard 2008). Even if Sendel erroneously assumed that amber was formed by soil in so-called "Gagat-Veins", as well as some inaccurate species determinations (Greven and Wichard 2010), the merit of this work is undisputed, due in part to the 13 rich lithographs by Christian Friedrich Boetius (1706–1782). Another breakthrough in amber research was achieved by Georg Carl Berendt with his "*Die Insekten im Bernstein*". Berendt was clearly ahead of his time, as he concluded "[…] *die Art ist verschwunden. Dass sie ausgestorben sei, lässt sich nicht behaupten* […] *wahrscheinlich ist sie durch das veränderte Klima nur verdrängt* […] " ([…] the species disappeared. It cannot be said it is extinct […] it has probably only been displaced by the changing climate [...]) (Berendt 1830, pp. 37). The issue of climate change is today more relevant than ever (Flannery 2009, Tollefson 2022), and amber inclusions can provide valuable evidence (Słodkowska 2013; Penney 2010; Penney et al. 2013; Solórzano-Kraemer et al. 2020). Moreover, Berendt was aware of the importance of inclusions for the study of earth's history, and he saw evidence against the constancy of species (Berendt 1830, pp. 5 and 6; Hinrichs 2007). With Berendt a modern state of amber research was reached, with a broad knowledge of insects, and cooperation between researchers with different taxonomic expertise. Furthermore, Berendt already distinguished between copal and true amber and was aware of the true origin of amber as a fossilized resin of a pine tree. Regardless of the theoretical basis of the time, new species were constantly described and the total number of described species from amber surely exceeds 4860 (Briggs 2018; Ross 2021), most of them being insects.

Far fewer specimens have been reported from copal, with a total of only about 120 species from these resins reported or described from East Africa and Madagascar (Solórzano-Kraemer et al. 2020), for example. Copal has been and still is largely undervalued as a scientific resource (Penney 2010; Penney and Preziosi 2013), although it has great potential for the study of recent biodiversity (Delclòs Martínez et al. 2020; Solórzano-Kraemer et al. 2020, 2022). Indeed, the young age of copal inclusions renders them ideal for documenting the loss of biodiversity, particularly since the colonial and industrial eras. Solórzano-Kraemer et al. (2020) recognized amber as > 2.58 Mya, Pleistocene and Holocene copals as between 2.58–0.0117 Mya and 0.0117 Mya–1760 AD, and Defaunation resin as younger than 1760 AD. Faced with the dual threats of global climate change and global deforestation, the intensive study of copal and Defaunation resin along with extant taxa may be our best and last chance to understand our contemporary biotic communities before it is too late.

Symington Grieve wrote in his book about the great auk in 1885:

> "*The following pages have been written in the hope of interesting some in the story of an extinct bird. The whole history of the Great Auk is a sad one – the continued slaughters of the helpless victims culminating in the final destruction of the race on the skerry, named Eldey, off the coast of Iceland, excites to pity. The last of the Great Auks has lived and died. The race was blotted out before naturalists, when too late, discovered it was gone. Regrets are now useless – the living Garefowl is extinct.*"

This happened, because of human influence, as it did for at least another 14 vertebrate species in the last 200 years (Piper 2009). One of the most well-known examples of anthropogenic extinction is the marsupial

Thylacine (*Thylacinus cynocephalus*), which was hunted relentlessly to the margins of extinction, till the last one died in 1936 at Hobart Zoo (Brook et al. 2023). Another famous and quite recent event of extinction, not only through hunting, but also due to habitat loss it that of the passenger pigeons (*Ectopistes migratorius*). Who would have thought that a bird, so common that flock size easily exceeded millions of individuals (Wright 1911), could go extinct? Of course, one key factor was that they were hunted as a food resource, the other on the deforestation, as due to their high specialization in tree nuts, they were not able to find enough food anymore (Guiry et al. 2020). These extinct species, victims of human activities, are today highly valued objects in museums, be it for display, teaching or scientific research.

Humans' fatal impact on environment extinction is progressing at an alarming rate, with a lot of species going extinct without ever being noticed (McKinney 1999; Régnier et al. 2015). Therefore, copal and Defaunation resin are not only a short window to the past, but they should also be a warning, of what is to come. Defaunation resin in particular is not only amenable to µ-CT analysis, as conducted here (Figs 3, 4, 6–11, 17), but also to genomic study, at least in some cases (Modi et al. 2021). With so many recent and near recent taxa to describe, let alone true amber fossils, it is imperative that we recognize the value of all biological specimens preserved in collections.

4.2.2. The Samland and Kleinkuhren localities

Samland, or the Kaliningrad Peninsula of today, is located on the south-eastern shore of the Baltic Sea, which has been part of the Soviet Union and Russia since 1945.

One direct locality (PMJ Pa 5827) from the collection is given as *Kleinkuhren* (in German), today known as Filino, which is located on the north-western tip of Samland. Most specimens contained in the piece were to be very untypical (see sect. 3.1.1. Biotic evidence) for the region of origin on the label, which drove us to further investigate on these localities.

Since the earliest written records of the region, the practice of "*Bernsteingräberey*" (amber mining or fishing) has been exercised by the inhabitants of the coast of Samland, which they also used to earn their living (Weber 1740; Hildt 1803). In 1861, Karl Mayer described the "faunula of Kleinkuhren", with 35 specimens to be found in the marine sandstone (Mayer 1861). According to these findings, he assigned the layer to the Rupelian (33.9 and 27.82 Ma). Noetling and A. von Koenen, came to the same conclusion some years later (Meyer 1914). The age of these sediments was questioned, however, and more recent investigations suggest that it is distinctly older, about 48 Ma (Ritzkowski 1997). Nevertheless, Perkovsky et al. (2007) pointed out that the results of Kaplan et al. (1977) are more reliable and suggested 37.7 Ma (Perkovsky et al. 2007), which in retrospect is closer to Mayer. The age estimations of all these researchers clearly indicate that no copal occurs in the sediments of the Samland region. Additionally, we were not able to find any report that copal has ever been found in the region of Kaliningrad-Oblast or its shores.

With the localities "Samland?" or "Samland, Bernsteinwerke Königsberg" and one with an original invoice (see section 3.1.1 above) the question when the collection was acquired could be further clarified. The Preußischen Bergwerks-Hütten-Aktiengesellschaft (Preussag) was founded on December the 13th in 1923; only a few years later they joined forces to form a manufacturing company known as "Staatliche Bernstein-Manufaktur GmbH' GmbH" (SBM) in 1926 (Erichson and Tomczyk 1998). In 1929, the VEBA (Vereinigte Elektrizitäts- und Bergwerks-AG, Berlin) was established for the uniform financing of the state economic enterprises (Winkler 2019). This indicates that Pa 5863 was purchased between 1923 and 1929. It was not uncommon that amber was sold to entomologists, which was advertised in a timely manner (Königsberg-Pr. 1937). Today, the amount of amber harvested from the Samland peninsula per year was 500 tons in the first decades of the 20th century (Causey 2011).

4.3. Biological conspectus

The primary data that can be captured from fossil organisms ranges from preserved anatomy—whether from sclerites or soft tissue (e.g., Pohl et al. 2010; Boudinot et al. 2022c; Richter et al. 2022)—to chemical composition (e.g., Trueman 2013; Barden et al. 2017; McCoy et al. 2017), with the two sources of information being nearly indistinguishable depending on the tools used and the scale of comparison (e.g., Modi et al. 2021; Jiang et al. 2022). In order to maximize the biological value of fossils, it is essential to identify the geological source unambiguously and to critically evaluate the plausible phylogenetic affinities of the inclusions. While the former requires the tracking or retracing of stone provenance often coupled with chemical tests (e.g., section 3.1.1 above and 4.3.2 below), the latter depends on: (1) the phylogenetic stability of the taxonomic system in question; (2) the quality of anatomical information obtained from the specimen; and (3) the availability of comparable information from extant taxa. In best case scenarios, both the phylogeny and phenotypic affinities of the fossils may be evaluated jointly (e.g., Klopfstein and Spasojevic 2019; Mongiardino Koch and Thompson 2021; Boudinot et al. 2022a) or in sequence, which nearly always requires substantial revision of fossil interpretations (e.g., Fikáček et al. 2020; Boudinot et al. 2022d; Schädel et al. 2022). A special issue of contemporary paleontological phylogenetics is to produce a classification that is both robust and systematically organizes diagnostic information, allowing future works to place fossils with certainty, or at least explicit uncertainty. Below, we highlight both issues via discussion of the Psocodea (section 4.3.1), which are grossly understudied anatomically, and *Dorylus* (section 4.3.2), which have been plagued by taphonomic uncertainty for

over a century. We conclude this section with a consideration of broader issues and methods for paleoentomology (section 4.3.3).

4.3.1. The case of barklice ("Psocoptera"), an underestimated and undeservedly spurned group

The barklice, or the psocopteran grade of the order Psocodea, are in a twilight zone of phylogenetic paleontology, as fossil material is very abundant from the present through the Mesozoic, yet the extant taxa are grossly understudied anatomically (Yoshizawa 2002; Mockford 2018; Kawata et al. 2022). Moreover, only the sub- and infraordinal relationships have been resolved via molecular systematics (de Moya et al. 2021), with the exception of a few families (Mockford 1999; Yoshizawa and Johnson 2008). As a consequence, a well-founded system to place fossils is lacking. The morphological assumptions of prior generations of taxonomists are largely untested, hence still dominant in the process of taxonomic determination and evolutionary inference. This is in addition to being problematic for understanding Psocodea for their own sake. This reduces the phylogenetic key role of the group as either sister to the Holometabola or the Condylognatha (Misof et al. 2014), which are issues of crucial importance to broader insect phylogenetics and evolutionary history.

Two extinct taxa directly highlighting the present difficulties of psocodean systematics are †*Arcantipsocus* and †*Paramesopsocus*, both originally placed in new, nominotypical families (Azar et al. 2008, 2009), and now considered to belong to Amphientomidae and Electrentomidae, respectively (Mockford et al. 2013). In both cases, the authors relied on the cladistic analysis of Yoshizawa (2002) for morphological characters. Azar et al. (2008, 2009) recognized that the taxonomic sampling of Yoshizawa (2002) was focused on Psocomorpha. Nevertheless, they placed their fossils using the characters of that study as the matrix was the most comprehensive that was available. As a consequence, both paleontological studies attributed the fossils to Psocomorpha, with overreliance on the thick pterostigma and presence of the nodus, which were considered as autapomorphies of the suborder (Yoshizawa 2002). By studying an expanded sample of fossil and extant taxa, Mockford et al. (2013) recognized that these characters are homoplastic among the suborders, and that other, less prominent features reasonably place †*Paramesopsocus* near Amphientomidae and †*Arcantipsocus* within this family. Even though this is certainly an improvement, these placements have yet to be incisively scrutinized using adequate data sets and analytical methods.

Both examples underline the problems with placing fossils into insufficiently founded systems, where relationships are often not supported by well-defined apomorphies, or where assumptions have yet to be tested. A specific problem in psocodean systematics is the almost exclusive use of characters of wing venation and genitalia, while most other body parts or organs are understudied and neglected during investigations. In a comparative sense, it is surprising that the shape and presence or absence of sclerites (except for genital structures) are very rarely used in systematic research on Psocodea, in contrast to other groups or insects (see, e.g., Pohl and Beutel 2005; Beutel et al. 2011). They are often the best-preserved characters in amber fossils besides the wings and might provide many phylogenetically informative features. It is conceivable that the missing access to new technologies may impede scientific progress in this field. Moreover, many fossils are simply not sufficiently preserved for detailed observation. With our present work, we hope to ignite interest in a more thorough morphological analysis of extant and fossil Psocodea, particularly using modern morphological methods such as μ-CT and computer rendering, which can reveal rich morphological data from limited material (Figs 7–11).

4.3.2. The case of *Dorylus*, a long historical arc

Ants of the genus *Dorylus* dominate Old World tropical ecosystems above and below ground, where they occur, and have long fascinated and challenged systematists working on ants (Gotwald 1995; Borowiec 2016; Boudinot et al. 2021). As such, the geological age and paleogeographic distribution of their crown clade is of considerable interest. Any fossils potentially attributable to *Dorylus* are thus of substantial evolutionary importance. In the present study, we identified one such species represented by dozens of individual specimens preserved in resins labeled as "Baltic amber" from the PMJ Pa collection (Figs 2, 3). The temptation to accept this assumption as a conclusion was powerful, yet we struggled to make sense of the initial qualitative tests. We therefore sent samples of the resin matrix for FT-IR, which contradicted the hypothesis that these specimens were from Eocene-aged succinite. Still not satisfied, we subjected one quality exemplar of this *Dorylus* species to SR-μ-CT scanning and 3D reconstruction (Appendix 1: Fig. A1).

With our μ-CT data, we were able to identify the PMJ Pa *Dorylus* as belonging to the extant subspecies *Dorylus nigricans molestus*, based on the key to subgenera from Gotwald (1982) and the key to the *D. nigricans* species group (former *Anomma*) of Santschi (1912). Specifically, the fossil has 11-merous antennae with flagellomeres that are longer than wide, the terminal abdominal tergum has well-defined ridges around its central depression, the spines of the frontal carinae and posterolateral corners of the head are lacking, the petiole widens posteriorly as seen in dorsal view, and the ventral posterolateral corners of the node angular and produced, rather than rounded. Coupled with the identification of the synincluded platypodine as a member of an extant metapopulation, we were forced to reject the succinite hypothesis. Subsequent ^{14}C analysis resulted in an estimated age of ~145 years for the *D. n. molestus*-bearing piece, squarely falling in the category of Defaunation resin. Although these specimens are not as ancient as we were led to believe by the original labels, they may yet be of systematic value: To resolve the species boundaries of this complex, a comprehensive

revision of *Dorylus nigricans* integrating sequence and morphological data is necessary (see Wilson and Brown 1953 on subspecies in myrmecology and Borowiec 2019 for further consideration in the context of Dorylinae).

The PMJ Pa *D. n. molestus* are far from the first positive subfossil members of *Dorylus* and the first false positive *Dorylus* from Baltic amber. Alongside the doryline *Neivamyrmex iridescens* from Colombian copal, DuBois (1998) previously reported *D. n. molestus* from confirmed East African copal *sensu lato*. Over a century before, F. Smith (1868) had identified a *Dorylus* ("being either *Anomma rubella* or a closely related species", p. 184) from what he assumed to be Baltic amber, but which was later determined to be East African copal (Grimaldi et al. 1994; O'Hara et al. 2013). Notably, "*Anomma rubella*" is currently considered to be *Dor. nigricans rubellus* (Savage, 1849), which suggests that the imperfect F. Smith may have handled material quite similar to, if not from the same source, as that of the PMJ Pa and those cited by DuBois (1998). Even more recently, Solórzano-Kraemer et al. (2022) figured multiple unidentified *Dorylus* specimens from Holocene copal (= Defaunation resin) from Tanzania (their fig. 11e, f), while the unavailable name †*Dissumulodorylus perseus* was provided for specimens of putative Baltic origin (Sosiak et al. 2022), which were later revealed via FT-IR to be sub-fossil resin by those authors (Sosiak et al. 2023a, b). Although moot due to unavailability, which we maintain, key structural details for species-level identification were not visible in their scans even after refined segmentation (Dubovikoff and Zharkov 2023). The work of Sosiak et al. (2022, 2023a, b) is an exemplary demonstration of biological hypothesis testing, and further underscores the necessity for a critical approach to the use of "amber" fossils for systematics and evolutionary influence.

4.3.3. Fossil evaluation: Further pitfalls

The two direct examples arising from the main part of this study illustrate the dual difficulties and importance of correctly identifying fossil provenance (section 4.3.2) and placing fossils in systems, when robust phylogenetic and anatomical documentation is lacking (section 4.3.1). With the deep and expanding backlog of amber fossils from Eocene Baltic and other sources (e.g., Peris et al. 2016; Delclòs et al. 2023), a true flood has become available with the intensive exploration of Burmese Kachin amber (e.g., Ross 2019, 2021; Boudinot 2020; Boudinot et al. 2020; Peris and Rust 2020; Pohl et al. 2021; Beutel et al. acc. pend. minor revision), all of which necessitates critical care in the treatment of anatomical information from these and other fossils, including adpression fossils, which may be older but are usually less well-preserved (e.g., Boudinot et al. 2022b). In addition to inadequacy of the phylogenetic system (point 1, section 4.3.1), insufficient morphological documentation (point 2, section 4.3.1), and failure to compare fossils to extant taxa (or absence of comparable information; point 3, section 4.3.1), we recognize three more shortcomings that, in variable combination, may lead to problematic inferences: (4) lack of taxonomic and evolutionary context, e.g., no keys, character lists or data matrices are provided; (5) inexpert knowledge of potentially related extant groups; and (6) inadequate phylogenetic evaluation. Because the literature is rapidly being filled with incautious conclusions, which are hard to correct, we find it unfortunately necessary to outline these issues and some examples so as to encourage finer comparative attention to detail.

The erroneous conclusions of two examples may have been emolliated via taxonomic specialist contribution (e.g., Li et al. 2022; see also Vitali 2019). Critical reevaluation of a putative mordellid larva from Cretaceous amber (Zippel et al. 2022) found that the insect in question is a sawfly (Batelka and Engel 2022), possibly belonging to the family Blasticomidae (Rasnitsyn and Müller 2023), while putative "triungulins" of Strepsiptera (Schawaroch et al. 2005) were eventually correctly placed based on piecemeal reconstruction of fine structures (Beutel et al. 2016, Batelka et al. 2019) with the final clarification provided by Pohl et al. (2018), wherein the first true strepsipteran primary larva enclosed in amber was identified. A third example, that of the putative new beetle family †Ptismidae (Kirejtshuk et al. 2016), was recognized as a synonym of the scirtiform family Clambidae after it was shown that this taxon was defined based on symplesiomorphies and gross rather than specific, structural similarities (Cai et al. 2019). As in many "high throughput" studies on amber fossils, the documentation and interpretation of morphological features were insufficient.

Beyond problems of nomenclature and systematics, lack of precise observation and identification may also lead to evolutionary misinterpretations that may have ramifying consequences for paleoecology. For example, there are presently only few events of pollination documented in the fossil record of the Cretaceous and Cenozoic and these should be taken with caution (e.g., Peña-Kairath et al. 2023). A new species of the cucujoid family Kateretidae was described by Tihelka et al. (2021), who suggested that the beetle was feeding on angiosperm pollen and was acting as a pollinator, thus seemingly revealing a very early event on beetle-angiosperm interaction. However, it was shown by Bao et al. (2022) that the pollen in question was in fact of gymnosperm origin and not ingested by the beetle via careful documentation and experimental replication of pollinivory.

An apparent and frequent problem in insect paleoentomology are fossil placements based more-or-less on intuition (e.g., Kirejtshuk et al. 2016; Kirejtshuk 2020), rather than arguments in the sense of synapomorphies or formal phylogenetic analyses based on maximum parsimony (MP) or Bayesian inference (BI). The placement of adpression fossils was formally evaluated by Fikáček et al. (2020) and Boudinot et al. (2022d), using morphological data sets and phylogenetic topologies based on comprehensive molecular data sets. A similar approach was recently applied to minute myxophagan beetles in Burmese amber (Fikáček et al. 2023). The characters were analyzed

in a Bayesian framework under different schemes of constraints, also using phylogenetic patterns based on molecular phylogenies. It is still a common practice in paleoentomology to erect and shift extant or extinct taxa without adequate analyses or at least phylogenetic arguments in the sense of apomorphies (e.g., Kirejtshuk 2020). However, this approach leads to random taxonomic and phylogenetic changes, lacks a solid basis, and does not help to understand the evolution of beetles and other groups (e.g., Fikáček et al. 2020; Boudinot et al. 2023).

4.4. Technological Conspectus: Phenomics

A key technology transforming the study of insect anatomy and evolution is micro-computed tomography (μ-CT), which allows for the non-destructive, replicable, quantitative sampling of structures at the submicron scale either preserved or in motion, in the case of x-ray kinematics (or cineradiography, e.g., van de Kamp et al. 2015; Wulff et al. 2017). The non-invasive generation of phenomic data further allows for the evaluation of complex functional interactions, such as for the metasoma of Scorpiones (Günther et al. 2021) and copulation in Strepsiptera (Peinert et al. 2016; Jandausch et al. 2023), Hymenoptera (Semple et al. 2021), and Lepidoptera (Zlatkov et al. 2023). For the purposes of paleoentomology, μ-CT has profound advantage as beam penetrance allows for the discovery of biological inclusions in opaque amber (Lak et al. 2008), phosphatized nodules (van de Kamp et al. 2018), and even Triassic coprolites (Qvarnström et al. 2021). In a pair of studies on Cretaceous stem ants (Boudinot et al. 2022c; Richter et al. 2022), it was discovered that soft tissue may be preserved in spectacular detail, including a nearly complete cephalic muscle set, glands, and elements of the central nervous system, and the utility of μ-CT was demonstrated for revisionary systematics and phylogenetic character discovery. That μ-CT is especially valuable for character discovery and phylogenetic hypothesis testing was also demonstrated in a study on the prosternum of extant Hymenoptera (Boudinot et al. in prep.), which expanded the available anatomical variables of this structure from 11 to 124. This study further showed potential for μ-CT as a tool for museomics, as a century-old specimen produced high-quality scan data, complementing genome capture from preserved material (e.g., Blaimer et al. 2016). Although relatively time-consuming, even simple surface renders may be highly informative (e.g., Garcia et al. 2019; Jałoszyński et al. 2020), especially for rare taxa or irreplaceable specimens (e.g., Simonsen and Kitching 2014) and when used as one prong of a multi-modal approach for phenotype documentation, alongside green-fluorescent light for fossils (e.g., Clarke et al. 2018; Boudinot et al. 2020, 2022c), and SEM, CLSM, and manual histology for extant taxa (e.g., Richter et al. 2019, 2023; see also Friedrich and Beutel 2008, Friedrich et al. 2014).

Even though the loss of information and amount of artefacts are usually very low, some aspects must be taken into account: (a) depending on fixation considerable deformation can occur, as for instance tissue preserved in ethanol can shrink through dehydration, depending on time and tissue properties up to a loss of 60% of the original volume (Hedrick et al. 2018; Leonard et al. 2022); (b) imaging contrast can be distinctly improved by iodine-staining (Metscher 2009) but this can demineralize specimens immersed for a longer time span (Early et al. 2020); (c) stained specimens can be de-stained very efficiently using thiosulfate solution, but this can increase calcium solubility and cause decalcification (Mataic and Bastani 2006; see Callahan et al. 2021 for a de-staining protocol); (d) desktop micro-CT scanners are still expensive and energy consuming, and not accessible for all scientists; (e) the post-processing of the data can be very time consuming; and (f) in the case of most synchrotron-scanned resin pieces a dark band occurs where the beam passed (e.g., Pohl et al. 2019; Sadowski et al. 2021), consequently thus it is also preferable that the piece should be carefully documented with photographs before scanning. Care should always be taken not to use an excessive level of energy of synchrotron radiation, as this can be destructive or leave behind an irreversible brownish band to the amber. The documentation of structural details can be enhanced by isolating individual structures of a certain specimen through physical preparation, or using an intact specimen; the target focal areas can be cleaned with chloroform (Ammar et al. 2015). Moreover, appropriate cleaning can distinctly reduce artifacts and thus accelerate the further processing. This can be further optimized with AI, for instance by using Biomedisa (Lösel et al. 2020).

Another major advantage of μ-CT data is that they can be made available to the community in suitable databases. A specimen gone through the three steps mentioned above can be distributed to scientists or the public in various forms. The data accessibility is crucial in different ways, but especially so for museum material and type specimens (Faulwetter et al. 2013), with cybertypes having use even beyond classificatory purposes (e.g., Naumann et al. 2020). For many active researchers, access to type material is often very difficult (Orr et al. 2020). Shipping is expensive and bears an enormous risk of damage or even losing specimens. In most cases, the scientific benefit and the entitlement of scientists to study the fauna of their country outweighs this risk (Dupérré 2020). However, μ-CT data can be made available electronically and thus open a new dimension of making specimens accessible, in the ideal case even including surface textures and color (Ijiri et al. 2018). Even though digital information can never fully replace the physical type specimens (Rogers et al. 2017), it is a highly efficient way to facilitate revisions and also to stimulate scientific inquiry and discussion in different contexts. Even if technical resources are limited, this can be extended using models from platforms like Sketchfab (Epic Games, Cary, North Carolina, USA) or MorphoSource (MorphoSource.org). In our study as well as in previous contributions (Aibekova et al. 2022; Tröger et al. 2023; Weingardt et al. 2023), these options were used to visualize complex

3-dimensional structures in an easily accessible way to contribute to a better understanding of insect morphology.

A final aspect of µ-CT data that confers unique advantage is for museums- and classroom-based pedagogy (e.g., Shelmerdine et al. 2018). School children and students can examine, disassemble, and assemble a wide variety of objects which enhances the understanding of complex 3D objects. The risk of damage is negligible compared to real specimens or wax models. This has been successfully demonstrated with the neurocranium of the mud-shark *Squalus acanthias* at the Institute of Zoology and Evolutionary Research of the Friedrich Schiller University (Jena, Germany) (Moritz pers. comm., 2022). 3D reconstructions are further advantageous as they can be scaled, which facilitates the visualization of structures or even entire animals which are otherwise hardly accessible. In the current project EntomonVR (Saqalaksari et al. 2023) demonstrated new opportunities to study and enhance the understanding of insect morphology in an engaging and appealing way. A less expensive way to present µ-CT results as 3D printed models was used in the exhibition of the Phyletisches Museum, where a copulating pair of leaf beetles (*Neocrepidodera ferruginea*) is on display, which was magnified forty times and airbrushed. With the above mentioned combination, a multisensory approach in museums can be boosted, as it is possible to conserve valuable objects, while allowing visitors to simultaneously handle an authentic copy (Wilson et al. 2017; Ziegler et al. 2020). This includes the option to make objects tangible for visually impaired visitors (Neumüller et al. 2014). The use of CT-scans to create highly realistic enlarged models of different organisms is now gaining great momentum, as for instance demonstrated by 10TONS (https://www.10tons.dk/) or Julia Stoess (https://www.insektenmodelle.de/de/).

5. Conclusion

The only direct documentation of the history of evolution in the dimension of time is the fossil record, for which the highest fidelity of preservation is afforded by exuded resins that may fossilize over the course of millions of years, thus forming amber. To be useful for biodiversity studies, it is critical that the source of inclusion-bearing resins be identified, as the difference in age between true amber and copal or Defaunation resin may profoundly influence ecological, biogeographical, and evolutionary inferences. The rediscovered amber collection of the Phyletisches Museum allowed us to starkly demonstrate this crux, as several pieces labeled as Baltic amber would have represented new generic records for the ant fauna of the Eocene, including the widespread and dominant genera *Crematogaster*, *Dorylus*, *Lepisiota*, and *Pheidole*. Through chemical (FT-IR, UV-VIS, ^{14}C), systematic (anatomical SR-µ-CT reconstruction), and historical investigation, we were able to not only correct the historical mislabeling of these and all other specimens in the amber collection, but to also review and revise the fossil record of *Amphientomum* and the Amphientomidae (Psocodea), several clades of Formicidae (Camponotini, *Crematogaster*, Dorylinae, *Pheidole*, Plagiolepidini, †*Yantaromyrmex*), the Nevrorthidae (Neuroptera), and two beetle genera (*Doliopygus*, Platypodinae; †*Baltistena*, Mordellidae). With respect to fossil resin provenance, we found that the study of historical records is highly useful where these exist, and that the generally recommended qualitative tests for amber identity fail spectacularly when benchmarked against quantitative tests, particularly FT-IR. In brief, when new records of taxa that are millions to tens of millions years older than the oldest known representative, great care should be taken to ensure that label data accurately reflect the source of the fossil material. With the rediscovered *Bernsteinsammlung*, the Phyletisches Museum is now known to comprise Defaunation resin, copal, and succinite (true Baltic amber) as well as Kachin amber. The biological value of subfossil material should not be overlooked.

Conflicts of interest

The authors declare no conflict of interest. The funders had no role in the design of the study; in the collection, analyses, or interpretation of data; in the writing of the manuscript; nor in the decision to publish the results.

Author contributions

Conceptualization: BEB, BLB. Methodology: BEB, BLB, MW, DT, KJ, JUH, HP. Software: JUH. Validation: BEB, BLB. Investigation: BEB, BLB, MW, DT, KJ, JUH, DL, OTDM, JB, AR. Resources: JUH. Data Curation: BEB, BLB, MW, JUH, JB. Writing, original draft: BEB, BLB, DT, MW, JB, DL. Writing, review & editing: RGB, AR, HP. Visualization: MW, DT, BLB. Supervision: RGB, HP. Project administration: BEB, BLB. Funding acquisition: BEB, DT, MW, AR.

Funding

This research was funded by the following.

- Boudinot: the Alexander von Humboldt Stiftung via a research fellowship (2020–2022) and a Peter S. Buck research fellowship at the Smithsonian Institute (2023).
- Richter: the Evangelisches Studienwerk Villigst eV via a scholarship (2020–2022).
- Förderverein Phyletisches Museum Jena e. V.
- Research of Jan Batelka was financed from operational program „Grant Schemes at CU "(reg. no. CZ .02.2.69/0.0/0.0/19_073/0016935).
- Tröger: scholarship of the Deutsche Bundesstiftung Umwelt (DBU) (2022–)
- Weingardt: Landesgraduiertenstipendium (2023–), Honours Programme University of Jena 2021–2022

Data availability statement

The original μ-CT datasets of ‡*Amphientomum knorrei* Weingardt, Bock & Boudinot, sp. nov. (PMJ Pa 5809), Archipsocidae gen. et sp. indet (PMJ Pa 5825), †*Baltistena nigrispinata* Batelka, Tröger & Bock, sp. nov. (PMJ Pa 5870), *Doliopygus* cf. *serratus* (PMJ Pa 5827), *Dorylus nigricans molestus* (PMJ Pa 5884), and the neotype of ‡*Pheidole cordata* (PMJ Pa 5889) are databased and assigned a unique identifier at the Phyletisches Museum (Jena, Germany) and additionally available at the data repository MorphoSource (URL: https://www.morphosource.org/projects/000547325?locale=en) with the reference numbers: 000549407 (†*Amphientomum knorrei* Weingardt, Bock & Boudinot, sp. nov.), 000549379 (Archipsocidae gen. et sp. indet.), 000549353 (*Dorylus nigricans molestus*), 000549006 (†*Baltistena nigrispinata* Batelka, Tröger & Bock, sp. nov.), 000548650 (*Doliopygus* cf. *serratus*), 000552612 (†*Pheidole cordata* Holl 1829, neotype).

Acknowledgments

We thank: Dietrich von Knorre and Matthias Krüger for sharing their profound knowledge of the whole PMJ collection; the International Amber Association (IAA) Gdańsk, Poland for chemical analysis; Brian Fisher, Michele Esposito, and Barry Bolton for AntWeb and AntCat; Charles Lienhard, Lulan Jie, Gurusamy Ramesh, Alexander Rasnitsyn, Christian Schmidt, and Dmitry Vassilenko for sharing Psocodea literature; Vincent Perrichot for loaning Ethiopian amber material; Feiyang Liang for confirming the genus identification of *Amphientomum* and providing additional information on amphientomid genitalia; Phil Ward and Rodolfo da Silva Probst for discussing the ideal treatment of the camponotine fossils; Alêxandre Ferreira for discussing the Defaunation resin *Pheidole*; Bjarte Jordal for identification of the platypodine, provision of literature, and discussion of *Doliopygus* systematics; Eva-Maria Sadowski, David Ware, and Andreas Abele-Rassuly for the possibility to take photographs at the MfN Berlin; and Jill Oberski for providing comment on a pre-submission version of the MS and for consistent discussion during the construction and revision of the work. We also thank Kazunori Yoshizawa and Phil Ward for their incisive and useful feedback on the manuscript, as well as the editor, Sonja Wedmann; we thank Phil once more for catching an embarrassing blunder, for which we are grateful.

We acknowledge the provision of beamtime related to the proposal BAG-20190010 at PETRA III beamline P05 of DESY, a member of the Helmholtz Association (HGF). We acknowledge the support during the beam times by Hereon team members Fabian Wilde, Julian Moosmann, and Felix Beckmann. This research was supported in part through the Maxwell computational resources operated at Deutsches Elektronen-Synchrotron DESY, Hamburg, Germany. Gunnar Brehm for the loan of his lepiLED. Additional support was provided by the Alexander von Humboldt Stiftung (BEB: 2020–2022; the Japan Society for the Promotion of Science (AR: 2023–), the Smithsonian Institute (BEB: 2023), Landesgraduiertenstipendium (MW: 2023–), the Honours Programme from University of Jena (MW: 2021–2022), the Evangelisches Studienwerk Villigst eV (AR: 2020–2022), the Deutsche Stiftung für Umwelt (DT 2022–), the Grant Schemes at Charles University (JB: reg. no. CZ.02.2.69/0.0/0.0/19_073/0016935), Susanne & Jens Wurdinger and the Förderverein Phyletisches Museum e.V.. We are very grateful to the Smithsonian's Biodiversity Heritage Library and the librarians who kindly permitted us to examine an original book (Schweigger 1819) and scanned the pages: Leslie Overstreet and Erin Rushing. Last but not least, we thank the Museum für Naturkunde (Berlin) for waiving the publication costs of our article.

References

Aarle WV, Palenstijn WJ, de Beenhouwer J, Altantzis T, Bals S, Batenburg KJ, Sijbers J (2015) The ASTRA Toolbox: A platform for advanced algorithm development in electron tomography. Ultramicroscopy 157: 35–47. https://doi.org/10.1016/j.ultramic.2015.05.002

Aarle WV, Palenstijn WJ, Cant J, Janssens E, Bleichrodt F, Dabravolski A, de Beenhouwer J, Batenburg KJ, Sijbers J (2016) Fast and flexible X-ray tomography using the ASTRA toolbox. Optics Express 24: 25129–25147. https://doi.org/10.1364/OE.24.025129

Agricola G (1546) De Natura Fossilium. Libri X, Basel.

Aibekova L, Boudinot BE, Beutel RG, Richter A, Keller RA, Hita-Garcia F, Economo EP (2022) The skeletomuscular system of the mesosoma of *Formica rufa* workers (Hymenoptera: Formicidae). Insect Systematics and Diversity 6: 1–26. https://doi.org/10.1093/isd/ixac002

Ammar E-D, Hentz M, Hall DG, Shatters Jr RG (2015) Ultrastructure of wax-producing structures on the integument of the melaleuca psyllid *Boreioglycaspis melaleucae* (Hemiptera: Psyllidae), with honeydew excretion behavior in males and females. PLoS ONE 10: e0121354. https://doi.org/10.1371/journal.pone.0121354

André E (1895) Notice sur les fourmis fossiles de l'ambre de la Baltique et description de deux espèces nouvelles. Bulletin de la Société Zoologique de France 20: 80–84.

Andrée K (1951) Der Bernstein – Das Bernsteinland und sein Leben. Kosmos, Stuttgart 95 pp.

AntWeb (2022) Version 8.77.4. California Academy of Science. https://www.antweb.org [last accessed 18 July 2022]

Assis AKT (2010) The experimental and historical foundations of electricity. Apeiron, Montreal, 268 pp. https://doi.org/10.1007/s11191-010-9318-z

Azar D, Hajar L, Indary C, Nel A (2008) Paramesopsocidae, a new Mesozoic psocid family (Insecta: Psocodea "Psocoptera": Psocomorpha). Annales de la Société Entomologique de France 44: 459–470. https://doi.org/10.1080/00379271.2008.10697581

Azar D, Nel A, Néraudeau D (2009) A new Cretaceous psocodean family from the Charente-Maritime amber (France) (Insecta, Psocodea, Psocomorpha). Geodiversitas 31: 117–127. https://doi.org/10.5252/g2009n1a10

Bachmayer F (1960) Insektenreste aus den Congerienschichten (Pannon) von Brunn-Vösendorf (südl. von Wien) Niederösterreich. Sitzungsberichte der Österreichischen Akademie der Wissenschaften. Mathematisch-Naturwissenschaftliche Klasse. Abteilung I 169: 11–16. https://doi.org/10.1007/978-3-662-25541-4_1

Badonnel A (1934) Recherches sur l'anatomie des Psoques. 241 pp. [80 figs]

Badonnel A (1948) Psocoptères du Congo Belge (2e note). Revue de Zoologie et de Botanique Africaines 40: 266–322.

Badonnel A (1949) Psocoptères du Congo Belge (3e note). Bulletin de l'Institut Royal des Sciences Naturelles de Belgique 25: 1–64.

Badonnel A (1955) Psocoptères de l'Angola. Publicacões Culturais da Companhia de Diamantes de Angola 26: 1–267.

Badonnel A (1959) Un psoque cavernicole du Moyen-Congo. Revue Suisse de Zoologie 66: 761–764. https://doi.org/10.5962/bhl.part.117922

Badonnel A (1967) Insectes Psocoptères. Faune de Madagascar 23: 1–235.

Badonnel A (1979) Psocoptères de la Côte d'Ivoire (2e note). Revue Suisse de Zoologie 86: 11–22. https://doi.org/10.5962/bhl.part.82275

Bao T, Wedmann S, Grímsson F, Beutel RG, Seyfullah L, Bao L, Jarzembowski EA (2022) Was the kateretid beetle *Pelretes* really a Cretaceous angiosperm pollinator? Nature Plants 8: 38–40. https://doi.org/10.1038/s41477-021-01044-3

Barden P, Herhold HW, Grimaldi DA (2017) A new genus of hell ants from the Cretaceous (Hymenoptera: Formicidae: Haidomyrmecini) with a novel head structure. Systematic Entomology 42: 837–846. https://doi.org/10.1038/s41477-021-01044-3

Baroni Urbani C (1995) Invasion and extinction in the West Indian ant fauna revisited: the example of *Pheidole* (Amber Collection Stuttgart: Hymenoptera, Formicidae. VIII: Myrmicinae, partim). Stuttgarter Beitrage zur Naturkunde. Serie B, Geologie und Palaontologie 222: 1–12.

Batelka J, Engel MS (2022) The 'first fossil tumbling flower beetle' larva is a symphytan (Hymenoptera). Acta Entomologica Musei Nationalis Pragae 62: 57–59. https://doi.org/10.37520/aemnp.2022.005

Batelka J, Prokop J, Pohl H, Bai M, Zhang W, Beutel RG (2019) Highly specialized Cretaceous beetle parasitoids (Ripiphoridae) identified with optimized visualization of microstructures. Systematic Entomology 44: 396–407. https://doi.org/10.1111/syen.12331

Batelka J, Rosová K, Prokop J (2023) Diversity and morphology of Eocene and Oligocene Mordellidae (Coleoptera). Acta Entomologica Musei Nationalis Pragae 63: 451–478. https://doi.org/10.37520/aemnp.2023.027

Beaver RA, Löyttyniemi K (1985) The platypodid ambrosia beetles of Zambia (Coleoptera: Platypodidae). Revue Zoologique Africaine 99: 113–134.

Berendt GC (1830) Die Insekten im Bernstein: Ein Beitrag zur Thiergeschichte der Vorwelt. Nicolai, Danzig, 38 pp.

Beutel RG, Friedrich F, Hörnschemeyer T, Pohl H, Hünefeld F, Beckmann F, Meier R, Misof B, Whiting MF, Vilhelmsen L (2011) Morphological and molecular evidence converge upon a robust phylogeny of the megadiverse Holometabola. Cladistics 27: 341–355. https://doi.org/10.1111/j.1096-0031.2010.00338.x

Beutel RG, Zhang WW, Pohl H, Wappler T, Bai M (2016) A miniaturized beetle larva in Cretaceous Burmese amber: Reinterpretation of a fossil "strepsipteran triungulin". Insect Systematics & Evolution 47: 83–91. https://doi.org/10.1163/1876312x-46052134

Beutel RG, Xu Ch-P, Jarzembowski E, Kundrata R, Boudinot BE, McKenna D, Goczał J (acc. pend. minor revision) The evolutionary history of Coleoptera (Insecta) in the late Paleozoic and the Mesozoic. Systematic Entomology [acc. pend. minor rev.].

Bisulca C, Nascimbene PC, Elkin L, Grimaldi DA (2012) Variation in the deterioration of fossil resins and implications for the conservation of fossils in amber. American Museum Novitates 2012: 1–19. https://doi.org/10.1206/3734.2

Blaimer BB, Brady SG, Schultz TR, Lloyd MW, Fisher BL, Ward PS (2015) Phylogenomic methods outperform traditional multi-locus approaches in resolving deep evolutionary history: A case study of formicine ants. BMC Evolutionary Biology 15(271): 1–14. https://doi.org/10.1186/s12862-015-0552-5

Blaimer BB, Lloyd MW, Guillory WX, Brady SG (2016) Sequence capture and phylogenetic utility of genomic ultraconserved elements obtained from pinned insect specimens. PLoS ONE 11: e0161531. https://doi.org/10.1371/journal.pone.0161531

Bolton B (1995) A new general catalogue of the ants of the world. Cambridge, Mass.: Harvard University Press, 504 pp.

Bolton B (2003) Synopsis and classification of Formicidae. Memoirs of the American Entomological Institute 71: 1–370.

Bolton B (2023) AntCat, an Online Catalog of the Ants of the World by Barry Bolton. https://antcat.org [accessed 31 October 2023]

Borgmeier T (1940) Duas notas myrmecologicas. Revista de Entomologia (Rio de Janeiro) 11: 606.

Borgmeier T (1950) Uma nova espécie do gênero *Neivamyrmex* Borgmeier (Hym. Formicidae). Revista de Entomologia (Rio de Janeiro) 21: 623–624.

Borowiec ML (2016) Generic revision of the ant subfamily Dorylinae (Hymenoptera, Formicidae). ZooKeys 608: 1–280. https://doi.org/10.3897/zookeys.608.9427

Borowiec ML (2019) Convergent evolution of the army ant syndrome and congruence in big-data phylogenetics. Systematic Biology 68: 642–656. https://doi.org/10.1093/sysbio/syy088

Boudinot BE, Probst RS, Brandão CRF, Feitosa RM, Ward PS (2016) Out of the Neotropics: Newly discovered relictual species sheds light on the biogeographical history of spider ants (*Leptomyrmex*, Dolichoderinae, Formicidae). Systematic Entomology 41: 658–671. https://doi.org/10.1111/syen.12181

Boudinot BE (2018) A general theory of genital homologies for the Hexapoda (Pancrustacea) derived from skeletomuscular correspondences, with emphasis on the Endopterygota. Arthropod Structure & Development 47: 563–613. https://doi.org/10.1016/j.asd.2018.11.001

Boudinot BE (2020) Systematic and Evolutionary Morphology: Case Studies on Formicidae, Mesozoic Aculeata, and Hexapodan Genitalia. University of California, Davis.

Boudinot BE, Perrichot V, Chaul JCM (2020) †*Camelosphecia* gen. nov., lost ant-wasp intermediates from the mid-Cretaceous (Hymenoptera, Formicoidea). ZooKeys 1005: 21–55. https://doi.org/10.3897/zookeys.1005.57629.figure13

Boudinot BE, Moosdorf OTD, Beutel RG, Richter A (2021) Anatomy and evolution of the head of *Dorylus helvolus* (Formicidae: Dorylinae): Patterns of sex- and caste-limited traits in the sausagefly and the driver ant. Journal of Morphology 282: 1616–1658. https://doi.org/10.1002/jmor.21410/v2/response1

Boudinot BE, Borowiec ML, Prebus MM (2022a) Phylogeny, evolution, and classification of the ant genus *Lasius*, the tribe Lasiini and the subfamily Formicinae (Hymenoptera: Formicidae). Systematic Entomology 47: 113–151. https://doi.org/10.1111/syen.12522

Boudinot BE, Khouri Z, Richter A, Griebenow ZH, van de Kamp T, Perrichot V, Barden P (2022b) Evolution and systematics of the Aculeata and kin (Hymenoptera), with emphasis on the ants (Formicoidea: †@@@idae fam. nov., Formicidae). bioRxiv, 450 pp. https://doi.org/10.1101/2022.02.20.480183

Boudinot BE, Richter A, Katzke J, Chaul JCM, Keller RA, Economo EP, Beutel RG, Yamamoto S (2022c) Evidence for the evolution of eusociality in stem ants and a systematic revision of †*Gerontoformica*

(Hymenoptera: Formicidae). Zoological Journal of the Linnean Society 195: 1355–1389. https://doi.org/10.1093/zoolinnean/zlab097

Boudinot BE, Yan EV, Prokop J, Luo X-Z, Beutel RG (2022d) Permian parallelisms: Reanalysis of †Tshekardocoleidae sheds light on the earliest evolution of the Coleoptera. Systematic Entomology 48: 69–96. https://doi.org/10.1111/syen.12562

Boudinot BE, Fikáček M, Liebermann ZE, Kusy D, Bocak L, Mckenna DD, Beutel RG (2023) Systematic bias and the phylogeny of Coleoptera—A response to Cai et al. (2022) following the responses to Cai et al. (2020). Systematic Entomology 48: 223–232. https://doi.org/10.1111/syen.12570

Briggs DE (2018) Sampling the insects of the amber forest. Proceedings of the National Academy of Sciences of the United States of America 115: 6525–6527. https://doi.org/10.1073/pnas.1807017115

Broadhead E (1950) A revision of the genus *Liposcelis* Motschulsky with notes on the position of this genus in the order Corrodentia and on the variability of ten *Liposcelis* species. Transactions of the Royal Entomological Society of London 101: 335–388. https://doi.org/10.1111/j.1365-2311.1950.tb00449.x

Broadhead E, Richards AM (1982) The Psocoptera of East Africa — A taxonomic and ecological survey. Biological Journal of the Linnean Society, Linnean Society of London 17: 137–216. https://doi.org/10.1111/j.1095-8312.1982.tb01545.x

Broadhead E, Wolda H (1985) The diversity of Psocoptera in two tropical forests in Panama. Journal of Animal Ecology 54: 739–754. https://doi.org/10.2307/4375

Brook BW, Sleightholme SR, Campbell CR, Jarić I, Buettel JC (2023) Resolving when (and where) the Thylacine went extinct. The Science of the Total Environment 877: 162878. https://doi.org/10.1016/j.scitotenv.2023.162878

Brost L, Dahlstrom A (1996) The Amber Book. Mountain Press Pub. Co., Missoula Mt, 134 pp.

Buchholz H (1961) Ein kurzer Führer durch die Sonderausstellung des Wandernden Museums Schleswig-Holstein. Bernstein - das Gold des Nordens. Schmidt & Klaunig, Kiel.

Buckley SB (1866) Descriptions of new species of North American Formicidae. Proceedings of the Entomological Society of Philadelphia 6: 152–172.

Cai C, Lawrence JF, Yamamoto S, Leschen RA, Newton AF, Ślipiński A, Yin Z, Huang D, Engel MS (2019) Basal polyphagan beetles in mid-Cretaceous amber from Myanmar: Biogeographic implications and long-term morphological stasis. Proceedings of the Royal Society B, Biological Sciences 286: 20182175. https://doi.org/10.1098/rspb.2018.2175

Callahan S, Crowe-Riddell JM, Nagesan RS, Gray JA, Davis Rabosky AR (2021) A guide for optimal iodine staining and high-throughput diceCT scanning in snakes. Ecology and Evolution 11: 11587–11603. https://doi.org/10.1002/ece3.7467

Carpenter FM (1930) The fossil ants of North America. Bulletin of the Museum of Comparative Zoology 70: 1–66.

Casadei-Ferreira A, Chaul JCM, Feitosa RM (2019) A new species of *Pheidole* (Formicidae, Myrmicinae) from Dominican amber with a review of the fossil records for the genus. ZooKeys 866: 117–125. https://doi.org/10.3897/zookeys.866.35756

Causey F (2011) Amber and the ancient world. Getty Publications, 144 pp. https://doi.org/10.1515/etst-2013-0005

Clarke DJ, Limaye A, McKenna DD, Oberprieler RG (2018) The weevil fauna preserved in Burmese amber—snapshot of a unique, extinct lineage (Coleoptera: Curculionoidea). Diversity 11: 1. https://doi.org/10.3390/d11010001

Chapuis F (1865) Monographie des Platypides. H. Dessain, Liège, 344 pp. https://doi.org/10.5962/bhl.title.9204

Chen C, Li B, Kanari M, Lu D (2019) 3. Epoxy adhesives. In: Rudawska A (Ed.) Adhesives and adhesive joints in industry applications. IntechOpen, 148 pp. https://doi.org/10.5772/intechopen.86387

Cockerell TDA (1915) British fossil insects. Proceedings of the United States National Museum 49: 469–499. https://doi.org/10.5479/si.00963801.49-2119.469

Corado R (2005) The importance of information on specimen labels. Ornitologia Neotropical 16: 277–278.

De Andrade ML (1998a) Fossil and extant species of *Cylindromyrmex* (Hymenoptera: Formicidae). Revue Suisse de Zoologie 105: 581–664. https://doi.org/10.5962/bhl.part.80052

De Andrade ML (1998b) First description of fossil *Acanthostichus* from Dominican amber (Hymenoptera: Formicidae). Mitteilungen der Schweizerische Entomologische Gesellschaft 71: 269–274.

Deharveng L, D'Haese CA, Grandcolas P, Thibaud J-M, Weiner WM (2017) Judith Najt. A life dedicated to Collembola and research support for systematics. Zoosystema 39: 5–14. https://doi.org/10.5252/z2017n1a1

Delclòs Martínez X, Peñalver Mollá E, Ranaivosoa V, Solórzano-Kraemer MM (2020) Unravelling the mystery of 'Madagascar copal': Age, origin and preservation of a Recent resin. PLoS ONE 15: e0232623. https://doi.org/10.1371/journal.pone.0232623

Delclòs Martínez X, Peñalver E, Barrón E, Peris D, Grimaldi DA, Holz M, Labandeira CC, Saupe EE, Scotese CR, Solórzano-Kraemer MM, Álvarez-Parra S, Arillo A, Azar D, Cadena EA, Dal Corso J, Kravčec J, Monleón-Getino A, Nel A, Peyrto D, Bueno-Cebollada CA, Gallardo A, González-Fernández B, Goula M, Jaramillo C, Kania-Kłosok I, López-Del Valle R, Lozano RP, Meléndez N, Menor-Salván C, Peña-Kairath C, Perrichot V, Rodrigo A, Sánchez-García A, Santer M, Sarto i Monteys V, Uhl D, Luis Viejo J, Pérez-de la Fuente R (2023) Amber and the Cretaceous Resinous Interval. Earth-Science Reviews 243: 104486. https://doi.org/10.1016/j.earscirev.2023.104486

Del Toro I, Pacheco JA, MacKay WP (2009) Revision of the ant genus *Liometopum* (Hymenoptera: Formicidae). Sociobiology 53: 299–369.

de Moya RS, Yoshizawa K, Walden KK, Sweet AD, Dietrich CH, Kevin PJ (2021) Phylogenomics of parasitic and nonparasitic lice (Insecta: Psocodea): combining sequence data and exploring compositional bias solutions in next generation data sets. Systematic Biology 70: 719–738. https://doi.org/10.1093/sysbio/syaa075

Dlussky GM (1988) Ants of Sakhalin amber (Paleocene?). Paleontologicheskii jurnal [Палеонтологический журнал] 1988: 50–61. [In Russian]

Dlussky GM (2009) The ant subfamilies Ponerinae, Cerapachyinae and Pseudomyrmecinae (Hymenoptera, Formicidae) in the Late Eocene ambers of Europe. Paleontological Journal 43: 1043–1086. https://doi.org/10.1134/s0031030109090068

Dlussky GM (2010a) Ants of the genus *Plagiolepis* Mayr (Hymenoptera, Formicidae) from Late Eocene ambers of Europe. Paleontologicheskii jurnal [Палеонтологический журнал] 2010: 64–73. https://doi.org/10.1134/s0031030110050096 [In Russian]

Dlussky GM (2010b) Ants of the genus *Plagiolepis* Mayr (Hymenoptera, Formicidae) from Late Eocene ambers of Europe. Paleontological Journal 44: 546–555. https://doi.org/10.1134/s0031030110050096

Dlussky GM, Dubovikoff DA (2013) *Yantaromyrmex* gen. n. – a new ant genus (Hymenoptera: Formicidae) from Late Eocene ambers of

Europe. Caucasian Entomological Bulletin 9: 305–314. https://doi.org/10.23885/1814-3326-2013-9-2-305-314

Dlussky GM, Perkovsky EE (2002) Ants (Hymenoptera, Formicidae) from the Rovno Amber. Vestnik Zoologii 36: 3–20. [In Russian]

Dlussky GM, Perfilieva KS (2014) Superfamily Formicoidea Latreille, 1802. In: Antropov AV, Belokobylskij SA, Compton SG, Dlussky GM, Khalaim AI, Kolyada VA, Kozlov MA, Perfilieva KS, Rasnitsyn AP (Eds) The Wasps, Bees and Ants (Insecta: Vespida=Hymenoptera) from the Insect Limestone (Late Eocene) of the Isle of Wight, UK. Earth and Environmental Science Transactions of the Royal Society of Edinburgh 104: 410–438. https://doi.org/10.1017/s1755691014000103

Dlussky GM, Putyatina TS (2014) Early Miocene ants (Hymenoptera, Formicidae) from Radoboj, Croatia. Neues Jahrbuch für Geologie und Paläontologie. Abhandlungen 272: 237–285. https://doi.org/10.1127/0077-7749/2014/0409

Dlussky GM, Wappler T, Wedmann S (2008) New middle Eocene formicid species from Germany and the evolution of weaver ants. Acta Palaeontologica Polonica 53: 615–626. https://doi.org/10.4202/app.2008.0406

Dlussky GM, Karl HV, Brauckmann C (2011) *Camponotites steinbachi* Dlussky, Karl and Brauckmann n. sp., 453–454. In: Dlussky GM, Karl HV, Brauckmann C, Gröning E, Reich M (2011) Two ants (Insecta: Hymenoptera: Formicidae: Formicinae) from the Late Pliocene of Willershausen, Germany, with a nomenclatural note on the genus *Camponotites*. Palaontologische Zeitschrift 85: 449–455. https://doi.org/10.1007/s12542-011-0104-2

Donisthorpe H (1920) British Oligocene ants. Annals & Magazine of Natural History 6: 81–94. https://doi.org/10.1080/00222932008632412

Donovan SK, Riley M (2013) The importance of labels to specimens: An example from the Sedgwick Museum. Geological Curators'. Group 509. https://doi.org/10.55468/GC51

DuBois MB (1998) The first fossil Dorylinae with notes on fossil Ecitoninae (Hymenoptera: Formicidae). Entomological News 109: 136–142.

Dubovikoff DA (2011) The first record of the genus *Pheidole* Westwood, 1839 (Hymenoptera, Formicidae) from the Baltic amber. Russian Entomological Journal 20: 255–257. https://doi.org/10.15298/rusentj.20.3.06

Dubovikoff DA, Zharkov DM (2023) A comment on: An Eocene army ant (2022) by Sosiak CE et al. Biology Letters 19: 20220603. https://doi.org/10.1098/rsbl.2022.0603

Dupérré N (2020) Old and new challenges in taxonomy: What are taxonomists up against? Megataxa 1: 59–62. https://doi.org/10.11646/megataxa.1.1.12

Early CM, Morhardt AC, Cleland TP, Milensky CM, Kavich GM, James HF (2020) Chemical effects of diceCT staining protocols on fluid-preserved avian specimens. PLoS ONE 15: e0238783. https://doi.org/10.1371/journal.pone.0238783

Emery C (1891) Le formiche dell'ambra Siciliana nel Museo Mineralogico dell'Università di Bologna. Memorie della Reale Accademia delle Scienze dell'Istituto di Bologna 1: 141–165. https://doi.org/10.5962/bhl.title.13914

Emery C (1903) Intorno ad alcune specie di *Camponotus* dell'America Meridionale. Rendiconti delle Sessioni della Reale Accademia delle Scienze dell'Istituto di Bologna (n.s.) 7: 62–81.

Emery C (1925) Hymenoptera. Fam. Formicidae. Subfam. Formicinae. Genera Insectorum 183: 1–302.

Enderlein G (1903) Die Copeognathen des indo-australischen Faunengebietes. Annales Historico-Naturales Musei Nationalis Hungarici 1: 179–344.

Enderlein G (1905) Zwei neue beschuppte Copeognathen aus dem Bernstein. Zoologischer Anzeiger 29: 39–43.

Enderlein G (1911) Die fossilen Copeognathen und ihre Phylogenie. Palaeontographica 58: 279–360.

Enderlein G (1917) 5. Beiträge zur Kenntnis der Copeognathen. IV. Zur Kenntnis der Copeognathen des Kongogebietes. Zoologischer Anzeiger 49: 254–256.

Enderlein G (1925) Beiträge zur Kenntnis der Copeognathen IX. Konowia (Vienna) 4: 97–108.

Engel MS (2016) A new species of the booklouse genus *Embidopsocus* in Baltic amber (Psocoptera: Liposcelididae). Novitates Paleoentomologicae 16: 1–9. https://doi.org/10.17161/np.v0i16.5706

Engel MS, Wang B (2022) A new species of embidopsocine barklouse in Langhian amber from Zhangpu, China (Psocoptera: Liposcelididae). Palaeoentomology 5: 487–492. https://doi.org/10.11646/palaeoentomology.5.5.10

Engelkes K, Friedrich F, Hammel JU, Haas A (2018) A simple setup for episcopic microtomy and a digital image processing workflow to acquire high-quality volume data and 3D surface models of small vertebrates. Zoomorphology 137: 213–228. https://doi.org/10.1007/s00435-017-0386-3

Erichson U, Tomczyk L (1998) Die Staatliche Bernstein-Manufaktur Königsberg: 1926–1945. Eigenverlag des deutschen Bernsteinmuseums, Ribnitz-Damgarten, 154 pp.

Ermisch K (1950) Die Gattungen der Mordelliden der Welt. Entomologische Blätter 45(46): 1.

Fabricius JC (1793) Entomologia systematica emendata et aucta. Secundum classes, ordines, genera, species, adjectis synonimis, locis observationibus, descriptionibus. Tome 2. C. G. Proft, Hafniae [= Copenhagen], 519 pp. https://doi.org/10.5962/bhl.title.125869

Faulwetter S, Vasileiadou A, Kouratoras M, Dailianis T, Arvanitidis C (2013) Micro-computed tomography: Introducing new dimensions to taxonomy. ZooKeys 263: 1. https://doi.org/10.3897/zookeys.263.4261

Federman D (1990) Amber. In: Modern jeweler's consumer guide to colored gemstones. Springer, 22–25. https://doi.org/10.1007/978-1-4684-6488-7_4

Fikáček M, Beutel RG, Cai C, Lawrence JF, Newton AF, Solodovnikov A, Ślipiński A, Thayer MK, Yamamoto S (2020) Reliable placement of beetle fossils via phylogenetic analyses – Triassic *Leehermania* as a case study (Staphylinidae or Myxophaga?). Systematic Entomology 45: 175–187. https://doi.org/10.1111/syen.12386

Fikáček M, Yamamoto S, Matsumoto K, Beutel RG, Maddison DR (2023) Phylogeny and systematics of Sphaeriusidae (Coleoptera: Myxophaga): minute living fossils with underestimated past and present-day diversity. Systematic Entomology 48: 233–249. https://doi.org/10.1111/syen.12571

Fischer G, Hita Jałoszyński F, Peters MK (2012) Taxonomy of the ant genus *Pheidole* Westwood (Hymenoptera: Formicidae) in the Afrotropical zoogeographic region: definition of species groups and systematic revision of the *Pheidole pulchella* group. Zootaxa 3232: 1–43. https://doi.org/10.11646/zootaxa.3232.1.1

Fisher BL, Bolton B (2016) Ants of the world. Ants of Africa and Madagascar. A guide to the genera. Berkeley: University of California Press [ix +] 503 pp. https://doi.org/10.1525/9780520962996

Flannery T (2009) Now or ever: Why we must act now to end climate change and create a sustainable future. Open Road+ Grove/Atlantic. https://doi.org/10.5860/CHOICE.47-4429

Forel A (1878) Études myrmécologiques en 1878 (première partie) avec l'anatomie du gésier des fourmis. Bulletin de la Société Vaudoise des Sciences Naturelles 15: 337–392.

Forel A (1886) Études myrmécologiques en 1886. Annales de la Société Entomologique de Belgique 30: 131–215.

Förster B (1891) Die Insekten des "Plattigen Steinmergels" von Brunstatt. Abhandlungen zur Geologischen Spezialkarte von Elsass-Lothringen 3: 333–594.

Franciscolo MF (1957) Coleoptera Mordellidae I. IN: South African Animal Life. Results of the Lund University Expedition in 1950–1951. Almqvist & Wiksells, Uppsala 4: 207–291.

Franciscolo ME (1967) Coleoptera, Mordellidae: A monograph of the South African genera and species. 3. Tribe Mordellistenini. South African Animal Life: 67–203.

Friedrich F, Beutel RG (2008) Micro-computer tomography and a renaissance of insect morphology. Developments in X-ray tomography VI, SPIE. https://doi.org/10.1117/12.794057

Friedrich F, Matsumura Y, Pohl H, Bai M, Hörnschemeyer T, Beutel RG (2014) Insect morphology in the age of phylogenomics: Innovative techniques and its future role in systematics. Entomological Science 17: 1–24. https://doi.org/10.1111/ens.12053

Frondel JW (1968) Amber Facts and Fancies. Economic Botany 22: 371–382. https://doi.org/10.1007/bf02908134

Garcia FH, Lieberman Z, Audisio TL, Liu C, Economo EP (2019) Revision of the highly specialized ant genus *Discothyrea* (Hymenoptera: Formicidae) in the Afrotropics with X-Ray Microtomography and 3D Cybertaxonomy. Insect Systematics and Diversity 3: 5. https://doi.org/10.1093/isd/ixz015

Georgiev D (2022a) New species of Psocoptera (Insecta) from East Africa. Historia Naturalis Bulgarica 44: 51–62. https://doi.org/10.48027/hnb.44.072

Georgiev D (2022b) New records of Psocoptera from East Sub-Saharan Africa. ZooNotes 12: 1–36. https://doi.org/10.48027/hnb.44.011

Germar EF (1837) Fauna insectorum Europae. Fasciculus 19. Insectorum protogaeae specimen sistens insecta carbonum fossilium. Kümmel, Halle, 25 pp.

Gerstäcker A (1859) Monatsberichte der Königlichen Preussischen Akademie der Wissenschaften zu Berlin 1858: 261–264. [Untitled. Introduced by: „Hr. Peters berichtete über sein Reisewerk, von dem die Insecten bis zum 64., die Botanik bis zum 34. Bogen gedruckt sind und teilte den Schluss der Diagnosen der von Hrn. Dr. Gerstäcker bearbeiteten Hymenopteren mit."]

Gessner C (1565)[-1566] De omni rerum fossilium genere, gemmis, lapidibus, metallis, et huiusmodi, libri aliquot, plerique nunc primum editi. Excudebat Iacobus Gesnerus, Tiguri.

Girón JC, Tarasov S, González Montaña LA, Matentzoglu N, Smith AD, Koch M, Boudinot BE, Bouchard P, Burks R, Vogt L, Yoder M, Osumi-Sutherland D, Friedrich F, Beutel RG, Mikó I (2023) Formalizing invertebrate morphological data: A descriptive model for cuticle-based skeleto-muscular systems, an ontology for insect anatomy, and their potential applications in biodiversity research and informatics. Systematic Biology 72: 1084–1100. https://doi.org/10.1093/sysbio/syad025

Goldenberg A (2004) Polish amber art. Thesis, Indiana University.

Gotwald Jr WH (1982) Army ants. In: Hermann HR (Ed.) Social Insects. Vol. 4. Academic Press, New York, 157–254. https://doi.org/10.1016/b978-0-12-342204-0.50010-3

Gotwald Jr WH (1995) Army ants: the biology of social predation. Cornell University Press, Ithaca, New York, [xviii +] 302 pp. https://doi.org/10.1086/419419

Greven H, Wichard W (2010) Schmetterlinge oder Köcherfliegen? Bemerkungen zum Kapitel „De papilionibus "aus der „Historia succinorum " (1742) des Nathanael Sendel. Entomologie Heute 22: 107–150.

Greving I, Wilde F, Ogurreck M, Herzen J, Hammel JU, Hipp A, Friedrich F, Lottermoser L, Dose T, Burmester H, Müller M, Beckmann F (2014) P05 imaging beamline at PETRA III: first results. In: Stuart RS (Ed.) Proceedings of SPIE - Developments in X-Ray Tomography IX, 9212, San Diego, 92120O-8. https://doi.org/10.1117/12.2061768

Grimaldi DA (1996) Amber: Window to the Past. Harry N. Abrams, 216 pp. https://doi.org/10.5860/choice.33-5724

Grimaldi D, Engel MS (2006) Fossil Liposcelididae and the lice ages (Insecta: Psocodea). Proceedings. Biological Sciences 273: 625–633. https://doi.org/10.1098/rspb.2005.3337

Grimaldi DA, Shedrinsky A, Ross A, Baer NS (1994) Forgeries in fossils in "amber": History, identification and case studies. Curator 37: 251–274. https://doi.org/10.1111/j.2151-6952.1994.tb01023.x

Guiry EJ, Orchard TJ, Royle TC, Cheung C, Yang DY (2020) Dietary plasticity and the extinction of the passenger pigeon (*Ectopistes migratorius*). Quaternary Science Reviews 233: 106225. https://doi.org/10.1016/j.quascirev.2020.106225

Günther KK (1989) *Empidopsocus saxonicus* sp. n., eine neue fossile Psocoptera-Art aus Sächsischem Bernstein des Bitterfelder Raumes (Insecta: Pscoptera: Liposcelidae). Mitteilungen aus dem Zoologischen Museum in Berlin 65: 321–325. https://doi.org/10.1002/mmnz.19890650214

Günther A, Drack M, Monod L, Wirkner CS (2021) A unique yet technically simple type of joint allows for the high mobility of scorpion tails. Journal of the Royal Society Interface, 18(182): 20210388.Hagen H (1865) Synopsis of the Psocina without ocelli. Entomologist's Monthly Magazine 2: 121–124. https://doi.org/10.1098/rsif.2021.0388

Hagen HA (1866) On some aberrant genera of Psocina. Entomologist's Monthly Magazine 2: 170–172.

Hagen HA (1882) Ueber Psociden in Bernstein. Entomologische Zeitung 43: 217–237.

Haibel A, Ogurreck M, Beckmann F, Dose T, Wilde F, Herzen J, Müller M, Schreyer A, Nazmov V, Simon M, Last A, Mohr J (2010) Micro- and nano-tomography at the GKSS Imaging Beamline at PETRA III. Developments in X-Ray Tomography VII, Vol. 7804 SPIE. https://doi.org/10.1117/12.860852

Hedrick BP, Yohe L, Linden AV, Dávalos LM, Sears K, Sadier A, Rossiter SJ, Davies KTJ, Dumont E (2018) Assessing soft-tissue shrinkage estimates in museum specimens imaged with diffusible iodine-based contrast-enhanced computed tomography (diceCT). Microscopy and Microanalysis 24: 284–291. https://doi.org/10.1017/S1431927618000399

Heer O (1849) Die Insektenfauna der Tertiärgebilde von Oeningen und von Radoboj in Croatien. Zweiter Theil: Heuschrecken, Florfliegen, Aderflüger, Schmetterlinge und Fliegen. W. Engelmann, Leipzig [vi +] 264 pp.

Heer O (1850) Die Insektenfauna der Tertiärgebilde von Oeningen und von Radoboj in Croatien. Zweite Abtheilung: Heuschrecken, Florfliegen, Aderflüger, Schmetterlinge und Fliegen. Neue Denkschriften der Allgemeinen Schweizerischen Gesellschaft für die Gesammten Naturwissenschaften 11: 1–264.

Hildt JA (1803) Magazin der Handels- und Gewerbskunde.

Hinrichs K (2007) Bernstein, das „Preußische Gold“ in Kunst-und Naturalienkammern und Museen des 16.-20. Jahrhunderts. Diss. Humboldt.-Universität.

Holl F (1829) Handbuch der Petrefactenkunde. Bd. 2 [part]. P. O. Hilschersche Buchhandlung, Dresden, 117–232.

Hong Y, Wu J (2000) The emendation of *Shanwangella palaeoptera* Zhang and its concerned problems. Geoscience (Beijing) 14: 15–20. [in Chinese]

Ijiri T, Todo H, Hirabayashi A, Kohiyama K, Dobashi Y (2018) Digitization of natural objects with micro CT and photographs. PLoS ONE 13: e0195852. https://doi.org/10.1371/journal.pone.0195852

ICZN (1999) International Code of Zoological Nomenclature. 4th edn. The International Trust for Zoological Nomenclature, London, UK. 306 pp. https://www.iczn.org/the-code/the-code-online/ [accessed: January 2024]

Jandausch K, van de Kamp T, Beutel RG, Niehuis O, Pohl H (2023) ‘Stab, chase me, mate with me, seduce me’: How widespread is traumatic insemination in Strepsiptera? Biological Journal of the Linnean Society. Linnean Society of London 140: 206–223. https://doi.org/10.1093/biolinnean/blad046

Jałoszyński P, Luo XZ, Hammel JU, Yamamoto S, Beutel RG (2020) The mid-Cretaceous †*Lepiceratus* gen. nov. and the evolution of the relict beetle family Lepiceridae (Insecta: Coleoptera: Myxophaga). Journal of Systematic Palaeontology 18: 1127–1140. https://doi.org/10.1080/14772019.2020.1747561

Jiang H, Tomaschek F, Muscente AD, Niu C, Nyunt TT, Fang Y, Schmidt U, Chen J, Lönartz M, Mähler B, Wappler T, Jarzembowski EA, Szwedo J, Zhang H, Rust J, Wang B (2022) Widespread mineralization of soft-bodied insects in Cretaceous amber. Geobiology 20: 363–376. https://doi.org/10.1111/gbi.12488

Johnson KP, Smith VS, Hopkins HH (2023) Psocodea Species File Online. Version 5.0/5.0. http://Psocodea.SpeciesFile.org [accessed: July 2023]

Jordal BH (2015) Molecular phylogeny and biogeography of the weevil subfamily Platypodinae reveals evolutionarily conserved range patterns. Molecular Phylogenetics and Evolution 92: 294–307. https://doi.org/10.1016/j.ympev.2015.05.028

van de Kamp T, dos Santos Rolo T, Baumbach T, Greven H (2015) X-ray radiography of a spraying stick insect (Phasmatodea). Entomologie Heute 27: 37–44.

van de Kamp T, Schwermann AH, dos Santos Rolo T, Lösel PD, Engler T, Etter W, Faragó T, Göttlicher J, Heuveline V, Kopmann A, Mähler B, Mörs T, Odar J, Rust J, Tan Jerome N, Vogelgesang M, Baumbach T, Krogmann L (2018) Parasitoid biology preserved in mineralized fossils. Nature Communications 9: 3325. https://doi.org/10.1038/s41467-018-05654-y

Kawata A, Ogawa N, Yoshizawa K (2022) Morphology and phylogenetic significance of the thoracic muscles in Psocodea (Insecta: Paraneoptera). Journal of Morphology 283: 1106–1119. https://doi.org/10.1002/jmor.21492

Kaplan AA, Grigelis AA, Strelnikova NI, Glikman LS (1977) Stratigraphy and correlation of Palaeogene deposits of South-Western cis-Baltic region. Sovetskaâ Geologiâ 4: 30–43.

King VT (1975) Labels are Important. Rocks and Minerals 50: 523–526. https://doi.org/10.1080/00357529.1975.11762911

King R (2022) Amber: From Antiquity to Eternity: Reaktion Books, 272 pp.

Kirejtshuk AG (2020) Taxonomic review of fossil coleopterous families (Insecta, Coleoptera). Suborder Archostemata: Superfamilies Coleopseoidea and Cupedoidea. Xiandai Dizhi 10: 73. https://doi.org/10.3390/geosciences10020073

Kirejtshuk AG, Chetverikov PE, Azar D, Kirejtshuk PA (2016) Ptismidae fam. nov. (Coleoptera, Staphyliniformia) from the lower Cretaceous Lebanese amber. Cretaceous Research 59: 201–213. https://doi.org/10.1016/j.cretres.2015.10.027

Klimeš P, Drescher J, Buchori D, Hidayat P, Nazarreta R, Potocký P, Rimandai M, Scheu S, Matos-Maraví P (2022) Uncovering cryptic diversity in the enigmatic ant genus *Overbeckia* and insights into the phylogeny of Camponotini (Hymenoptera: Formicidae: Formicinae). Invertebrate Systematics 36: 557–579. https://doi.org/10.1071/IS21067

Klopfstein S, Spasojevic T (2019) Illustrating phylogenetic placement of fossils using RoguePlots: An example from ichneumonid parasitoid wasps (Hymenoptera, Ichneumonidae) and an extensive morphological matrix. PLoS ONE 14: e01212942. https://doi.org/10.1371/journal.pone.0212942

Knorre Dv (1983) Die zoologisch-paläontologischen Sammlungen des Phyletischen Museums. Friedrich-Schiller-Universität Jena, Bernd Wilhelmi, Jena.

Knorre Dv, Beutel RG (2018) Jena: The Palaeontological Collections at the Phyletisches Museum in Jena. Paleontological Collections of Germany, Austria and Switzerland, Springer: 339–346. https://doi.org/10.1007/978-3-319-77401-5_33

Köhler UBG (2019) Dr. Dietrich von Knorre - der Malakologe, Museologe und Naturschützer sowie einer der letzten klassischen Zoologen Deutschlands wurde 80 Jahre. Mitteilung der Deutschen Malakozoologischen Gesellschaft 100: 49–62.

Königsberg-Pr. Pd B (1937) Bernstein-Einschlüsse. Entomologisches Nachrichtenblatt (Troppau) 1: 3.

Krogmann L, Knorre Dv, Beutel RG (2007) Die Chalcidoidea-Sammlung von Ferdinand Rudow (1840–1920) im Phyletischen Museum (Jena). Mitteilungen aus dem Hamburgischen Zoologischen Museum und Institut 104: 129–140.

Krüger L (1923) Neuroptera succinica baltica. Die im baltischen Bernstein eingeschlossenen Neuropteren des Westpreußischen Provinzial-Museums (heute Museum für Naturkunde und Vorgeschichte) in Danzig. Stettiner Entomologische Zeitung 84: 68–92.

Lak M, Néraudeau D, Nel A, Cloetens P, Perrichot V, Tafforeau P (2008) Phase contrast X-ray synchrotron imaging: Opening access to fossil inclusions in opaque amber. Microscopy and Microanalysis 14: 251–259. https://doi.org/10.1017/s1431927608080264

LaPolla JS (2005) Ancient trophophoresy: a fossil *Acropyga* (Hymenoptera: Formicidae) from Dominican amber. Transactions of the American Entomological Society 131: 21–28.

LaPolla JS, Greenwalt DE (2015) Fossil ants (Hymenoptera: Formicidae) of the Middle Eocene Kishenehn Formation. Sociobiology 62: 163–174. https://doi.org/10.13102/sociobiology.v62i2.163-174

Larsson L (2010) A double grave with amber and bone adornments at Zvejnieki in northern Latvia. Archaeologia Baltica 13: 80–90.

Leach WE (1815) Entomology. In: Brewster D (Ed.) The Edinburgh encyclopedia. William Blackwood, Edinburgh 9: 57–172. https://doi.org/10.5962/bhl.title.66019

Leonard KC, Worden N, Boettcher ML, Dickinson E, Hartstone-Rose A (2022) Effects of long-term ethanol storage on muscle architecture. The Anatomical Record 305: 184–198. https://doi.org/10.1002/ar.24638

Li F (1999) Psocids (Psocoptera) of Fujian Province, China. Fauna of insects, Fujian Province of China 3.

Li F (2002) Psocoptera of China. National Natural Science Foundation of China: [xlvi +] 1976 pp. (2 Vols) [1547 figs, 10 pl. at the end of the 2nd Vol.].

Li YD, Ruta R, Tihelka E, Liu ZH, Huang DY, Cai Ch-Y (2022) A new marsh beetle from mid-Cretaceous amber of northern Myanmar (Coleoptera: Scirtidae). Scientific Reports 12: 13403. https://doi.org/10.1038/s41598-022-16822-y

Lienhard C (1991) New records and species of *Belaphopsocus* (Psocoptera: Liposcelididae). The Raffles Bulletin of Zoology 39: 75–85.

Lienhard C (1998) Psocoptères euro-méditerranéens. Faune de France 83, [XX+] 517 pp. [148 figs, 11 plates]

Lienhard C (2003) Nomenclatural amendments concerning Chinese Psocoptera (Insecta), with remarks on species richness. Revue Suisse de Zoologie 110: 695–721. https://doi.org/10.5962/bhl.part.80207

Lienhard C (2016) Country checklists of the Psocoptera species of the world. Extracted from Lienhard C, Smithers CN (2002) Psocoptera (Insecta) world catalogue and bibliography. Psocid News I(Special Issue): 1–123.

Lösel PD, van de Kamp T, Jayme A, Ershov A, Faragó T, Pichler O, Tan Jerome N, Aadepu N, Bremer S, Chilingaryan SA, Heethoff M, Kopmann A, Odar J, Schmelzle S, Zuber M, Wittbrodt J, Baumbach T, Heuveline V (2020) Introducing Biomedisa as an open-source online platform for biomedical image segmentation. Nature Communications 11: 5577. https://doi.org/10.1038/s41467-020-19303-w

Lund PW (1831) Lettre sur les habitudes de quelques fourmis du Brésil, adressée à M. Audouin. Annales des Sciences Naturelles 23: 113–138. https://doi.org/10.5962/bhl.part.7282

Matuschek O (2020) Goethes Elefanten. Insel Verlag, Berlin.

Mayer C (1861) Die Faunula des marinen Sandsteines von Kleinkuhren bei Königsberg. [Publisher not ascertainable]

Mayr G (1861) Die europäischen Formiciden. Nach der analytischen Methode bearbeitet. C. Gerolds Sohn, Wien, 80 pp. https://doi.org/10.5962/bhl.title.14089

Mayr G (1862) Myrmecologische Studien. Verhandlungen der Kaiserlich-Königlichen Zoologisch-Botanischen Gesellschaft in Wien 12: 649–776.

Mayr G (1867) Vorläufige Studien über die Radoboj-Formiciden, in der Sammlung der k. k. geologischen Reichsanstalt. Jahrbuch der Kaiserlich-Königlichen Geologischen Reichsanstalt Wien 17: 47–62.

Mayr G (1868) Die Ameisen des baltischen Bernsteins. Beiträge zur Naturkunde Preussens 1: 1–102.

Mayr G (1870) Neue Formiciden. Verhandlungen der Kaiserlich-Königlichen Zoologisch-Botanischen Gesellschaft in Wien 20: 939–996.

Mayr G (1887) Südamerikanische Formiciden. Verhandlungen der Kaiserlich-Königlichen Zoologisch-Botanischen Gesellschaft in Wien 37: 511–632.

McCoy VE, Boom A, Kraemer MMS, Gabbott SE (2017) The chemistry of American and African amber, copal, and resin from the genus *Hymenaea*. Organic Geochemistry 113: 43–54. https://doi.org/10.1016/j.orggeochem.2017.08.005

McKinney ML (1999) High rates of extinction and threat in poorly studied taxa. Conservation Biology 13: 1273–1281. https://doi.org/10.1046/j.1523-1739.1999.97393.x

Mercati M (1717) Michaelis Mercati Samminiatensis Metallotheca: Hauptw (Vol. 1). Salvioni.

Mataic D, Bastani B (2006) Intraperitoneal sodium thiosulfate for the treatment of calciphylaxis. Renal Failure 28: 361–363. https://doi.org/10.1080/08860220600583781

Menon MGR (1938) Coxal interlocking in the Lepidopsocidae and its probable taxonomic value. Current Science 7: 66–67.

Metscher BD (2009) MicroCT for comparative morphology: Simple staining methods allow high-contrast 3D imaging of diverse non-mineralized animal tissues. BMC Physiology 9: 1–14. https://doi.org/10.1186/1472-6793-9-11

Meyer E (1914) [Neue Nr. 1186] Germau [Russkoje, Русское]/Geologische Karte.

Misof B, Liu S, Meusemann K, Peters RS, Donath A, Mayer C, et al. (2014) Phylogenomics resolves the timing and pattern of insect evolution. Science 346: 763–767. https://doi.org/10.1126/science.1257570

Mockford EL (1969) Fossil insects of the Order Psocoptera from Tertiary amber of Chiapas, Mexico. Journal of Paleontology 43: 1267–1273.

Mockford EL (1993) North American Psocoptera (Insecta). CRC Press, New York, 1–455. https://doi.org/10.1201/9780203745403-1

Mockford EL (1999) A Classification of the Psocopteran Family Caeciliusidae (Caeciliidae Auct.). Transactions of the American Entomological Society 125: 325–417.

Mockford EL (2018) Biodiversity of Psocoptera. In: Foottit RG, Adler PH (Eds) Insect Biodiversity: Science and Society, Vol. II. 417–456. https://doi.org/10.1002/9781118945582

Mockford EL, Lienhard C, Yoshizawa K (2013) Revised classification of 'Psocoptera' from Cretaceous amber, a reassessment of published information. Insecta Matsumurana (N.S.) 69: 1–26.

Modi A, Vergata C, Zilli C, Vischioni C, Vai S, Tagliazucchi GM, Lari M, Caramelli D, Taccioli C (2021) Successful extraction of insect DNA from recent copal inclusions: Limits and perspectives. Scientific Reports 11: 1–8. https://doi.org/10.1038/s41598-021-86058-9

Mongiardino Koch N, Thompson JR (2021) A total-evidence dated phylogeny of Echinoidea combining phylogenomic and paleontological data. Systematic Biology 70: 421–439. https://doi.org/10.1093/sysbio/syaa069

Moosmann J, Ershov A, Weinhardt V, Baumbach T, Prasad MS, LaBonne C, Xiao X, Kashef J, Hoffmann R (2014) Time-lapse X-ray phase-contrast microtomography for in vivo imaging and analysis of morphogenesis. Nature Protocols 9: 294–304. https://doi.org/10.1038/nprot.2014.033

Mukherjee AJ, Roßberger E, James MA, Pfälzner P, Higgitt CL, White R, Peggie DA, Azar D, Evershed RP (2008) The Qatna lion: Scientific confirmation of Baltic amber in late Bronze Age Syria. Antiquity 82: 49–59. https://doi.org/10.1017/s0003598x00096435

Najt J (1987) Le Collembole fossile *Paleosminthurus juliae* est un Hyménoptère. Revue Française d'Entomologie 9: 152–154. [Nouvelle Série]

Nakahara W (1915) On the Hemerobiinae of Japan. Annotationes Zoologicae Japonenses 9: 11–48.

Nakamine H, Yamamoto S, Takahashi Y, Liu XY (2023) A remarkable new genus of Nevrorthidae (Neuroptera, Osmyloidea) from mid-Cretaceous Kachin amber of northern Myanmar. Deutsche Entomologische Zeitschrift 70: 113–120. https://doi.org/10.3897/dez.70.98873

Naumann B, Reip HS, Akkari N, Neubert D, Hammel JU (2020) Inside the head of a cybertype–three-dimensional reconstruction of the head muscles of *Ommatoiulus avatar* (Diplopoda: Juliformia: Julidae) reveals insights into the feeding movements of Juliformia. Zoological Journal of the Linnean Society 26: 954–75. https://doi.org/10.1093/zoolinnean/zlz109

Nel A, de Ploëg G, Azar D (2004) The oldest Liposcelididae in the lowermost Eocene amber of the Paris Basin (Insecta: Psocoptera). Geologica Acta 2: 31–36.

Nel A, Prokop J, de Ploeg G, Millet J (2005) New Psocoptera (Insecta) from the lowermost Eocene Amber of Oise, France. Journal of Systematic Palaeontology 3: 371–391. https://doi.org/10.1017/S1477201905001598

Neumüller M., Reichinger A, Rist F, Kern C (2014) 3D printing for cultural heritage: Preservation, accessibility, research and education. 3D research challenges in cultural heritage: a roadmap in digital heritage preservation: 119–134. https://doi.org/10.1007/978-3-662-44630-0_9.

O'Hara JE, Raper CM, Pont AC, Whitmore D (2013) Reassessment of *Paleotachina* Townsend and *Electrotachina* Townsend and their removal from the Tachinidae (Diptera). ZooKeys 361: 27–37. https://doi.org/10.3897/zookeys.361.6448

Orr MC, Ascher JS, Bai M, Chesters D, Zhu CD (2020) Three questions: How can taxonomists survive and thrive worldwide? Megataxa 1: 19–27. https://doi.org/10.11646/megataxa.1.1.4

Özdikmen H (2010) New names for the preoccupied specific and subspecific epithets in the genus *Camponotus* Mayr, 1861 (Hymenoptera: Formicidae). Munis Entomology & Zoology 5: 519–537.

Palenstijn WJ, Batenburg KJ, Sijbers J (2011) Performance improvements for iterative electron tomography reconstruction using graphics processing units (GPUs). Journal of Structural Biology 176: 250–253. https://doi.org/10.1016/j.jsb.2011.07.017

Paleobio DB (2022) The Paleobiology Database: Revealing the History of Life. https://paleobiodb.org/#/ [accessed: 18 July 2022]

Pearman JV (1935) Two remarkable amphientomids (Psocoptera). Stylops 4: 134–137. https://doi.org/10.1111/j.1365-3113.1935.tb00576.x

Pearman JV (1936) The taxonomy of the Psocoptera: Preliminary sketch. Proceedings Royal Entomological Society of London (B) 5: 58–62. https://doi.org/10.1111/j.1365-3113.1936.tb00596.x

Peinert M, Wipfler B, Jetschke G, Kleinteich T, Gorb SN, Beutel RG, Pohl H (2016) Traumatic insemination and female counter-adaptation in Strepsiptera (Insecta). Scientific Reports 6: 25052. https://doi.org/10.1038/srep25052

Peña-Kairath C, Delclòs X, Álvarez-Parra S, Peñalver E, Engel MS, Ollerton J, Peris D (2023) Insect pollination in deep time. Trends in Ecology & Evolution 38: 749–759. https://doi.org/10.1016/j.tree.2023.03.008

Penney D (2010) Biodiversity of fossils in amber from the major world deposits. Siri Scientific Press.

Penney D, Preziosi RF (2013) Sub-fossils in copal: An undervalued scientific resource. Paper presented at the Abstracts and Proceedings of the International Amber Researcher Symposium (Deposits—Collections—The Market). Gdansk International Fair Co. Amberif.

Penney D, Wadsworth C, Green DI, Kennedy SL, Preziosi RF, Brown TA (2013) Extraction of inclusions from (sub) fossil resins, with description of a new species of stingless bee (Hymenoptera: Apidae: Meliponini) in Quaternary Colombian copal. Paleontological Contributions 2013: 1–6. https://doi.org/10.17161/PC.1808.11103

Peris D, Rust J (2020) Cretaceous beetles (Insecta: Coleoptera) in amber: the palaeoecology of this most diverse group of insects. Zoological Journal of the Linnean Society 189: 1085–1104. https://doi.org/10.1093/zoolinnean/zlz118

Peris D, Ruzzier E, Perrichot V, Delclòs X (2016) Evolutionary and paleobiological implications of Coleoptera (Insecta) from Tethyan-influenced Cretaceous ambers. Geoscience Frontiers 7: 695–706. https://doi.org/10.1016/j.gsf.2015.12.007

Perkovsky EE (2016) Tropical and Holarctic ants in Late Eocene ambers. Vestnik Zoologii 50: 111–122. https://doi.org/10.1515/vzoo-2016-0014

Perkovsky E, Rasnitsyn A, Vlaskin A, Taraschuk M (2007) A comparative analysis of the Baltic and Rovno amber arthropod faunas: Representative samples. African Invertebrates 48: 229–245.

Pictet FJ (1854) Classe insectes. Traité de Paléontologie: ou, Histoire Naturelle des Animaux Fossiles Considérés dans Leurs Rapports Zoologiques et Géologiques 2: 301–405. https://doi.org/10.5962/bhl.title.13903.

Pierce WD, Gibron SJ (1962) Fossil arthropods of California. 24. Some unusual fossil arthropods from the Calico Mountains nodules. Bulletin of the Southern California Academy of Sciences 61: 143–151.

Pileckaitė R (2001) Amber jewelry of Sigitas Virpilaitis: Postmodern approach. Acta Academiae artium Vilnensis. Dailė 22: 213–218.

Piper R (2009). Extinct animals: an encyclopedia of species that have disappeared during human history, Bloomsbury Publishing USA. https://doi.org/10.5040/9798400649219

Piton L (1935) [New species *Camponotus obesus* attributed to Piton]. In: Piton L, Théobald N (Eds) La faune entomologique des gisements Mio-Pliocènes du Massif Central. Revue des Sciences Naturelles d'Auvergne (n.s.) 1: 65–104 [pp. 68].

Pohl H, Beutel RG (2016) †*Kinzelbachilla ellenbergeri*–a new ancestral species, genus and family of Strepsiptera (Insecta). Systematic Entomology 41: 287–297. https://doi.org/10.1111/syen.12158

Pohl H, Beutel RG (2005) The phylogeny of Strepsiptera. Cladistics 21: 328–374. https://doi.org/10.1111/j.1096-0031.2005.00074.x

Pohl H, Beutel RG, Kinzelbach R (2005) Protoxenidae fam. nov. (Insecta, Strepsiptera) from Baltic amber—A 'missing link' in strepsipteran phylogeny. Zoologica Scripta 34: 57–69. https://doi.org/10.1111/j.1463-6409.2005.00173.x

Pohl H, Wipfler B, Grimaldi D, Beckmann F, Beutel RG (2010) Reconstructing the anatomy of the 42-million-year-old fossil *Mengea tertiaria* (Insecta, Strepsiptera). Naturwissenschaften 97: 855–859. https://doi.org/10.1007/s00114-010-0703-x

Pohl H, Batelka J, Prokop J, Müller P, Yavorskaya MI, Beutel RG (2018) A needle in a haystack: Mesozoic origin of parasitism in Strepsiptera revealed by first definite Cretaceous primary larva (Insecta). PeerJ 6: e5943. https://doi.org/10.7717/peerj.5943

Pohl H, Hammel JU, Richter A, Beutel RG (2019) The first fossil free-living late instar larva of Strepsiptera (Insecta). Arthropod Systematics & Phylogeny 77: 125–140. https://doi.org/10.26049/ASP77-1-2019-06

Pohl H, Wipfler B, Boudinot BE, Beutel RG (2021) On the value of Burmese amber for understanding insect evolution: Insights from †*Heterobathmilla*–an exceptional stem group genus of Strepsiptera (Insecta). Cladistics 37: 211–229. https://doi.org/10.1111/cla.12433

Qvarnström M, Fikáček M, Wernström JV, Huld S, Beutel RG, Arriaga-Varela E, Ahlberg PE, Niedźwiedzki G (2021) Exceptionally preserved beetles in a Triassic coprolite of putative dinosauriform origin. Current Biology 31: 3374–3381. https://doi.org/10.1016/j.cub.2021.05.015

Radchenko AG, Dlussky GM (2019) First record of the ant genus *Crematogaster* (Hymenoptera: Formicidae) from the Late Eocene European ambers. Annales Zoologici (Warsaw) 69: 417–421. https://doi.org/10.3161/00034541anz2019.69.2.008

Radchenko AG, Perkovsky EE (2021) Wheeler's dilemma revisited: First *Oecophylla-Lasius* syninclusion and other ants syninclusions in the Bitterfeld amber (late Eocene). Invertebrate Zoology 18: 47–65. https://doi.org/10.15298/invertzool.18.1.05

Rafiqi AM, Rajakumar A, Abouheif E (2020) Origin and elaboration of a major evolutionary transition in individuality. Nature 585: 239–244. https://doi.org/10.1038/s41586-020-2653-6

Ramesh G, Babu R, Subramanian KA (2020) New species of *Soa* Enderlein, 1904 (Psocodea: 'Psocoptera': Lepidopsocidae) from the Western Ghats of India. Zootaxa 4881: 383–392. https://doi.org/10.11646/zootaxa.4881.2.11

Rasnitsyn AP, Müller P (2023) Identity of the insect larva described by Zippel et al. (2022) in the mid–Cretaceous Burmese (Kachin) amber (Hymenoptera, Tenthredinoidea, Blasticotomidae = Xyelotomidae, syn. nov.). Palaeoentomology 6: 13–16. https://doi.org/10.11646/palaeoentomology.6.1.4

Régnier C, Achaz G, Lambert A, Cowie RH, Bouchet P, Fontaine B (2015) Mass extinction in poorly known taxa. Proceedings of the National Academy of Sciences of the United States of America 112: 7761–7766. https://doi.org/10.1073/pnas.1502350112

Richter A, Keller RA, Rosumek FB, Economo EP, Garcia FH, Beutel RG (2019) The cephalic anatomy of workers of the ant species *Wasmannia affinis* (Formicidae, Hymenoptera, Insecta) and its evolutionary implications. Arthropod Structure & Development 49: 26–49. https://doi.org/10.1016/j.asd.2019.02.002

Richter A, Boudinot BE, Yamamoto S, Katzke J, Beutel RG (2022) The first reconstruction of the head anatomy of a Cretaceous insect, †*Gerontoformica gracilis* (Hymenoptera: Formicidae), and the early evolution of ants. Insect Systematics and Diversity 6: 4. https://doi.org/10.1093/isd/ixac013

Richter A, Boudinot BE, Garcia FH, Billen J, Economo EP, Beutel RG (2023) Wonderfully weird: The head anatomy of the armadillo ant, *Tatuidris tatusia* (Hymenoptera: Formicidae: Agroecomyrmecinae), with evolutionary implications. Myrmecological News 33. https://doi.org/10.25849/myrmecol.news_033:035

Riou B (1999) Descriptions de quelques insectes fossiles du Miocène supérieur de la Montagne d'Andance (Ardèche, France). EPHE Biologie et Evolution des Insectes 11/12: 123–133.

Ritzkowski S (1997) K-Ar-Altersbestimmungen der bernsteinführenden Sedimente des Samlandes (Paläogen, Bezirk Kaliningrad). Metalla (Sonderheft) 66: 19–23.

Roesler R (1943) Über einige Copeognathengenera. Stettiner Entomologische Zeitung 104: 1–14.

Roesler R (1944) Die Gattungen der Copeognathen. Stettiner Entomologische Zeitung 105: 117–166.

Roger J (1862) Einige neue exotische Ameisen-Gattungen und Arten. Berliner Entomologische Zeitschrift 6: 233–254. https://doi.org/10.1002/mmnd.47918620118

Rogers DC, et al. (2017) Images are not and should not ever be type specimens: A rebuttal to Garraffoni & Freitas. Zootaxa 4269: 455–459. https://doi.org/10.11646/zootaxa.4269.4.3

Ross AJ (2019) Burmese (Myanmar) amber checklist and bibliography 2018. Palaeoentomology 2: 22–84. https://doi.org/10.11646/palaeoentomology.2.1.5

Ross AJ (2021) Supplement to the Burmese (Myanmar) amber checklist and bibliography, 2020. Palaeoentomology 4: 57–76. https://doi.org/10.11646/palaeoentomology.4.1.11

Sado A (2022) Amber on Fashion Week. Bursztynisko. The Amber Magazine 46: 6.

Sadowski E-M, Schmidt AR, Seyfullah LJ, Solórzano-Kraemer MM, Neumann C, Perrichot V, Hamann C, Milke R, Nascimbene PC (2021) Conservation, preparation and imaging of diverse ambers and their inclusions. Earth-Science Reviews 220: 103653. https://doi.org/10.1016/j.earscirev.2021.103653

Salata S, Fisher BL (2020) *Pheidole* Westwood, 1839 (Hymenoptera, Formicidae) of Madagascar – an introduction and a taxonomic revision of eleven species groups. ZooKeys 905: 1–235. https://doi.org/10.3897/zookeys.905.39592

Salata S, Fisher BL (2022) Taxonomic revision of the *Pheidole megacephala* species-group (Hymenoptera, Formicidae) from the Malagasy Region. PeerJ 10: e13263. https://doi.org/10.7717/peerj.13263

Samšińák K (1967) *Camponotus novotnyi* sp. n., eine neue tertiäre Ameise aus Böhmen. Vestník Ustredního Ustavu Geologického 42: 365–366.

Santschi F (1911) Nouvelles fourmis du Congo et du Benguela. Revue Zoologique Africaine (Brussels) 1: 204–217.

Santschi F (1912) Fourmis d'Afrique et de Madagascar. Annales de la Société Entomologique de Belgique 56: 150–167. https://doi.org/10.5962/bhl.part.5816

Santschi F (1926) Trois notes myrmécologiques. Annales de la Société Entomologique de France 95: 13–28. https://doi.org/10.1080/21686351.1926.12280094

Sarnat EM, Fischer G, Guénard B, Economo EP (2015) Introduced *Pheidole* of the world: Taxonomy, biology and distribution. ZooKeys 543: 1–109. https://doi.org/10.3897/zookeys.543.6050

Savage TS (1849) The driver ants of western Africa. Proceedings of the Academy of Natural Sciences of Philadelphia 4: 195–200.

Schädel M, Yavorskaya M, Beutel RG (2022) The earliest beetle †*Coleopsis archaica* (Insecta: Coleoptera)–morphological re-evaluation using Reflectance Transformation Imaging (RTI) and phylogenetic assessment. Arthropod Systematics & Phylogeny 80: 495–510. https://doi.org/10.3897/asp.80.e86582

Schedl KE (1939) Die Einteilung und geographische Verbreitung der Platypodidae. 56. Beitrag zur Morphologie und Systematik der Scolytidae und Platypodidae. In: Jordan K, Hering EM (Eds) Verhandlungen, VII. Internationaler Kongress für Entomologie. Vol. 1. Selbstverlage der Internationalen Kongresse für Entomologie, Weimar, 377–410.

Schindelin J, Arganda-Carreras I, Frise E, Kaynig V, Longair M, Pietzsch T, Preibisch S, Rueden C, Saalfeld S, Schmid B, Tinevez J-T, White DJ, Hartenstein V, Eliceiri K, Tomancak P, Cardona A (2012) Fiji: An open-source platform for biological-image analysis. Nature Methods 9: 676–682. https://doi.org/10.1038/nmeth.2019

Schawaroch V, Kathirithamby J, Grimaldi D (2005) Strepsiptera and triungula in Cretaceous amber. Insect Systematics & Evolution 36: 1–20. https://doi.org/10.1163/187631205788912787

Schweigger AF (1819) Beobachtungen auf naturhistorischen Reisen. Anatomisch-physiologische Untersuchungen über Corallen; nebst einem Anhange, Bemerkungen über den Bernstein enthaltend. Reimer, Berlin, 127 pp. https://doi.org/10.5962/bhl.title.14416

Scudder SH (1877) The first discovered traces of fossil insects in the American Tertiaries. Bulletin of the United States Geological and Geographical Survey of the Territories 3: 741–762.

Seeger W (1975) Funktionsmorphologie an Spezialbildungen der Fühlergeißel von Psocoptera und anderen Paraneoptera (Insecta); Psocodea als monophyletische Gruppe. Zeitschrift für Morphologie der Tiere 81: 137–159. https://doi.org/10.1007/bf00301153

Semple TL, Vidal-García M, Tatarnic NJ, Peakall R (2021) Evolution of reproductive structures for in-flight mating in thynnine wasps (Hymenoptera: Thynnidae: Thynninae). Journal of Evolutionary Biology 34: 1406–1422. https://doi.org/10.1111/jeb.13902

Sendel N (1742) Historia succinorum corpora aliena involventium et naturae opere pictorum et caelatorum ex regis augustorum cimeliis Dresdae conditis aeri insculptorum conscripta a Nathanaeli Sendelio: apud Io. Fridericum Gleditschium. https://doi.org/10.5962/bhl.title.150129

Shelmerdine SC, Simcock IC, Hutchinson JC, Aughwane R, Melbourne A, Nikitichev DI, Ong J-l, Borghi A, Cole G, Kingham E, Calder

AD, Capelli C, Akhtar A, Cook AC, Schievano S, David A, Ourselin S, Sebire NJ, Arthurs OJ (2018) 3D printing from microfocus computed tomography (micro-CT) in human specimens: Education and future implications. The British Journal of Radiology 91: 20180306. https://doi.org/10.1259/bjr.20180306

Simonsen TJ, Kitching IJ (2014) Virtual dissections through micro-CT scanning: A method for non-destructive genitalia 'dissections' of valuable Lepidoptera material. Systematic Entomology 39: 606–618. https://doi.org/10.1111/syen.12067

Singer GG (2008) Amber in the ancient Near East. Centro de Estudios de Historia del Antiguo Egipto-Universidad Católica Argentina. Disponível em. https://www.academia.edu/241848/Amber_in_the_Ancient_Near_East [Acesso em, 1]

Singer GNG (2016) Amber exchange in the Late Bronze Age Levant in cross-cultural Perspective. Paper presented at the International Conference about the Ancient Roads in San Marino.

Słodkowska B, Kramarska R, Kasiński JR (2013) The Eocene Climatic Optimum and the formation of the Baltic amber deposits. Paper presented at the The international amber researcher symposium."Amber. Deposits-Collections-The Market". Gdansk, Poland: Gdansk International fair Co. Amberif.

Smith F (1857) Catalogue of the hymenopterous insects collected at Sarawak, Borneo; Mount Ophir, Malacca; and at Singapore, by A. R. Wallace. Journal of the Proceedings of the Linnean Society of London. Zoology 2: 42–88. https://doi.org/10.1111/j.1096-3642.1857.tb01759.x [part]

Smith F (1868) Explanation of the plate of organic remains found in amber, in Amber; its origin and history, as illustrated by the geology of Samland. Quarterly Journal of Science 5: 183–184.

Smith MR (1943) A generic and subgeneric synopsis of the male ants of the United States. American Midland Naturalist 30: 273–321. https://doi.org/10.2307/2421283

Smithers CN (1964) On the Psocoptera of Madagascar. Revue de Zoologie et de Botanique Africaines 70: 209–294.

Smithers CN (1990) Key to the families and genera of Psocoptera (Arthropoda: Insecta). Technical Reports of the Australian Museum 2: 1–82. https://doi.org/10.3853/j.1031-8062.2.1990.77

Smithers CN (1999) New species and new records of Psocoptera from Tanzania. African Entomology 7: 91–106.

Snelling RR (2006) Taxonomy of the *Camponotus festinatus* complex in the United States of America (Hymenoptera: Formicidae). Myrmecologische Nachrichten 8: 83–97.

Solórzano-Kraemer MM, Delclòs X, Engel MS, Peñalver E (2020) A revised definition for copal and its significance for palaeontological and Anthropocene biodiversity-loss studies. Scientific Reports 10: 19904. https://doi.org/10.1038/s41598-020-76808-6

Solórzano-Kraemer MM, Kunz R, Hammel JU, Peñalver E, Delclòs X, Engel MS (2022) Stingless bees (Hymenoptera: Apidae) in Holocene copal and Defaunation resin from Eastern Africa indicate Recent biodiversity change. The Holocene 32: 414–432. https://doi.org/10.1177/09596836221074035

Sosiak CE, Borowiec ML, Barden P (2022) An Eocene army ant. Biology Letters 18: 20220398. https://doi.org/10.1098/rsbl.2022.0398

Sosiak CE, Borowiec ML, Barden P (2023a) Retraction: An Eocene army ant. Biology Letters 19: 20230059. https://doi.org/10.1098/rsbl.2023.0059

Sosiak CE, Borowiec ML, Barden P (2023b) An invited reply to: A comment on: An Eocene army ant (2022) by Sosiak CE et al. Biology Letters 19: 20230140. https://doi.org/10.1098/rsbl.2023.0140

Steward GA, Beveridge AE (2010) A review of New Zealand kauri (*Agathis australis* (D. Don) Lindl.): Its ecology, history, growth and potential for management for timber. New Zealand Journal of Forestry Science 40: 33–59.

Strohmeyer H (1912) Neue Platypodiden aus Deutsch-Ostafrika, Kamerun und Franzosisch-Kongo. Entomologische Blätter 8: 78–86.

Saqalaksari MP, Talebi AA, van de Kamp T, Haghighi SR, Zimmermann D, Richter A (2023) EntomonVR: a New Virtual Reality Game for Learning Insect Morphology. bioRxiv, 25 pp. https://doi.org/10.1101/2023.02.01.526587

Takahashi Y, Aiba H (2023) Winged formicine ant fossils (Hymenoptera, Formicidae) from the Chibanian (Middle Pleistocene) Shiobara Group, Tochigi Prefecture, Japan. Chishitsugaku Zasshi 129: 573–578. https://doi.org/10.5575/geosoc.2023.0023

Taylor B (2022) The Ants of (sub-Saharan) Africa (Hymenoptera: Formicidae). Profusely illustrated with original drawings and photographs and Catalogue notes on all ant species described from sub-Saharan Africa. 12th edn. https://antsofafrica.org/ [accessed: 18 July 2022]

Taylor CK (2013) The genus *Lithoseopsis* (Psocodea: Amphientomidae) in the Western Australian fauna, with description of the male of *Lithoseopsis humphreysi* from Barrow Island. Records of the Western Australian Museum 83: 245–252. https://doi.org/10.18195/issn.0313-122x.83.2013.245-252

Tihelka E, Li L, Fu Y, Su Y, Huang D, Cai C (2021) Angiosperm pollinivory in a Cretaceous beetle. Nature Plants 7: 445–451. https://doi.org/10.1038/s41477-021-00893-2

Tollefson J (2022) Climate change is hitting the planet faster than scientists originally thought. Nature 28. https://doi.org/10.1038/d41586-022-00585-7

Tröger D, Stark H, Beutel RG, Pohl H (2023) The morphology of the free-living females of Strepsiptera (Insecta). Journal of Morphology 284: e21576. https://doi.org/10.1002/jmor.21576

Trueman CN (2013) Chemical taphonomy of biomineralized tissues. Palaeontology 56: 475–486. https://doi.org/10.1111/pala.12041

Turner BD (1975) The Psocoptera of Jamaica. Transactions of the Royal Entomological Society of London 126: 533–609. https://doi.org/10.1111/j.1365-2311.1975.tb00860.x

Uschmann G (1959) Geschichte der Zoologie und der zoologischen Anstalten in Jena 1779–1919, Gustav Fischer Verlag, Jena.

Varela-Hernández F, Riquelme F (2021) A new ant species of the genus *Pheidole* Westwood, 1839 from Miocene Mexican amber. Southwestern Entomologist 46: 75–82. https://doi.org/10.3958/059.046.0107

Valentini MB (1714) Musei museorum, oder, der vollständigen Schaubühne fremder Naturalien: die raresten Naturschätze aus allen bis daher gedruckten Kunstkammern, Reißbeschreibungen und anderen curiosen Büchern enthalten, und benebenst einer neu ausgerichteten Zeug- und Rüstkammer der Natur auch vielen curiosen Kupferstücken vorgestellen sind. Von D. Michael Bernhard Valentini. https://doi.org/10.5962/bhl.title.150208

Vijande Vila E, Domínguez-Bella S, Cantillo Duarte JJ, Martínez López J, Barrena Tocino A (2015) Social inequalities in the Neolithic of southern Europe: The grave goods of the Campo de Hockey necropolis (San Fernando, Cádiz, Spain). Comptes Rendus. Palévol 14: 147–161. https://doi.org/10.1016/j.crpv.2014.11.004

Vishnyakova VN (1975) Psocoptera in Late Cretaceous insect-bearing resins from the Taimyr. Entomological Review 54: 63–75.

Vitali F (2019) Systematic notes on the Cerambycidae (Insecta: Coleoptera) described from Burmese amber. Palaeoentomology 2: 215–218. https://doi.org/10.11646/palaeoentomology.2.3.3

von Kéler S (1966) Zur Mechanik der Nahrungsaufnahme bei Corrodentien. Zeitschrift für Parasitenkunde (Berlin, Germany) 27: 64–79. https://doi.org/10.1007/BF00261218

Wappler T, Dlussky GM, Reuter M (2009) The first fossil record of Polyrhachis (Hymenoptera: Formicidae: Formicinae) from the Upper Miocene of Crete (Greece). Palaontologische Zeitschrift 83: 431–438. https://doi.org/10.1007/s12542-009-0035-3

Ward PS, Boudinot BE (2021) Grappling with homoplasy: taxonomic refinements and reassignments in the ant genera *Camponotus* and *Colobopsis* (Hymenoptera: Formicidae). Arthropod Systematics & Phylogeny 79: 37–56. https://doi.org/10.3897/asp.79.e66978

Ward PS, Brady SG, Fisher BL, Schultz TR (2010) Phylogeny and biogeography of dolichoderine ants: Effect of data partitioning and relict taxa on historical inference. Systematic Biology 59: 342–362. https://doi.org/10.1093/sysbio/syq012

Ward PS, Blaimer BB, Fisher BL (2016) A revised phylogenetic classification of the ant subfamily Formicinae (Hymenoptera: Formicidae), with resurrection of the genera *Colobopsis* and *Dinomyrmex*. Zootaxa 4072: 343–357. https://doi.org/10.11646/zootaxa.4072.3.4

Weber FC (1740) Das veränderte Rußland: In welchem Die jetzige Verfassung des Geist- und Weltlichen Regiments, Der Kriegs-Staat zu Lande und zu Wasser, Der wahre Zustand der Rußischen Finantzen, die geöffneten Berg-Wercke, die eingeführte Academien, Künste, Manufacturen, ergangene Verordnungen, Geschäfte mit denen Asiatischen Nachbahren und Vasallen, nebst der allerneuesten Nachricht von diesen Völckern, Ingleichen Die Begebenheiten des Czarewitzen Und was sich sonst merckwürdiges in Rußland zugetragen; Nebst verschiedenen bisher unbekannten Nachrichten vorgestellt werden. 3: Die Regierung der Kayserin Catharina und des Kaysers Petri Secundi und sonst alle vorgefallene Merkwürdigkeiten in sich haltend. 243.

Weidner H (1972) Copeognatha (Staubläuse). Handbuch der Zoologie 4: 2. [Hälfte, Berlin.]

Weingardt M, Beutel RG, Pohl H (2023) *Xenos vesparum* (Strepsiptera: Xenidae)—A new insect model and its endoparasitic secondary larva. Insect Systematics and Diversity 7: 4. https://doi.org/10.1093/isd/ixad003

Westwood JO (1839) An introduction to the modern classification of insects; founded on the natural habits and corresponding organisation of the different families. Volume 2. Part XI. London: Longman, Orme, Brown, Green and Longmans, 193–224. https://doi.org/10.5962/bhl.title.34449

Wheeler WM (1915) ["1914"] The ants of the Baltic Amber. Schriften der Physikalisch-Ökonomischen Gesellschaft zu Königsberg 55: 1–142. https://doi.org/10.5962/bhl.title.14207

Wheeler WM (1921) Chinese ants. Bulletin of the Museum of Comparative Zoology 64: 529–547.

Wichard W (2009) Taxonomic names. Aquatic Insects in Baltic Amber: 1–335.

Wichard W, Buder T, Caruso C (2010) Aquatic lacewings of family Nevrorthidae (Neuroptera) in Baltic amber. Denisia 29: 445–457.

Wichard W (2016) Overview and descriptions of Nevrorthidae in Baltic amber (Insecta, Neuroptera). Palaeodiversity 9: 95–111. https://doi.org/10.18476/pale.v9.a7

Wichard W (2017) Family Nevrorthidae (Insecta, Neuroptera) in mid-Cretaceous Burmese amber. Palaeodiversity 10: 1–5. https://doi.org/10.18476/pale.v10.a1

Wichard N, Wichard W (2008) Nathanael Sendel (1686–1757) Ein Wegbereiter der paläobiologischen Bernsteinforschung. Palaeodiversity 1: 93–102.

Wilde F, Ogurreck M, Greving I, Hammel JU, Beckmann F, Hipp A, Lottermoser L, Khokhriakov I, Lytaev P, Dose T, Burmester H, Müller M, Schreyer A (2016) Micro-CT at the imaging beamline P05 at PETRA III. AIP Conference Proceedings 1741: 030035. https://doi.org/10.1063/1.4952858

Wilson EO (1985a) Ants of the Dominican amber (Hymenoptera: Formicidae). 1. Two new myrmicine genera and an aberrant Pheidole. Psyche (Cambridge) 92: 1–9. https://doi.org/10.1155/1985/17307

Wilson EO (1985b) Ants of the Dominican amber (Hymenoptera: Formicidae). 2. The first fossil army ants. Psyche (Cambridge) 92: 11–16. https://doi.org/10.1155/1985/63693

Wilson EO (2003) *Pheidole* in the New World. A dominant, hyperdiverse ant genus. Cambridge, Mass.: Harvard University Press, [ix +]794 pp.

Wilson EO, Brown Jr WL (1953) The subspecies concept and its taxonomic application. Systematic Zoology 2: 97–111. https://doi.org/10.2307/2411818

Wilson PF, Stott J, Warnett JM, Attridge A, Smith MP, Williams MA (2017) Evaluation of touchable 3D-printed replicas in museums. Curator 60: 445–465. https://doi.org/10.1111/cura.12244

Winkler HJ (2019) Preußen als Unternehmer 1923–1932. In Preußen als Unternehmer 1923–1932: de Gruyter. https://doi.org/10.1515/9783110830682

Wright AH (1911) Other early records of the passenger pigeon (concluded). The Auk 28: 427–449. https://doi.org/10.2307/4070951

Wulff NC, van de Kamp T, dos Santos Rolo T, Baumbach T, Lehmann GU (2017) Copulatory courtship by internal genitalia in bushcrickets. Scientific Reports 7: 42345. https://doi.org/10.1038/srep42345

Yoshizawa K (2002) Phylogeny and higher classification of suborder Psocomorpha (Insecta: Psocodea:'Psocoptera'). Zoological Journal of the Linnean Society 136: 371–400. https://doi.org/10.1046/j.1096-3642.2002.00036.x

Yoshizawa K, Johnson KP (2008) Molecular systematics of the barklouse family Psocidae (Insecta: Psocodea:'Psocoptera') and implications for morphological and behavioral evolution. Molecular Phylogenetics and Evolution 46(2): 547–559. https://doi.org/10.1016/j.ympev.2007.07.011

Yoshizawa K, Lienhard C (2010) In search of the sister group of the true lice: A systematic review of booklice and their relatives, with an updated checklist of Liposcelididae (Insecta: Psocodea). Arthropod Systematics & Phylogeny 68: 181–195. https://doi.org/10.3897/asp.68.e31725

Zhang J (1989) Fossil insects from Shanwang, Shandong, China. [In Chinese.]. Jinan, China: Shandong Science and Technology Publishing House, 459 pp.

Zhang J, Sun B, Zhang X (1994) Miocene insects and spiders from Shanwang, Shandong. [In Chinese.]. Beijing: Science Press, [v +] 298 pp.

Ziegler MJ, Perez VJ, Pirlo J, Narducci RE, Moran SM, Selba MC, Hastings AK, Vargas-Vergara C, Antonenko PD, MacFadden BJ (2020) Applications of 3D paleontological data at the Florida Museum of Natural History. Frontiers of Earth Science 8: 1–20. https://doi.org/10.3389/feart.2020.600696

Zippel A, Haug C, Müller P, Haug JT (2022) First fossil tumbling flower beetle-type larva from 99 million year old amber. Palaontologische Zeitschrift 96: 219–229. https://doi.org/10.1007/s12542-022-00608-8

Zlatkov B, Vergilov V, Pérez Santa-Rita JV, Baixeras J (2023) First 3-D reconstruction of copulation in Lepidoptera: Interaction of genitalia in *Tortrix viridana* (Tortricidae). Frontiers in Zoology 20: 22. https://doi.org/10.1186/s12983-023-00500-4

Appendix 1

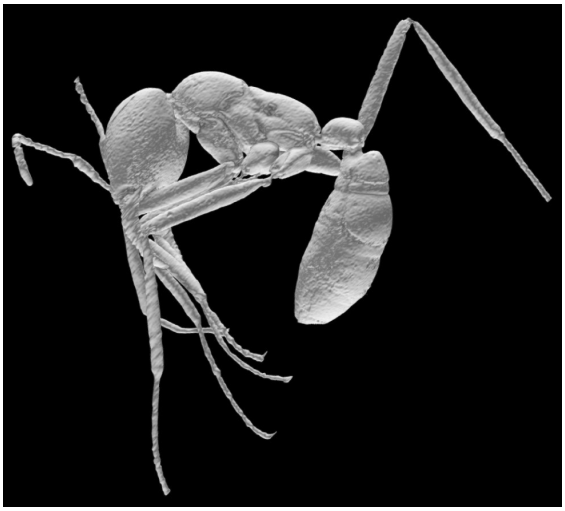

Figure A1. Model 1 of *Dorylus nigricans molestus* (Formicidae: Dorylinae) preserved in piece PMJ Pa 5884. An interactive version of this model is available in the HTML version of this article online and on Sketchfab: URL: https://sketchfab.com/3d-models/dorylus-sp-94769aba51364c5ab51ec8b92485609a.

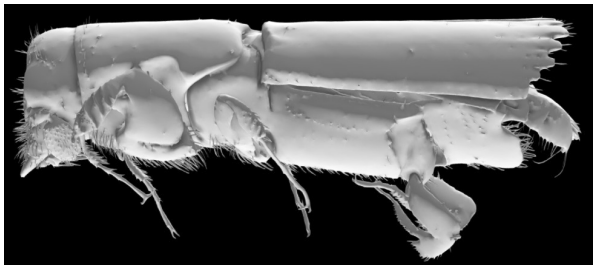

Figure A2. Model 2 of *Doliopygus* cf. *serratus* (Curculionidae: Platypodinae) in piece PMJ Pa 5827. An interactive version of this model is available in the HTML version of this article online and on Sketchfab: URL: https://sketchfab.com/3d-models/platypodidae-e6d79e10baf6456ea137888f814e0925.

Figure A3. Model 3 of the holotype specimen of ‡*A. knorrei* Weingardt, Bock & Boudinot, sp. nov. (Amphientomidae: Amphientominae) preserved in piece PMJ Pa 5809. An interactive cybertype is available in the HTML version of this article online and on Sketchfab: URL: https://sketchfab.com/3d-models/amphientomum-knorrei-a7e0f1c0c6234093a384a51c2be48730.

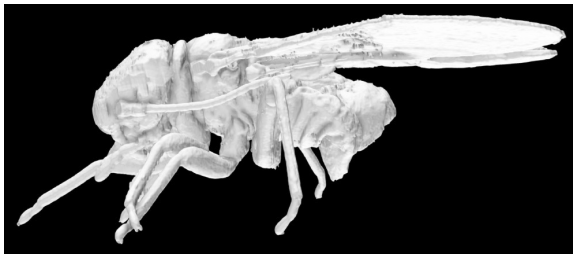

Figure A4. Model 4 of Archipsocidae gen. et sp. indet. preserved in kaori gum piece PMJ Pa 5825. An interactive version of this model is available in the HTML version of this article online and on Sketchfab: URL: https://sketchfab.com/3d-models/archipsocidae-21ac330840f14ab5ac6d50898aba3a4d.

Figure A5. Model 5 of the neotype of ‡*Pheidole cordata* Holl, 1829 preserved in copal piece PMJ Pa 5889. An interactive cybertype is available in the HTML version of this article online and on Sketchfab: URL: https://sketchfab.com/3d-models/pheidole-cordata-695385c99247469ebb28bc4049b9e301.

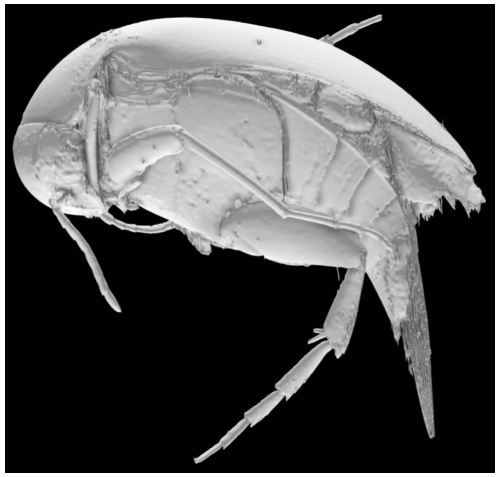

Figure A6. Model 6 of the holotype of †*Baltistena nigrispinata* Batelka, Tröger & Bock, sp. nov. (Mordellidae) preserved in piece PMJ Pa 5870. An interactive cybertype is available in the HTML version of this article online and on Sketchfab: URL: https://sketchfab.com/3d-models/baltistena-nigrispinata-0b8819500b854c42b782b42b79c781c4.

Supplementary material 1

Amber and copal specimens of the Phyletisches Museum collection

Authors: Brendon E. Boudinot, Bernhard L. Bock, Michael Weingardt, Daniel Tröger, Jan Batelka, Di LI, Adrian Richter, Hans Pohl, Olivia T. D. Moosdorf, Kenny Jandausch, Jörg U. Hammel, Rolf G. Beutel

Data type: docx

Explanation note: Amber and copal specimens of the Phyletisches Museum collection sorted by inventory number with the number of pieces given for each, what source they had according to the label and what source they are after identifying.

Link: https://doi.org/10.3897/dez.71.112433.suppl1

Supplementary material 2

Protocol of the IAA

Authors: Brendon E. Boudinot, Bernhard L. Bock, Michael Weingardt, Daniel Tröger, Jan Batelka, Di LI, Adrian Richter, Hans Pohl, Olivia T. D. Moosdorf, Kenny Jandausch, Jörg U. Hammel, Rolf G. Beutel

Data type: pdf

Link: https://doi.org/10.3897/dez.71.112433.suppl2